Grid Flexibility by Electrifying Energy Systems for Sustainable Aviation

A thesis submitted for the degree of Doctor of Philosophy

By

Zekun Guo

Principal Supervisor: Prof Gareth Taylor

Brunel Interdisciplinary Power Systems Research Centre
Department of Electronic and Electrical Engineering
College of Engineering, Design and Physical Sciences
Brunel University London

May 2023

Abstract

Decarbonisation of aviation goals set by Flightpath 2050 Europe's Vision for Aviation requires that the airports become emission-free by 2050. This thesis original contribution to knowledge is to explore the incorporation of aviation electrification technologies, including electric aircraft (EA), electrified ground support equipment (GSE), and airport parking electric vehicles (EVs), into power systems, evaluating their influence on grid infrastructure and operations, as well as their potential to support the grid operation.

A comprehensive review of aviation electrification technologies revealed a research gap in the integration of these technologies into the power systems. The thesis contributes to electricity network infrastructure planning for electrification of aviation and airport-based distributed energy resources (DER) that provide ancillary services to the power grid.

A multi-objective airport microgrid planning framework is developed, comparing EA charging strategies and revealing that battery swap performs better. Vehicle-to-grid (V2G) strategy with parking EVs improves the microgrid's performance. A techno-economic assessment of wireless charging systems for electric airport shuttle buses shows better economic performance than conventional buses and other charging options.

A novel Aviation-to-Grid (A2G) flexibility concept provides frequency response services to the GB power system using EA battery charging systems, with typical A2G service capacity showing significant variation across eight UK airports. A deep reinforcement learning (DRL)-based A2G dispatch approach evaluates the impact of EA charger capacity on energy dispatch results, with higher capacities leading to higher revenue and lower operation costs.

To summarise, this thesis addresses the research gaps in integrating aviation electrification technologies into power systems, offering valuable insights for airport operators aiming to decarbonise air transport activities through the adoption of these technologies. The study also provides an understanding of the impacts on grid operators in terms of infrastructure planning and operations. This comprehensive approach ensures a cohesive understanding of the challenges and opportunities presented by aviation electrification and its integration into power systems.

Acknowledgements

Firstly, I would like to express my deepest gratitude to my previous principal supervisor, Prof. Xin Zhang, for his exceptional guidance, encouragement, and support throughout this doctorate. Prof. Zhang's expertise in research methodology, critical thinking, and innovative ideas, as well as his dedication during our regular meetings, have been instrumental in shaping the direction and success of my work. His ability to provide constructive feedback and challenge me to push the boundaries of my research has been truly inspiring. I am also grateful to Prof. Gareth Taylor for sharing his knowledge and research experience, Dr. Chun Sing Lai for his valuable advice at Brunel University London, and Prof. Patrick Luk at Cranfield University for his insightful comments and recommendations. Their collective guidance and help have been instrumental in the completion of this thesis, and I am sincerely grateful to all of them.

Secondly, I would also thank my colleagues and friends at the Brunel Institute for Power Systems at Brunel University London. I will treasure the memories that we played card games, celebrated birthdays and festivals, had amazing dinners as well as went on trips together. Without their accompanying the time spent completing the thesis would have been much less enjoyable.

Last but not least, I want to show my thankfulness to my parents who brought me to this world and inspired me to choose my own career path. I would like to express my heartfelt thanks to my wife Mrs. Hongyu Jiang for accompanying with me; with her accompanying, I will no longer feel lonely when facing new challenges in the future.

Author’s Declaration

The work described in this thesis has not been previously submitted for a degree in this or any other university and unless otherwise referenced it is the author’s own work.

Zekun Guo

May 2023

List of Contents

List of Figures

List of Tables

Abbreviation

A2G	Aviation-to-Grid
AC	Alternating current
AVR	Automatic voltage regulator
BFS	Backward forward sweep
CAA	Civil Aviation Authority
CAPEX	Capital expenditure
COVID	Coronavirus Disease
CRF	Capital recovery factor
DC	Direct current
DER	Distributed Energy Resource
DG	Distributed Generator
DOD	Depth of discharge
DPD	Design peak day
DPH	Design peak hour
DQN	Deep Q Network
DRL	Deep Reinforcement Learning
DWC	Dynamic wireless charging
EA	Electric aircraft
EISY	Enter into service year
EMS	Energy Management System
EPI	Energy performance indicators
ESS	Energy Storage System
EV	Electric vehicle
FFR	Fast Frequency Response
FFY	First flight year
G2V	Grid to Vehicle
GHG	Greenhouse Gas
GSE	Ground support equipment
GSEE	Global Solar Energy Estimator
GT	Gas turbine
HVAC	Heating, ventilation, and air conditioning

HVDC	High-voltage direct current
IAG	International Airlines Group
ICT	Information and communications technology
KAIST	Korea Advanced Institute of Science and Technology
KCL	Kirchhoff's Current Law
KVL	Kirchhoff's Voltage Law
MABM	Multi-agent-based Model
MDP	Markov decision process
MILP	Mixed-integer linear programming
NSGA	Non-dominated Sorting Genetic Algorithm
OPEX	Operating expense
PAX	Passenger
PCC	Point of Common Coupling
PEM	Polymer electrolyte membrane
PEV	Plug-in electric vehicle
PFR	Primary frequency response
PSS	power system stabilizer
PSU	Power supply unit
PV	Photovoltaic
PVR	Peak-to-valley ratio
PWM	Pulse width modulation
QWC	Quasi-dynamic wireless charging
RF	Resilience factor
RoCoF	Rate of change of frequency
RSCR	Renewable generation self-consumption rate
SFR	Secondary frequency response
SOC	State of charge
SWC	Static wireless charging
TOU	Time of use
V2G	Vehicle-to-Grid
WPT	Wireless power transfer
WT	Wind turbine

Chapter 1 Introduction

1.1 Motivation and Background

Flightpath 2050, the European Commission's vision for aviation, requires that the aviation industry achieves a 75% reduction in CO_2 emissions per passenger mile and airports become emission-free by 2050 [1]. The civil aviation develops substantially over the past decades and contributes to around 2% of the global greenhouse gas emission. To limit or reduce the aviation-related climate impact, alternative power source aircraft technology and the more efficient energy infrastructure become necessary measures, as shown in Figure 1-1.

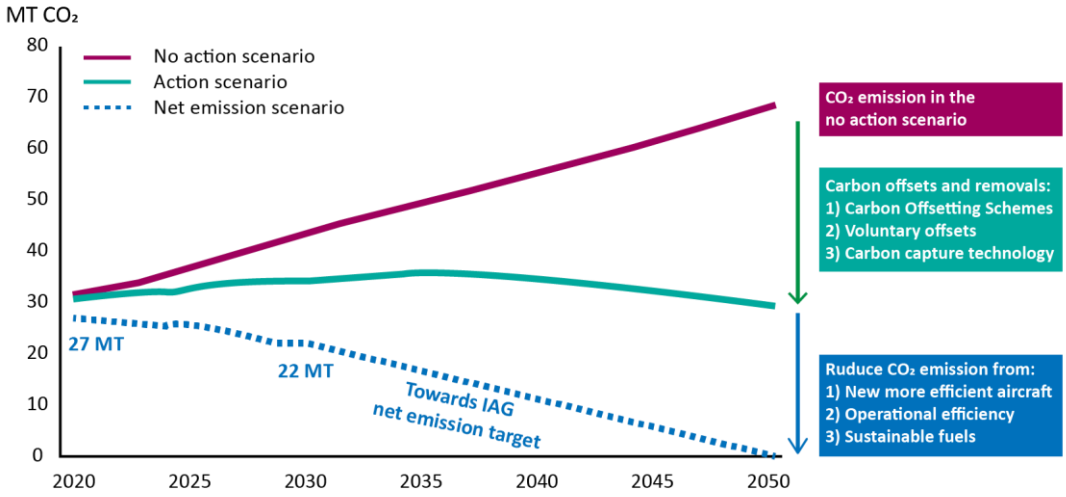

Figure 1-1 International Airlines Group (IAG) CO_2 road-map for global aviation [2]

In recent years, the design innovation of electrically powered aircraft has advanced rapidly with over 200 innovation projects targeting a service date between 2020 and 2030 with some of them already commercially viable. An increasing number of aircraft designers including Airbus, Rolls Royce, NASA, etc., are working on the electric propulsion system for electric aircraft (EA) [3]. EA has been identified as one of the promising approaches to reduce CO_2 emissions and NO_x pollution from aviation industry. EA can be generally classified as fully electric (also known as universally electric), hybrid-electric and turboelectric aircraft. However, due to the limitation of energy density of on-board batteries, fully electric and battery-powered aircraft propulsion system is not

recommended as a high-priority approach for long distance commercial aircraft [4]. For regional and single-aisle aircraft, all-electric and hybrid-electric aircraft propose feasible solutions to utilise electrical energy to reduce fuel burn and emissions. By considering the 20-year projections and state of art development for battery powered electric propulsion technologies, medium-haul routes (1,500 and 4,000 km) are envisioned as viable application scenarios for hybrid-electric aircraft and all-electric aircraft. However, with the electrification of aviation industry, the EA charging will have significant impact on ground energy systems, in particular the extra charging demand and infrastructure. The study in Ref. [5] indicates that the global electricity consumption will increase by 112-344 TWh (0.6-1.7% of 2015 global electricity consumption) if all the short haul flights with 400-600 nautical-mile (nm) are operated by all-electric aircraft. In the UK, additional 1.2-3.6 GW electricity generation capacity is required even if the daily first morning flight is electrified which requires the EA batteries to be recharged overnight. Electric aircraft such as air taxis with 1-4 passengers over a distance of around 100 km require battery specific energy of 200Wh/kg [5]. The existing fast charger (10-50kW) for electric vehicle is not quick enough for aircraft charging (4-20 hours) due to the high-power consumptions of aircraft propulsion system and constrained flight turnaround time. As advancements in fast charging technology continue to unfold, the increasing demand for charging EA batteries may place a significant strain on the existing electrical grid infrastructure [6]. However, the EA charging has potentials to provide grid flexibility through the large EA batteries and their charging infrastructure. In order to eliminate the airport local ground emission of CO_2 and NO_x, the electrification of ground support equipment (GSE) also plays an important role in aviation decarbonisation. Therefore, the ground-side electrification technologies for GSE and the energy management of the airport energy systems are also emerging challenges for both aviation industry and power system [7].

The rapid integration of renewable energy sources and electrification of transportation, including aviation, poses significant challenges to the power grid [8]. These challenges include the need for additional flexibility services, frequency response, and generation capacity. The reduction of system inertia due to the increasing penetration of power electronics-interfaced renewable energy sources calls for the development of innovative solutions to maintain frequency stability and robustness [9].

To address these challenges, this thesis aims to create a new aviation-energy nexus by exploring methods to integrate aviation electrification technologies with the power grid, focusing on grid-side challenges and motivations. The research will consider the increased demand for flexibility services from both the aviation and grid sectors, as well as the integration of aviation electrification with broader transport electrification initiatives.

Motivated by the need to maintain power system stability in the face of low-inertia challenges, the thesis will investigate various technologies and strategies, including novel control methods, distributed energy resources (DER) such as micro gas turbines and electrified transport, and the integration of EA batteries as a potential source of frequency response services. By addressing these grid-side challenges comprehensively, the research aims to contribute meaningfully to both the aviation and power grid sectors, providing valuable insights for infrastructure planning, operations, and grid operators' impacts.

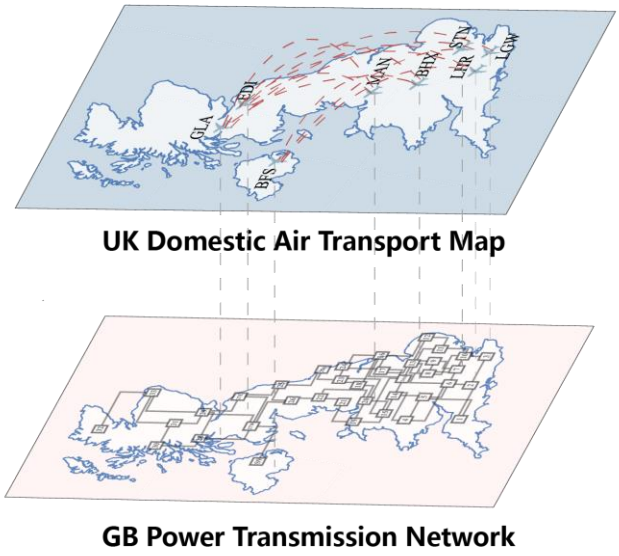

Figure 1-2 The new nexus between major UK airports and GB power network

This thesis presents approaches and frameworks for planning and design the aviation-energy nexus through integrating these aviation electrification technologies into the grid. One example nexus between UK aviation transport and the GB power transmission network is shown in Figure 1-2, where lines and links represent the connections between power system components, such as substations, and aviation infrastructure like airports.

This thesis also presented a novel concept of "Aviation-to-Grid (A2G)", which enables the EA battery charging system to provide ancillary services to the grid when there is a frequency drop event. The A2G concept addresses the emerging nexus between power systems and electrified aviation. As electrification progresses in the aviation sector, it is crucial to integrate these two systems effectively to maintain stability and reliability. A2G enables electrified aviation to provide flexibility and support the frequency of power system while managing its electricity supply and demand.

To effectively implement the A2G concept, electrified aviation must be integrated into ground energy infrastructure. Moreover, power systems must provide sufficient electricity to meet the demands of electrified aviation, and significant charging infrastructure investments are crucial. By addressing these challenges and developing innovative solutions, the A2G concept can help ensure the long-term sustainability and reliability of both the power and aviation industries.

1.2 Research Aim and Objectives

The aim of this thesis is to explore the new nexus between the electricity network and aviation sectors, focusing on the coordinated planning and operation of infrastructure for the electrification of aviation and the integration of airport-based DER. This research seeks to understand the interaction, interdependency, and interoperability between these two sectors, providing a comprehensive framework for their synergistic development. To achieve this aim, the research objectives of the thesis have been defined as follows:

1) A comprehensive review of sustainable aviation electrification technologies, renewable energy and airport demand patterns, and potential technologies for aviation-energy nexus. Identify the research gap in the integration of aviation electrification technologies into power systems.
2) Develop plans and designs of airport microgrids that are capable to accommodate airport-based renewable generation, EA, and parking EVs. Investigate the impact of two different EA charging strategies (plug-in charge and batter swap) on the airport microgrid operation stability and cost.
3) Integrate the electric airport ground support vehicles (e.g., electric airport shuttle buses) into the airport power networks through wireless charging systems. Conduct a

techno-economic assessment of wireless charging systems for electric airport shuttle buses from the perspective of the power system operation.

4) Investigate the impact of energy demand and charging demand from aviation electrification on the power grid, considering flight schedules and other factors, as a crucial and novel aspect of the research.
5) Analyse the volume, capacity, and effectiveness of frequency response services that Aviation-to-Grid can provide to the power grid, examining their impact on frequency nadirs and restoration levels.
6) Assess the role and value of Aviation-to-Grid flexibility, including the quantification of benefits, costs, and revenues associated with providing such services to the grid.

1.3 Major Contributions

Based on the abovementioned research aim and objectives, the principal contributions of the thesis can be summarised as follows:

1) A comprehensive review of sustainable aviation electrification technologies, renewable energy and airport demand patterns, and potential technologies for aviation-energy nexus. The review work helps the readers to understand the technical path of aviation electrification and the research gaps in integrating aviation electrification into the power systems.
2) A multi-objective airport microgrid planning framework for airport microgrid to accommodate parking EVs and EAs. The difference between two different scheduling approaches for charging EA batteries (plug-in charge and batter swap) and the impact of Vehicle-to-Grid (V2G) on the airport microgrid are assessed as well.
3) A techno-economic assessment of wireless charging systems for electric airport shuttle buses through a bi-level hybrid algorithm of (Non-dominated Sorting Genetic Algorithm-III) NSGA-III and mixed integer linear programming (MILP). A multi-agent-based model for airfield shuttle bus transport network simulation is designed based on Anylogic software for generating shuttle bus position and energy consumption profiles.
4) A novel concept of A2G flexibility to provide frequency response services to the GB power system with EA battery charging systems. EA batteries and gas turbines are

controlled coordinatively to provide combined primary and secondary frequency responses to grid disturbance.

5) A deep reinforcement learning (DRL)-based A2G dispatch approach for providing fast frequency response services to the grid. The results of the A2G frequency response are validated based on the reduced GB power system simulations in DIgSILENT PowerFactory.

1.4 Selection Rationale for Study Sites and Data Sources

The choice of research objects for this study, namely airports and the power system, were determined by our research objectives and backgrounds. Specifically, this investigation places a strong emphasis on airports within the United Kingdom (UK) and the Great Britain (GB) power system. Depending on the specific objectives of the research, various airports are chosen as reference points. Middle-sized airports, for instance, are selected when examining airport energy systems with commuting EA or airport electric ground support vehicles. Major airports, on the other hand, are chosen when investigating medium range EA.

In Chapter 4, the focus is on airport microgrids that can accommodate parking EVs and EAs, with the implementation of renewable energy. East Midland Airport was selected as the case study due to its commitment to emission reduction through the adoption of wind power [10]. In Chapter 5, the objective is to explore the wireless charging systems for electric airport shuttle buses. London City Airport was chosen due to its unique layout, where shuttle buses are used to minimise terminal size and maximise aircraft servicing capacity [11].

Chapters 6 and 7 aim to examine Aircraft-to-Grid (A2G) flexibility in providing frequency response services to the GB power system with EA battery charging systems. For these chapters, eight major UK airports are selected for electrification assumptions. The electricity demand data, electricity price data, and flight demand data used in the study are primarily based on data available in 2019. For the projected cases in 2050, flight schedules were forecasted using the method detailed in Appendix C. In consideration of data availability, the electricity prices and frequency response revenues from 2019 were utilized as inputs for the research presented in Chapters 6 and 7.

1.5 List of Publications Arising from the PhD

1.5.1 Journal publications

[J1] **Z. Guo**, J. Zhang, R. Zhang and X. Zhang, "Aviation-to-Grid Flexibility Through Electric Aircraft Charging", *IEEE Transactions on Industrial Informatics*, vol. 18, no. 11, pp. 8149-8159, Nov. 2022, doi: 10.1109/TII.2021.3128252.

[J2] **Z. Guo**, C. S. Lai, P. Luk, and X. Zhang, "Techno-economic assessment of wireless charging systems for airport electric shuttle buses", *Journal of Energy Storage*, vol. 64, p. 107123, 2023, doi: 10.1016/j.est.2023.107123.

[J3] **Z. Guo**, B. Li, Y. Yuan, X. Zhang, "Infrastructure Planning for Airport Microgrid Integrated with Electric Aircraft and Parking Lot Electric Vehicles", *eTransportation*, vol. 17, p. 100257, 2023, doi: 10.1016/j.etran.2023.100257.

1.5.2 Conference Publications

[C1] **Z. Guo**, X. Zhang. Aviation to Grid: Airport Charging Energy Systems for Electric Aircraft, *Proceedings of the 12th International Conference on Applied Energy (ICAE2020), Bangkok, Thailand [virtual]*, 1-10 December 2020, 10 (2), pp. 1-6.

[C2] **Z. Guo**, X. Zhang, Rui Zhang. A multi-agent microgrid *energy* management solution for air transport electrification, *IET Conference Proceedings*, p. 318-324, doi: 10.1049/icp.2021.2351

[C3] B. Li, **Z. Guo**, Y. Yuan and X. Zhang, "Study on the Impact of Aviation Electrification on Voltage Deviation of the GB Transmission System," *2022 57th International Universities Power Engineering Conference (UPEC)*, 2022, pp. 1-6, doi: 10.1109/UPEC55022.2022.9917970.

1.6 Structure of the Thesis

Figure 1-3 shows the flowchart for the organisation of the thesis. The outline of the thesis is provided to summarise the main content of each following chapter:

Chapter 2 - Literature Review

This chapter presents a comprehensive review on the sustainable aviation electrification technologies, renewable energy and airport demand patterns, and potential technologies for aviation electrification. The research gap in the integration of aviation electrification

technologies into the power systems is found through critical analysis of existing literature.

Chapter 3 – Technology Background

This chapter presents a comprehensive overview of the technology behind electrified aviation, emphasising the importance of effective scheduling methods for efficient energy use and proper charging of electric aircraft. The chapter also explores the potential of wireless charging systems for public transportation, specifically focusing on airport electric shuttle buses. The concept of aviation-to-grid is presented as a new nexus between power systems and electrified air transport, highlighting the need for effective strategies to integrate aviation and power systems to provide efficient frequency response services to the grid.

Chapter 4 - The Coordination between Electric Aircraft and Airport Parking of EVs

In this chapter, a multi-objective infrastructure planning framework for airport microgrid to accommodate parking EVs and EAs is developed, and the impact of V2G on the airport microgrid is assessed as well. The dispatch problem of airport microgrid is formulated as a heuristic optimisation problem and the NSGA-II algorithm is adopted to find the Pareto Fronts and optimal solutions. There are two different scheduling strategies for charging EA: plug-in charge and battery swap. The economic and technological assessments for both strategies are conducted and compared. Sensitivity analyses for different EA implementation levels and renewable generation uncertainties are carried out to investigate the cost of future potential investment for increasing the number of EA flights and fluctuations of renewable power output.

Chapter 5 - Infrastructure Design for Airport Shuttle Bus Electrification

In this chapter, the feasibility of wireless charging facilities implemented in the airfield of commercial airport for recharging the electric shuttle buses is evaluated. The input traffic data of airport shuttle buses is simulated from a multi-agent-based model (MABM) based on Anylogic software. To evaluate the techno-economic potential of the wireless charging technology, a hybrid bi-level optimisation framework is presented for seeking the optimal design of proposed wireless charging system. The optimisation approach

combines the multi-objective NSGA-III and MILP algorithm to handle the large number of decision variables and constraints generated from the investigated problem.

Chapter 6 - Power Grid Ancillary Services through Aviation-to-Grid Flexibility

This chapter proposes the novel concept of A2G that utilises EA charging to provide flexibility to the power grid. Smart EA charging system with battery swap method is developed using photovoltaic, gas turbine, and grid electricity. Hourly energy dispatch strategy is produced based on the mixed integer linear programming method to meet electrified aviation charging demand and provide A2G frequency response to the power grid. The A2G frequency response services will be further enhanced by coordinating with airport gas turbines which are primarily used to provide off-grid and high-power charging to the swappable EA batteries. Case studies are conducted in 8 major UK airports considering seasonal flight schedules and power system operation scenarios.

Chapter 7 – Aviation-to-Grid Flexibility through Deep Reinforcement Learning

This chapter proposes a novel DRL-based dispatch approach for EA battery recharging systems to provide FFR services to the power grid with the A2G capability. The feasibility of the proposed approach is demonstrated by a case study conducted in 8 major UK airports and the GB power system and solved with the Deep Q network (DQN) approach. The simulations for the reduced GB power system model were implemented in DIgSILENT PowerFactory.

Chapter 8 - Conclusion and Further Works

This chapter summarises the overall findings of the whole research work and discusses the key contributions of this project and implies some further research directions in the future.

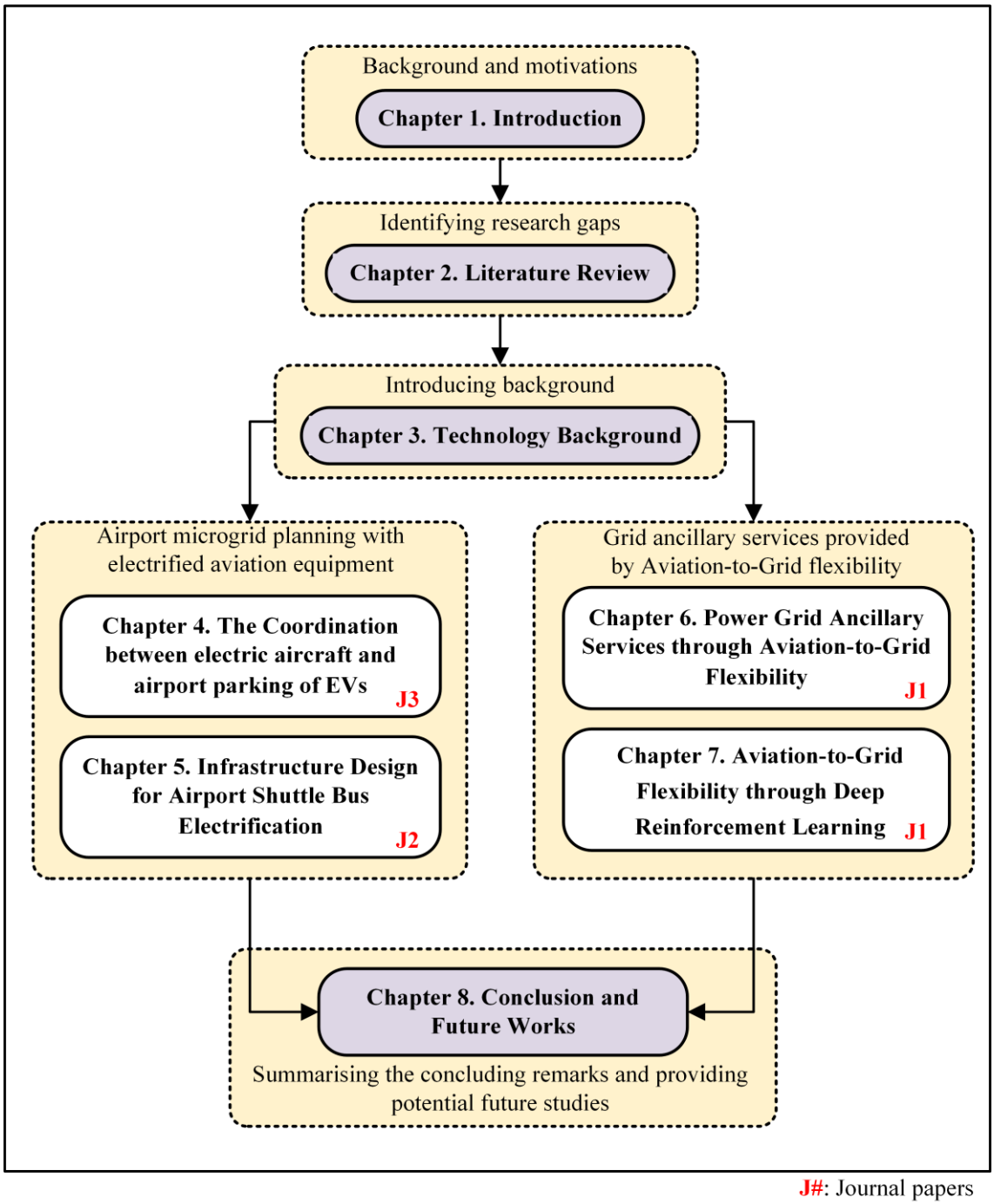

Figure 1-3 Flowchart for thesis structure organisation

Chapter 2 Literature Review

2.1 Introduction

Airports are vital hubs that transport people and cargos in regional, national, and international commerce. Identifying the common energy patterns of airports is essential to solving energy supply problems, adopting advanced new aviation electrification technologies, and introducing innovative aviation-energy nexus into both power and aviation industries. In this chapter, a comprehensive review on the electrification of aviation sector is presented, including sustainable aviation electrification technologies, renewable energy and airport demand patterns, and potential technologies for aviation electrification. A particular focus is placed on examining the existing literature on power system frequency response services and outlining various research projects exploring power system inertia and frequency response services. These projects highlight the benefits and difficulties encountered in maintaining frequency stability in the grid, which is crucial for ensuring seamless integration of aviation electrification technologies. This review will help the researchers to understand the state of the art of the sustainable aviation electrification technologies and to provide a reference for the potential aviation-energy nexus in the future.

2.2 Aviation Electrification Technologies

To achieve net-zero emissions in air transport industry and align with defined CO_2 mitigation objectives in "Flightpath 2050" [12], electrically powered aircraft as part of electrified aviation have become increasingly attractive technologies. In recent years, numerous electric aircraft prototypes for short-haul commuting air transport have been designed, with the majority expected to be deployed in the real airports by 2030 – 2035 [13]. This section presents a comprehensive survey of the current development trends and progress in aviation electrification, examining various aspects of this emerging field.

This section delves into three main areas of aviation electrification: hybrid-electric aircraft, all-electric aircraft, and ground operation challenges for aviation electrification. Each of these aspects plays a vital role in the development and deployment of electric aviation technologies.

Hybrid-electric aircraft utilise a combination of conventional propulsion systems and electric motors, providing a transitional path towards full electrification. All-electric aircraft rely entirely on electric propulsion systems, powered by batteries. These aircraft have the potential to significantly reduce emissions, noise, and operating costs, making them an attractive option for short-haul and regional flights. The successful integration of electric aircraft into the aviation ecosystem also requires addressing various ground operation challenges. As the aviation industry continues to embrace electrification, the environmental and economic benefits of electric aircraft will become increasingly apparent, paving the way for a more sustainable and efficient air transportation system.

2.2.1 Hybrid-Electric Aircraft

Generally, the hybrid-electric propulsion systems can be categorised into two types: series hybrid-electric and parallel hybrid-electric. Series hybrid-electric propulsion systems generate electricity using both combustion engines and batteries, with power delivered to the motor and fan/propeller through converters. In contrast, parallel hybrid-electric propulsion systems directly supply combustion power directly to the fan/propulsor by mounting the gas turbines on a shaft [14].

Most current plans for decarbonising the general aviation sector envision the hybrid-electric aircraft entering service for domestic fleet in the UK by 2030 [15]. Figure 2-1illustrates the technical schematic of parallel and series hybrid-electric aircraft propulsion systems. In a parallel hybrid-electric propulsion system, both gas turbine and a battery-powered motor are mounted on a shaft to drive the ducted fan. This configuration allows either or both power sources to provide aircraft propulsion at any given time during the flight mission. In contrast, in a series hybrid-electric propulsion system, the turbine drives an electric generator, which drives the motor with electricity output. With this design, the electricity generated by the generator can be stored with energy storage units when the electrical output exceeds the required propulsive effort. The primary advantage of the series architecture is that the turbine, not being mechanically coupled to thrust generation, can consistently operate at its optimal power and speed. Furthermore, the simplicity of the concept facilitates straightforward propulsion control.

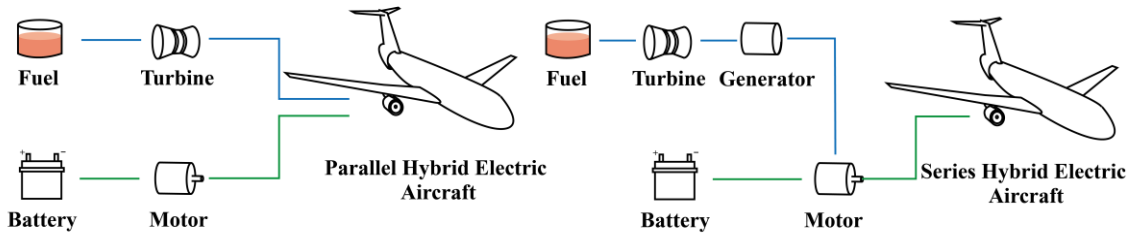

Figure 2-1 Parallel hybrid-electric and Series hybrid-electric propulsion systems

A standard flight mission profile involves all phases from taking off at the origin to landing at the destination, including take off, initial climb, cruise climb, cruise, descent, holding, approach, and landing [16], is shown in Figure 2-2. Batteries in hybrid-electric aircraft not only provide energy for propulsion during one or more flight phases, reducing direct combustion emissions, but also allows for a smaller gas turbine with lower specific fuel consumption and a reduced NOx emission index [5].

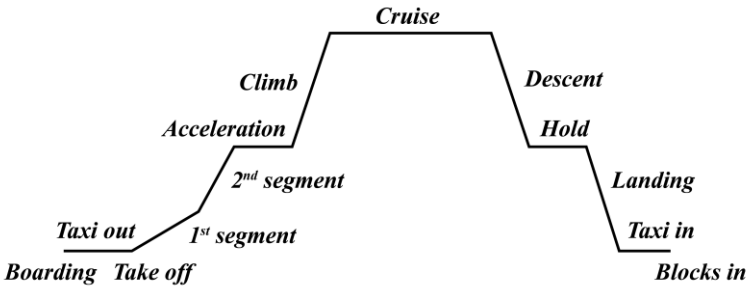

Figure 2-2 standard flight mission profile

2.2.2 All-Electric Aircraft

The all-electric aircraft is the only potential technology emerging in aviation industry that could achieve net-zero emissions [17]. In all-electric propulsion system, batteries are the only power source for the fan/propeller, as shown in Table 2-1. All-electric aircraft is a high-efficiency and economic technology to eliminating the environment impacts of air transport. Eviation Alice is the world's first all-electric aircraft designed to accommodate 2 crew members and 9 passengers with a 900-kWh battery, as shown in Figure 2-3. The prototype has conducted its first flew on 27th September 2022 [18]. This aircraft was ordered by DHL to transport cargos from 2024 [19]. With the electrification of aviation, all-electric aircraft have the potential to reduce aviation's environmental impact significantly. In addition to eliminating various air contaminants, they might also

contribute to resolving the global warming issue. Furthermore, All-electric aircraft (EA) could considerably lower noise with electric propulsion systems, particularly during take-off and landing [20]. In the last few years, Numerous companies are working in a variety of directions to realise the concept of all-electric flight and overcome significant obstacles, including increasing battery energy capacity and proposing novel electric propulsion systems [21]. Electric propulsion systems shows potential for the future of aviation, and further electrification of future aircraft can be foreseen [22].

Figure 2-3 “Eviation Alice” aircraft [18]

The key progress in designing all-electric aircraft to date is shown in Table 2-1.

Table 2-1 Progress in designing and applications of all-electric aircraft to date

Name	Design Remarks	Ref
Airbus E-Fan	2-seat electric aircraft for pilot training, with 60 min flight endurance, FFY: 2014	[23]
Magnus eFusion	2-seat training electric aircraft, serving as a testbed for sub-100 kW electric propulsion system, FFY: 2016	[24]
Siemens Extra 330 LE	2-seat aerobatic electric aircraft, serving as a testbed for 0.25 to 0.5 MW electric motors, FFY: 2016	[24]
NASA X-57 “Maxwell”	2-seat electric aircraft, maximum operational altitude: 14,000 ft, cruise speed: 172 mph, FFY: 2020	[25]
Rolls Royce/YASA ACCEL Project	1-PAX light sport and training electric aircraft, flight range: 200 miles, FFY: 2020	[26]
Eviation Alice	9-PAX commuting electric aircraft, maximum cruise speed: 250 kts, flight range:440 nmi, EISY: 2024	[18]
Easy Jet	100-PAX large commercial electric aircraft, with 1-hour flight endurance, EISY: 2026	[27]
Rolls-Royce/Siemens CleanSky 2 ELICA	19-PAX commuting electric aircraft, flight range: 400nmi, EISY: 2060	[28]

** FFY: first flight year, EISY: enter into service year, PAX: passenger*

2.2.3 Ground Operation Challenges for Aviation Electrification

While the aircraft designers and aerospace engineers are pushing the boundary of the electric propulsion system, little research has been focusing on the energy infrastructure to support the future air transport electrification. While adopting aviation electrification technologies to decarbonise the air transport activities, the attention on common operating problems occurred in airport management should also be paid.

One of the compulsory infrastructures for adopting EA is the high-power EA charging system [29]. The traditional airport consumes a large amount of electricity, and the adoption of EA in the airports will require additional high energy demand. In order to avoid increase the turnaround time of electric flight missions, battery swap technology should be adopted to recharge the EA batteries. Battery swap is a technology that directly swaps the empty batteries from the arrival vehicles with a fully charged battery. The empty batteries will be charged off-board in a scheduled period when the power system is not in congestion. As a result, battery swap is recognised as a flexible charging strategy particularly for large capacity batteries. Battery swap technology has been extensively studied for use in electric public transportation. In most of the existing literatures, the battery swap process is formulated by various linear integer or mixed integer program with different optimisation algorithms to solve this problem. A population-based evolutionary algorithm is proposed to optimise the allocation of distributed generation and battery swap stations [30]. In [31] , an electric vehicle transportation network routing problem is presented with battery swapping stations located in the city. Battery swap is adopted to recharge a fleet of electric commuter aircraft aiming to minimise the operation costs and charging infrastructure expenditures in [32]. The battery swap process is formulated with a state flow model and to assess the operation cost of the battery swap station in [33][34][35].

Another emerging technology to eliminate airport ground emissions is electrified Ground support equipment (GSE), which refers to support equipment in an airport that is adopted to conduct ground services for the aircraft between flight missions. The main duties of GSE include aircraft movement, ground power supply, cargo and passenger loading process, aircraft refuelling, etc. In modern airports, GSE is typically powered by diesel or petrol fuels and becomes a nonnegligible part of airport emission source. One way to cut

airport greenhouse gas (GHG) emission is to adopt zero-emission GSE, such as electric-powered GSE and hydrogen-powered GSE. Most of the GSE that is responsible for easier tasks like catering, transporting passenger and cargos is prone to be electrified, because these GSE can be replaced by electric trucks of similar size [36]. However, tug vehicles are a special type of GSE that is hard to be electrified due to high power requirement of motors. The electric tugs that are responsible to carry the aircraft to taxi-in or taxi-out are called electric taxi (e-Taxi) equipment [37]. In the conventional taxi-out process, aircraft will detach with electric tugs after it has been pushed out. A new taxi-out procedure was introduced in [38] to improve the taxi-out efficiency, which detach the electric tugs and aircraft after carrying the aircraft to the holding point in Figure 2-4.

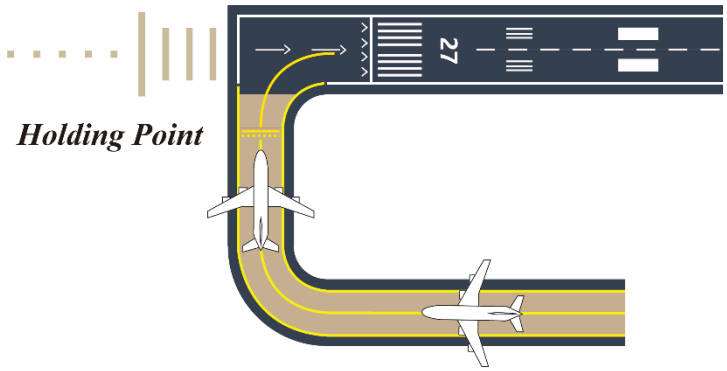

Figure 2-4 Aircraft ground taxi-out process

2.3 Renewable Energy and Airport Demand

Airports are high-energy consumption public transportation infrastructures, requiring significant amounts of energy to support the numerous air transport activities they facilitate. Serving as essential hubs for both passenger and freight transportation, airports have experienced a sharp increase in air transport operations over the past few decades, leading to a significant rise in their energy demand in order to meet the growing air transport requirements [16]. Concurrently, emissions from the aviation industry have continued to grow rapidly. As a result, airport operators are actively exploring strategies to reduce energy consumption and enhance energy efficiency.

In this context, renewable energy resources have emerged as a promising option for supporting airport ground energy systems. By integrating renewable energy resources, such as solar and wind, airports can decrease reliance on traditional fossil fuels, reduce

the carbon footprint, and contribute to the global efforts towards tackling unprecedented climate change challenges. Additionally, incorporating renewable energy systems can provide economic benefits for airports by reducing energy bills and securing a stable on-site energy supply.

2.3.1 Energy Demand in Airports

Airports serve as essential transportation hubs for passengers and cargos, necessitating significant energy consumption for efficient and effective operations. Airports operate like cities that require large-scale public infrastructure to accommodate the vast number of air travellers. The energy demand patterns at airports are influenced by various factors, including air transport activities, weather conditions, and the behaviours of passengers and employees. Consequently, airport energy consumption exhibits nonlinear, stochastic, and dynamic characteristics [39].

Table 2-2 EPI in European airports in 2009 [40]

Airport	EPI (kWh/pax·year)	Airport	EPI (kWh/pax·year)
London (LHR)	13.57	Mallorca (PMI)	3.87
Paris (CDG)	17.93	Munich (MUC)	11.53
Frankfurt (FRA)	15.69	Barcelona (BCN)	6.30
Madrid (MAD)	7.19	Brussels (BRU)	10.90
Amsterdam (AMS)	7.61	Lisbon (LIS)	8.52
Rome (FCO)	7.24	Edinburgh (EDI)	3.95
Istanbul (IST)	8.00	Manchester (MAN)	12.48
Zurich (ZRH)	13.96	Oslo (OSL)	4.31

[*] *the information in this table is not based on recent data and is presented only for illustrative purposes.*

Energy consumption costs comprise a considerable percentage of the total expenses of an airport. For instance, data from 2010 suggests that in the United States, energy bills made up roughly 10% to 15% of overall operation costs at airports [41]. Energy performance indicators (EPI) are utilised as benchmarks for evaluating the energy efficiency of an airport, typically measured on a per passenger basis (kWh/passenger (pax)). Table 2-2 shows the EPI of European airports in 2009, illustrating that the EPI performance does

not have a linear relationship with the size of airport or the number of passengers due to the influence of multiple complex factors [40]. As a result, a detailed study examining the energy demand patterns in different airport areas is crucial for evaluating the overall energy performance of an airport.

Airports can be divided into two main areas based on operational functions, an: the airside and the landside [42]. On the airside, aircraft and related activities are the primary energy consumers. Typical airside traffic operation processes, such as landing, taking off, and directing aircraft to aprons, are shown in Figure 2-5. Several structures and facilities are constructed to organise and control airside operations, including the air traffic control tower, airfield lighting system, firefighting buildings, and hangers [43].

On the landside, air travellers are the most important customers, with their demands prioritised. Passenger-related operations involve organising and controlling passenger flows, baggage, and freight at the terminal buildings. Common land side constructions at airports include terminal buildings, cargo terminals, and airport parking lots. The majority of energy demand at airports is dedicated to supporting activities on both the airside and landside.

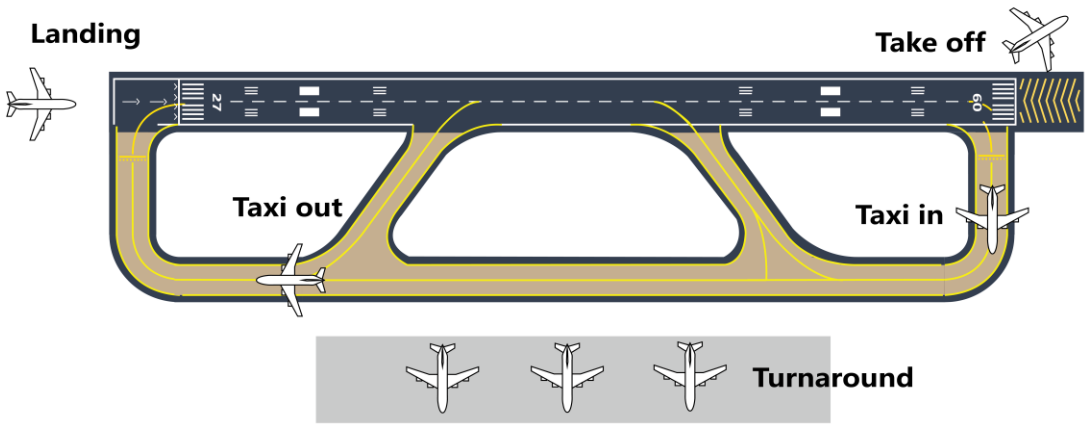

Figure 2-5 Standard traffic pattern in airports [44]

On the landside, the terminal building is the largest energy consumer in the airport, as it serves as a hub for processing passenger and cargo movement activities [45]. A variety of facilities are required to support airport terminal building operations, such as heating, ventilation, and air conditioning (HVAC), information and communications technologies (ICT) systems, and lighting system. With the increasing penetration level of electric

vehicles (EV), more and more customers and airport employees require charging facilities for their EVs. The EV charging demand in airport parking lots is becoming a high-energy consumption facility in airports.

Within the airside of an airport, the majority of energy is consumed by the air traffic control tower, hangers, radio navigation systems, ground support equipment, and the airfield lighting system. Airfield lighting system takes around 7% of the total airport energy demand, which is the largest share of energy consumption within airfield [40]. The amount of airfield energy demand is mainly influenced by the size of the airfield operation areas, because it is proportional to the number of lights installed in the airfield and the airfield operating time. For busy airports, the aircraft usually have to conduct flight missions during night, and the airfield lighting system should be switched on. Moreover, there is a growing trend towards electrifying GSE, such as electric shuttle buses, tractors, and de-icing vehicles, etc. As this technology becomes more widespread, the charging demand for electric GSE will emerge as a significant energy demand within the airfield in the future.

Airport demand is typically determined by considering design peak day (DPD) or design peak hour (DPH) loads, which represent traffic levels exceeded only rarely during a target period [42]. The goal is to ensure airport facilities have sufficient capacity to handle demand at an acceptable level of service throughout the year without overdesigning for extreme peaks. To estimate DPD and DPH loads, planners must carefully analyse historical data to understand seasonal, monthly, daily, and hourly peaking patterns at the airport and use their judgment to predict how these patterns might change in the future. As traffic grows, demand peaking at airports generally becomes less pronounced, and planners must take care to differentiate between peaking characteristics of passengers and air traffic, as well as arriving and departing passengers.

Figure 2-6 illustrates flight schedules in two typical design days at London Gatwick Airport. The provided flight schedules represent hourly flight frequencies for winter and summer over a 24-hour period. Both schedules display a similar pattern, with peak demand occurring during the morning hours, particularly at hour 9. The lowest flight frequencies are observed in the early morning hours (1-6 am) for both seasons. In the

majority of airports, flight demand tends to be significantly lower during the initial six hours of the day.

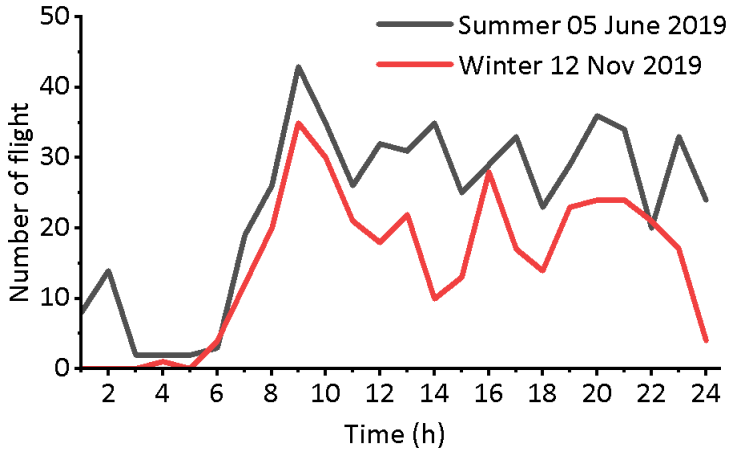

Figure 2-6 Two typical design day flight schedules at London Gatwick Airport

2.3.2 Airport-based Renewable Generation

Renewable energy resources, which are naturally replenishing and almost inexhaustible on a human timescale, including biomass, hydro, geothermal, solar, wind, ocean thermal, wave and tidal [46]. In recent years, airport operators have made significant efforts to minimise the environmental impact by adopting sustainable energy supply technologies. Given that the geographic and structural characteristics of airports, renewable energy resources such as solar, wind, hydroelectric, and geothermal energy technologies are suitable for supplying the energy demand at airports.

Solar Photovoltaic (PV) technology, which converts sunlight into electricity, is increasingly being utilised in airport building rooftops. Airports usually offer large shading-free space, providing an ideal platform for the implementation of solar PV panels. However, the adoption of solar PV energy at airports can raise some safety concerns. In some sunlight conditions (suns position, tilt angle), solar PV panels might cause glare that might reduce the visibility of pilots and air traffic controllers [47]. There are some potential solutions such as glare prediction through computational simulations [48], and setup regulations and guidance on glare assessment [49].

Wind energy has a physical conflict with aircraft. As a result, it is impossible to install a large-scale wind farm near airports. However, wind turbines with height less than 50 m

above ground is in compliance with airspace protection regulations. Alternatively, installing 10 to 20 small-scale wind turbines on the rooftop of airport buildings can also provide renewable energy supply to the airport buildings.

2.4 Airport Microgrids

Renewable energy resources and DER have become promising energy sources due to the increasing requirements on emission reduction. The interconnection of DER has initiated the concept of microgrid which is the aggregation of DER, energy storage units, and loads [50]. In modern present power system and air transport scenario, airports are still one of customers of electricity from the national main grid [10]. However, the airport is also developing DER to provide on-site electrical power generation like other consumers of the grid [51][52]. This trend is making the adoption of microgrids become a reliable and profitable choice. When referring to airport microgrids, the airport facilities include terminal buildings, airport parking lots, airfield electrification utilities and other power consumption elements of the airports should be covered.

2.4.1 Airport Microgrid Infrastructure

A microgrid is a collection of interconnected loads, local energy storage system, energy management system and DER that operates as a single, controllable entity in relation to the grid and is contained within well-defined electrical boundaries [53]. Microgrids can operate in both grid-tied and islanded mode by connecting or disconnecting from the main grid [54]. In order to achieve the connection mode exchanging, the primary infrastructure named Point of Common Coupling (PCC) is required at the connection between the microgrid and the main grid [55].

The PCC allows the airport import or export power according to the situation regarding with technical or commercial conditions. To allow the airport operators effectively control the DER generation and local energy demands, another essential infrastructure, referred to as the Energy Management System (EMS), is required to monitor and control the microgrid [56]. For example, when the electricity generated by solar and wind energy exceeds the real-time airport electrical demand, the EMS will monitor the situation and control the energy storage to store the renewable generation to balance the generation and loads. The most important infrastructure to balance the renewable generation and demand,

especially in the context of the microgrid, is the energy storage system (ESS) [57]. The ESS enables the microgrid operators to store the excessive power generation and discharge power to meet the load when generation is not able to fully satisfy the demand.

There are limited examples of implementing microgrids in commercial airport and other public transport infrastructures.

2.4.2 Airport Microgrid Stability and Resilience

Microgrids offer numerous benefits to airports, including profit generation, locally controlled DER electricity generation, and protection from regional or even national grid failure [58]. This enables airports to maintain air transport operations even during power loss events. Aviation industry experts and airport stakeholders consider four crucial project indicators when evaluating advanced technology adoption: reliability, resiliency, affordability, and sustainability [59]. Microgrids have the potential to achieve all four project metrics while reducing overall costs and carbon emissions.

Airport microgrid stability and resilience play crucial roles in maintaining seamless airport and public transit operations. Reliability is a key concern, as power instability and poor power quality can adversely impact these sectors. For instance, on 17th December 2017, Hartsfield-Jackson Atlanta International Airport experienced an 11-hour power outage, resulting in 1,150 cancelled flights and an inability to serve 30,000 travellers [60]. A fire caused the power outage by cutting off the feeders connecting the airport distribution network to the main grid. Adopting microgrids in airports could prevent such situations. Well-designed microgrids with an advanced energy management and control systems can secure the power supply reliability and stability, enhancing overall airport operations and mitigating the impact of unforeseen power disruptions.

2.5 Power System Frequency Response Services

Power system stability, as described in [61], refers to the capacity of an electrical power network to re-establish a balanced operating state from a specific initial condition after experiencing a physical disruption, while ensuring that the majority of system variables remain within acceptable limits, thus preserving the system's integrity.

One key challenge for power system operators is the real time balancing of electricity generation and demand. The imbalance between generation and load will be reflected in frequency deviation of the power system [62]. The inertia stored in the synchronous generators can reduce the frequency deviation. However, with the increasing penetration of renewable power generation which is expected to reach over 60% in the future GB power grid [63], the system inertia will reduce significantly due to the power electronics-interfaced renewable energy that do not provide conventional inertia to the grid.

Frequency serves as the primary indicator reflecting this balance between generation and load. It is essential to keep the power system's frequency as close as possible to its nominal value, which is 50 Hz for the GB power system. This section primarily concentrates on the aspect of frequency stability and reviews the existing literature on power system frequency response services. The section outlines various research projects exploring power system inertia and frequency response services, highlighting the benefits and difficulties encountered.

2.5.1 Power System Inertia and Frequency Response Services

Essentially, power system inertia represents the capacity of an electrical grid to counteract energy variations stemming from external disruptions [64]. In conventional power systems, this inertia is preserved as kinetic energy stored within the spinning mass of synchronous generators [65].This stored kinetic energy is valuable during major power plant failure events, because it can provide a temporary compensation to the loss of power from the connected generators. The kinetic energy (E_k) of a power system can be expressed as Equation (2.1) [66]:

$$E_k = \sum_{m=1}^{N_m} \left(\frac{1}{2} J_m \omega_m^2 \right) \tag{2.1}$$

where J_m and ω_m denote the inertia (in $kg \cdot m^2$) and the angular speed of the rotor of the m-th rotating machine, respectively. N_m is the number of connected synchronous machines.

The total inertia constant of a power system is determined by calculating the ratio of the total stored kinetic energy (in MJ) to the base power rating (in MVA) of the power system:

$$H_{sys} = \frac{E_k}{S_{base}} \quad 2.2$$

where S_{base} represents the MVA base apparent power of the power system. It is evident that the total power system inertia is contingent on the number of connected synchronous generators and the kinetic energy stored within their rotating mass. Consequently, a decrease in the number of synchronous machines connected to the power system can lead to a reduction in system inertia, making it more susceptible to instability during fluctuations in generation and demand.

The integration of renewable energy resources can bring significant challenges to the power system frequency stability. The power system inertia will be greatly reduced because the renewable energy generators that do not contribute to system inertia is replacing the spinning synchronous generators. In this context, the power system inertia is essential for the future power grids with high penetration levels of renewable energy resources. Therefore, the provision of additional inertia from auxiliary sources may help mitigate frequency deterioration in the future power systems. Consequently, offering inertia support from supplementary sources can play a crucial role in maintaining frequency stability. This additional inertia can be provided by thermal generators, rotating loads, or even wind generators. By designing thermal generators and rotating loads with a higher inertia constant, they can contribute effectively to system stability. Moreover, wind generators have the potential to provide "synthetic inertia" through the implementation of an extra control loop in the wind turbine controller, as demonstrated by several studies [67], [68]. Grid-scale energy storage units can also contribute to inertia support by emulating the mechanical inertia of synchronous generators [66]. Although these technologies have been developed to support power system inertia, existing market mechanisms do not sufficiently incentivize participants to supply such services. This lack of financial encouragement may hinder the widespread adoption and implementation of these solutions.

Given these challenges, the need for frequency response services becomes even more critical. To ensure secure system operation from a frequency performance perspective, system operators must satisfy three key criteria:

- The Rate-of-Change-of-Frequency (RoCoF) must remain within a specific limit

to prevent RoCoF-sensitive relay tripping.

- The frequency nadir, or minimum frequency value, must stay above a designated level to avoid triggering Under-Frequency Load Shedding.
- The quasi-steady-state frequency deviation, identified as the stable frequency value 60 seconds after a power outage, must not exceed a predetermined threshold.

By scheduling specific frequency response services to be activated in case of frequency drops, system operators can maintain frequency within these secure ranges consistently. To demonstrate the mechanism of different frequency response services, here the standard of GB power system is given as an example. The GB power system frequency steady-state limits are 50 ± 0.5 Hz, but normally the operational range of frequency is 50 ± 0.2 Hz [69], as shown in Figure 2-7. It is important to mention that this research is grounded in the state of the GB power system frequency response services as they were in 2019. Modifications or evolution of these frequency services in the future have not been factored into our analysis, and can be found in [70].

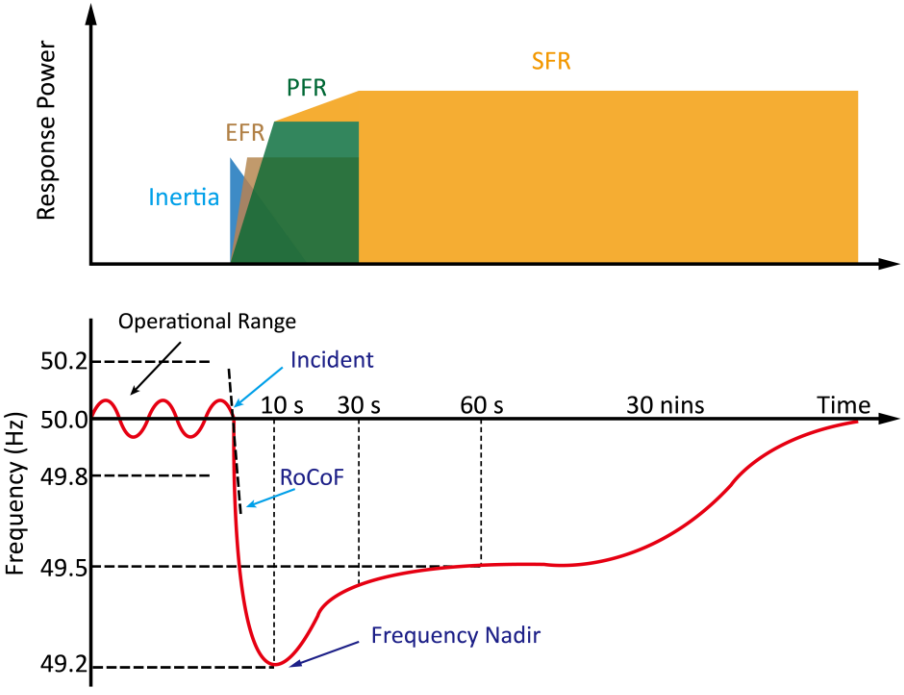

Figure 2-7 Post-contingency frequency evolution and power system frequency control in GB power system, along with different types of frequency response services: inertia, Enhanced Frequency Response (EFR), Primary Frequency Response (PFR) and Secondary Frequency Response (SFR) (National Grid regulation [69])

The initial RoCoF at the beginning of the incident can be expressed as:

$$RoCoF = \frac{f_0}{2H_{sys}} \cdot \frac{\Delta P}{S_{base}} \quad 2.3$$

where ΔP is the disturbance power and f_0 represents the nominal power system frequency. I can be seen that the initial RoCoF is inversely proportional to the level of inertia in the power grid.

A specific fast-responding frequency response service, known as Enhanced Frequency Response (EFR) in the GB, necessitates that service providers respond to power system incidents within 1 second and maintain their response for at least 15 minutes after the incident occurs [71] [72]. When the frequency deviation surpasses the 'trigger level' set point (49.7 Hz), primary (PFR) and secondary frequency response (SFR) services are deployed to restore the system frequency to its normal operational range. PFR serves to prevent the frequency nadir point (occurs at least 20 seconds) [73] [74] from falling below the Infrequent Infeed Loss Risk (defined as below 49.5 Hz) [75], while SFR aims to bring the frequency back to operational points (at least 30 minutes) [76].

Currently, frequency response services are predominantly provided by conventional generation units [77], although energy storage units are emerging as increasingly important contributors. As the penetration of renewable power generation increases and replaces traditional synchronous machines, system inertia will significantly decline due to fewer synchronous machines containing rotational kinetic energy [78]. Consequently, the real-time balancing mechanism will necessitate supplementary frequency response services from new, flexibility-enabled energy sources [79].

2.5.2 Future Low-inertia Challenges and Solutions

As discussed in previous sections, the increasing penetration of renewable power generation is replacing conventional synchronous machines, significantly reducing system inertia due to the decreased presence of synchronous machines containing rotational kinetic energy [78]. Consequently, new and additional frequency response services are urgently required for frequency stability in a low-inertia power system [79].

Various frequency control methods have been proposed to address these challenges. For instance, a novel tuning method has been introduced, enabling a fuzzy hierarchical control

structure to supplement conventional control and improve power system stability and robustness [80]. Furthermore, DERs have been investigated as potential sources of frequency regulation services. One major type of future DERs, micro gas turbines, could provide firm frequency response services [81]. Advanced gas turbine technologies have been developed, improving ramp-up rates, start-up rates, and compliant load to enhance their frequency response capabilities.

Electrified transport is emerging as an attractive DER for providing ancillary services to the power system, including frequency response services. Research indicates that electrically powered GB trains could provide response power ranging from 300 MW to 850 MW to the power system [82]. With the higher penetration level of electric vehicles, the GB power system has introduced a new frequency response service called fast frequency response (FFR) [83], which requires idling battery energy storage systems to reserve power to prevent power loss issues [84].

In the context of aviation, electrified aviation technologies have become an attractive solution for achieving emission reduction goals in the industry. When adopted in airports, these technologies will connect to the grid as potential DER flexibility resources through charging systems, forming a new aviation-energy nexus. However, managing the FFR reserve power and EA battery recharging schedule simultaneously requires a smart scheduling dispatch approach, as the price of FFR will interact instantaneously with the EA battery charging systems.

In summary, various technologies and strategies have been proposed to tackle the challenges of low-inertia power systems. These include novel control methods, DERs such as micro gas turbines and electrified transport, and the integration of EA technology as a potential source of frequency response services. As the aviation industry continues to electrify and renewable energy sources become more prevalent, innovative solutions must be further developed and implemented to maintain power system stability and robustness in the face of low-inertia challenges.

2.6 Conclusions

In this chapter, a comprehensive review of aviation electrification, airport energy demand, and airport-based renewable energy resources is presented, along with an in-depth exploration of power system frequency stability.

The identified research gap in the integration of aviation electrification technologies into the power systems not only covers the general interactions, but also specifically includes an exploration of the technological details of interactions between EA and EVs in airport parking, as well as the planning and design of wireless charging systems for electric airport shuttle buses. Furthermore, the investigation extends to the provision of Aviation-to-Grid frequency response services. The decarbonisation of aviation and the grid can be enabled simultaneously by adopting emerging Aviation-to-Grid technologies, including EA charging systems, wireless charging technology for GSE, and V2G from parking EVs. A particular focus is placed on examining the existing literature on power system frequency response services and outlining various research projects exploring power system inertia and frequency response services. These projects highlight the benefits and difficulties encountered in maintaining frequency stability in the grid.

In the following chapters, we will further investigate deep reinforcement learning approaches for dispatching EA charging systems, the interactions between EA, airport parking EVs and airport-based renewable energy resources, the planning and design of wireless charging systems for electric airport shuttle buses, as well as the practical implementation of frequency response services in the context of aviation electrification technologies.

Chapter 3 Technology Background

3.1 Introduction

This chapter provides a comprehensive overview of the technology backgrounds for electrified aviation. Section 3.2 focuses on the microgrid architecture and presents two EA charging scheduling methods. This section discusses the need for effective scheduling methods to ensure the efficient use of energy resources and the proper charging of electric aircraft. This section also presents the airport parking EV scheduling approach that can coordinatively interact with EA charging system. The Section 3.3 presents a dynamic wireless charging system for airport electric shuttle buses. This section discusses the technology behind wireless charging and its potential as a solution for the electrification of public transportation systems. The Section 3.4 explores the Aviation-to-Grid concept and its potential as a new nexus between power systems and electrified air transport. This section highlights the importance of developing effective strategies for integrating aviation and power systems to provide efficient frequency response services to the grid.

3.2 Airport Microgrid Architecture with EV and EA

3.2.1 Introduction to Microgrid Architecture with EV

In recent years, many research studies are conducted on microgrid for electrified transportation, particularly concerning the integration of EVs and renewable energy sources. As mentioned in the literature review, various studies have focused on different aspects of microgrids and their potential applications.

Existing energy system research work is mainly focused on the optimal design of energy systems with energy resource integration, and various novel techniques have been increasingly implemented on both the demand and supply side of energy systems [85][86]. To determine the potential of integrating electric vehicles (EVs) to the grid, [87] proposed a multi-agent system to simulate the operation of an energy hub with EVs and integrated a novel dispatch algorithm into the charging strategy, considering varied penetration levels and charging patterns of EVs.

In recent research, electrified airports present an attractive application case for integrated energy systems. In [88], Sensitivity analyses of critical system parameters including a wide variety of uncertainties were conducted to inform the design of an integrated energy system with 5 integration scenarios for an electrified airport. Additionally, the study analyses the financial and environmental benefits of integration. [89] investigated the integration of EVs into an electrified airport energy system.

The microgrid is an emerging framework for adopting distributed energy resources. Microgrids can be classified into two categories: island microgrids and grid-tied microgrids. Island microgrids operate independently from the main grid, while grid-tied microgrids are connected to the main grid [50]. [90] investigated microgrid integration at maritime ports and developed a holistic framework to evaluate the benefits of microgrid adoption in addressing challenges in the ports and generating economic and social value through comprehensive planning. [91] adopted a coordinated scheduling model for microgrids with hydrogen fuelling stations, taking multiple uncertainty variables into account. By addressing power generation and system load uncertainty using a data-driven chance-restricted method and electricity pricing uncertainty using a distributionally robust optimisation strategy, the study aimed to create a more robust and efficient microgrid system. [92] developed an integrated energy system with a hydrogen station considering hydrogen generation and storage processes, whilst a sensible power to heat and hydrogen model with various constraints is also proposed, and generation-load uncertainties are addressed using random and robust optimisation methods. [93] proposed a multi-agent stochastic programming model for optimal design and dispatch of an energy system, where the influence of the uncertainties on energy system is also investigated. In the work reported in [94], to enhance the flexibility of the energy system, a model for a set of energy hubs is established and the bi-directional energy flows between energy consumer and the main grid are also analysed. [95] presented a multi-energy system for a microgrid with renewable coupled with a hydrogen fuel cell system and proposed a power management strategy to reduce the fluctuations of wind generation. In [96], a genetic algorithm-based multi-objective optimisation technique is implemented to solve a multi-agent system framework for achieving flexible demand response in low-voltage distribution networks. [97] proposed a bi-level optimisation approach for day-ahead operation management of a building-level integrated energy system with potential

benefits provided by the energy storage system, which proves the potential benefits provided by energy storage. In [98], a steady-state model of an energy system with multiple energy resources had been established, which considers the electricity-gas-thermal coupling interaction characteristics. Generally, the integration of sophisticated and novel technology is critical for energy system transitions. These real-world case studies have demonstrated the numerous economic and environmental benefits of integrating energy systems with renewable energy sources and hydrogen energy systems may deliver.

The existing research has demonstrated the numerous economic and environment benefits of integrating microgrid with renewable energy resources, hydrogen energy systems, and EV charging systems. However, there is still a gap in research when it comes to airport microgrid planning for adopting EA. This thesis will focus on exploring the flexibility potential of EA charging demand to participate in the operation of the airport energy system, enabling airports to further enhance their sustainability and efficiency.

3.2.2 Charging Infrastructure for EA

The development of charging infrastructure is a critical aspect of incorporating EA into commercial airports as part of aviation electrification. A few studies have explored EA charging systems and their potential benefits. In [99], a multi-agent real-time microgrid energy scheduling solution was designed to address the stochastic electric aircraft charging requirements of electrified air transport. Optimal airport charging infrastructure for EA is investigated in [100], where battery swap and plug-in charging systems are proposed and compared in terms of charging schedule flexibility, costs, and revenue with different EA penetration levels. In that case, the adoption of V2G and A2G technology could offer not only socio-economic profits (emission free and lower energy costs) but also operational benefits by providing services to the grid.

While there are limited existing works focusing on the EA charging infrastructure planning, charging system designs for heavy-duty electric trucks can serve as alternative references for adopting EA in airports. The smart charging system for heavy EVs designed in [101] achieved a 46% reduction in monthly cost compared to the uncontrolled charge scenarios. In [102], the battery swap strategy for charging heavy electric trucks was proved to be a more economical solution under medium recharge distance.

However, the existing research predominantly examines EA charging systems independently from EV energy systems, without combining the flexibility of EA and EV charging systems to support energy system operation. Moreover, the comprehensive evaluation of different charging strategies (plug-in charge and battery swap) for EA has not been investigated with a focus on their impact on power system operations.

Figure 3-1 illustrates two distinct charging scenarios for EA based on the analysis of existing literature: plug-in charging and battery swapping. In the plug-in charging scenario, EA is directly connected to the busbar through dedicated chargers, facilitating power transfer for recharging their batteries. On the other hand, the battery swapping scenario involves EA exchanging depleted batteries with fully charged ones at a battery swap station. The swap station, in turn, connects to the busbar through chargers to recharge the depleted batteries. These two strategies showcase alternative methods for maintaining the energy requirements of electric aircraft while considering their potential impact on power system operations.

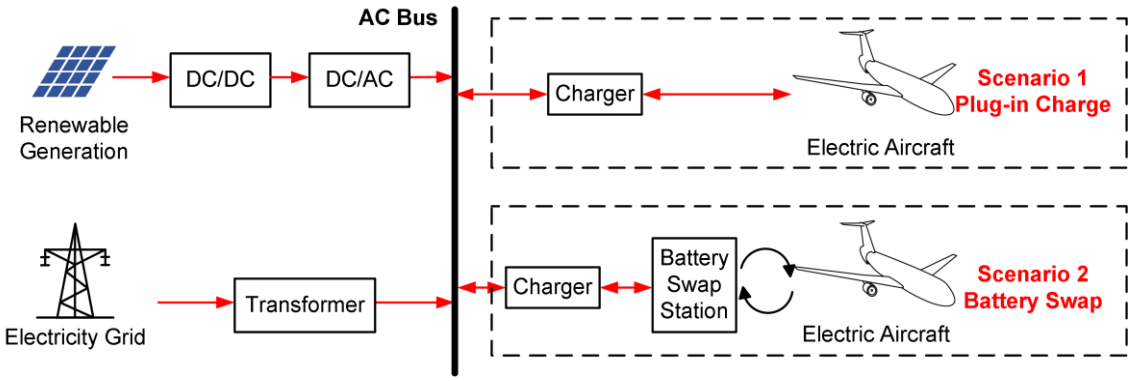

Figure 3-1 Electric aircraft charging scenarios (plug-in charge and battery swap)

3.2.3 EV Charging and Vehicle-to-Grid Technology

Vehicle-to-grid (V2G) technology presents new opportunities for value-added services in EVs, enabling efficient and seamless operation of power generation and distribution factors. [102] proposes a model that classifies EVs into distinct clusters based on their state of storage charge (SoC) and dwell time, helping meet the electrical demands of the main grid while utilising the flexibility potential of EVs. A robust optimisation approach is used to analyse the optimal procurement strategies for the microgrid under worst-case scenarios of electricity price uncertainty.

[103] suggest an optimising strategy for energy system planning that incorporates V2G technology into integrated energy systems. The benefits of V2G on energy system design are evaluated using a modified Non-dominated Sorting Genetic Algorithm- II (NSGA-II) algorithm. An electric vehicle charging dispatch optimisation model based on the NSGA-II algorithm is constructed in [103], considering demand-side response service participation and the impact of uncertainties of renewable generation resources and demand. The results indicate that the NSGA-II algorithm is an effective algorithm for solving multi-objective energy dispatch problems. [104] proposes an intelligent energy management system to optimise emissions, energy costs, and battery SoC based on the NSGA-II algorithm, contributing to a more cost-effective and environmental-friendly power supply. The benefits of adopting EVs in energy systems are also witnessed in [105]. Additionally, with advancements in battery and charging technology, electrified aviation and bi-directional power exchange between the main grid and airport energy management systems could provide greater flexibility for both airport microgrids as well as the main power grids.

[106] review the concepts of G2V (EVs operate as electrical loads) and V2G (EVs operate as distributed energy storage), examining the future development trends of EV grid integration and analysing both the positive and negative impacts of EV integration on the grid. In [107], to support the consumption of wind energy and ensure a robust system, EVs are introduced in V2G mode as both a load and a source, and a multi-agent optimisation scheduling model is adopted with the worst-case strategy. In [108], a multi-objective model for EVs management system in consideration of EVs travel pattern and V2G capability is constructed. The adopted scheduling strategy is evaluated over a 24-hour period on a 33-bus distribution test system. [110] investigated the financial benefit of the interaction between EVs and the electrical grid and found that the overall electricity costs could be reduced by adopting V2G technology. In consideration of battery life, [109] investigated the influence on EV batteries of adopting V2G technology and proposed a battery degradation model based on long-term ageing data. The model was tested using multiple real-world usage cycles. In [110], battery degradation is also included in the objective functions, the authors proposed a stochastic model for battery management and EVs charge/discharge power in V2G strategies and investigated the economic benefit of V2G implementation in active distribution networks.

To utilise V2G functionality of the plug-in EV, a charging and discharging strategy are developed in [111], considering the limited EVs battery capacity and reverse power flow induced by excess PV energy. [112] developed a V2G aggregator dispatching strategy with two calculation modules to calculate the SOC of the battery and optimise the financial benefits of the aggregator for its performance in frequency control services. In the work reported in [113], considering the potential battery degradation cost, an energy management strategy for integration of EVs with V2G into the operation of grid-connected microgrids is developed based on the forecast accuracy of various variables. Previous works have focused on the formulation of the V2G strategy, however, there remains a need for an efficient approach to plan for the airport microgrid integrated with EA and Parking EV.

V2G technology offers opportunities for efficient power generation and distribution, as well as value-added services in EVs. Various studies have proposed models and strategies to optimise energy system planning, EV management systems, and charging dispatch, considering factors such as battery life, economic benefits, and renewable resource uncertainties. The integration of electrified aviation and bi-directional power flow between the main grid and airport energy management systems could enhance flexibility for both airport microgrids and main power grids. Although previous research has focused on V2G strategy formulation, there is still a need for efficient planning approaches for airport microgrids integrated with electrified aviation and parking EVs.

3.2.4 Coordinative Interaction with Airport Parking EV

In the context of future airports, the adoption of charging infrastructure to support EA and EV is expected to significantly increase energy consumption. This increase in energy demand results in a supply gap that can be addressed by incorporating a high penetration of DER. To effectively manage the electric load of the airport building, EA and EV charging loads, the hydrogen systems, PV and wind turbines (WT), an airport microgrid system is proposed.

The architecture of airport microgrid system is shown in Figure 3-2, which is designed to provide a comprehensive energy management solution for airports, integrating a diverse range of renewable energy and DER. to optimise the energy supply and consumption within the airport. The proposed airport microgrid system can potentially foster greater

flexibility in energy management, facilitate the integration of renewable energy sources and promote the transition towards a more sustainable and environmentally responsible aviation industry.

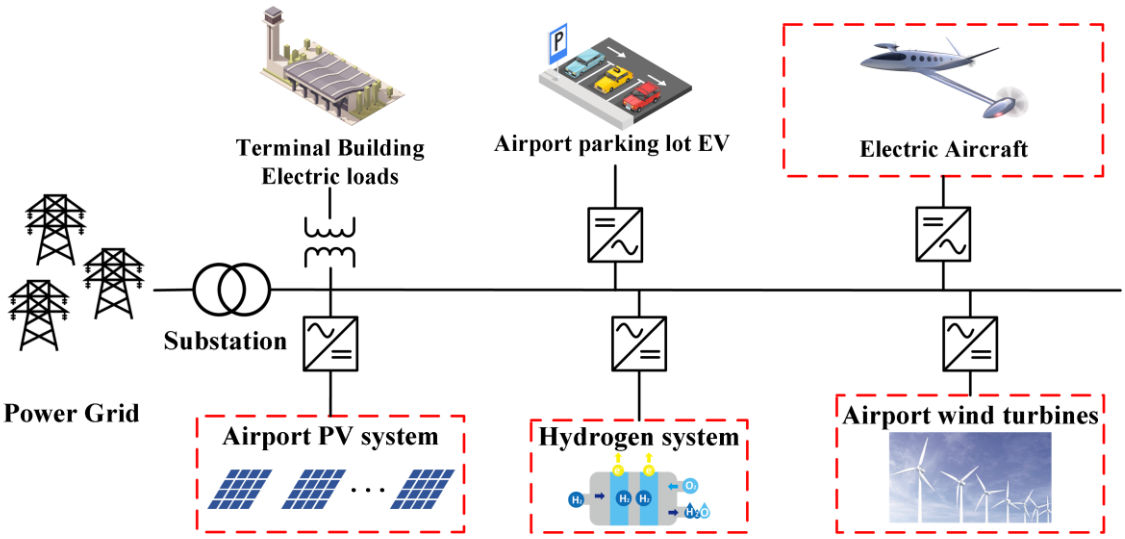

Figure 3-2 Airport Microgrid architecture

This thesis proposes an architecture of airport microgrid system involves various components that interact with each other to manage the energy consumption of the airport building, EA and EV charging loads, PV, hydrogen systems, and micro-WT. The PV, micro-WT, and hydrogen systems are adopted as distributed energy resources for the microgrid, while the terminal building electric loads, parking EVs, and electric aircraft represent the loads.

To enable interactions between the airport microgrid and the main power grid, a substation connects the two systems. This connectivity ensures that the airport microgrid has access to the main grid's power supply and can also supply excess energy back to the main grid. This bi-directional power flow not only provides a more secure energy supply for the airport but also helps reduce demand congestion on the main grid, especially during peak hours of electricity demand and flight missions.

Another advantage of adopting a microgrid in the airport is its ability to operate in an islanded mode. In case of a power outage or disruption in the main grid's electricity supply, the airport microgrid can continue to operate independently and provide uninterrupted power supply to critical airport operations with adequate protection and power balance.

Gas turbines are commonly used as distributed generation resources in airport energy systems. However, many airport operators are now striving for carbon neutrality and emission reduction [114]. To achieve these goals, the hydrogen system is a promising alternative to decarbonize airport energy systems and reduce ground carbon dioxide emissions. In this context, the proposed airport energy system assumes the existence of on-site hydrogen fuel cells with an external hydrogen supply, replacing the fossil fuel generation system. This means the airport operator will purchase hydrogen from the external supplier based on day-ahead energy dispatch results every day. The hydrogen system consists of the hydrogen storage tank and fuel cell, acting as a distributed generator in the airport energy system.

In summary, the proposed airport microgrid system offers a decentralized energy generation approach that guarantees energy security, reduces demand congestion on the main grid, and enables the airport to operate in an islanded mode, providing a more reliable energy supply for critical airport operations.

3.3 Dynamic Wireless Charging System for Airport Electric Shuttle Buses

3.3.1 Introduction to Wireless Charging Technology

As transport electrification emerges as a crucial strategy for reducing emissions and mitigating pollution, the methods for recharging EVs have become a popular research topic [106][115]. However, in underdeveloped areas where charging facilities are inadequate, the scarcity of charging infrastructure for EVs away from home emerges as a significant challenge. Wireless power transfer technology employed in EV charging could help overcome the limitations of wired charging infrastructure, as it does not require a physical connection between the power supply and EVs [116]. The technology enables EV charging both when stationary and in motion by installing wireless chargers underneath the ground surface and pick-up devices on EVs [117].

Wired EV charging systems are a mature technology with established standards [118]. These systems necessitate a physical (ohmic) connection between EVs and the power grid through electric circuits, comprising the AC-DC rectifier and DC-DC converters or a converter with power factor correction circuits that directly transition from low-frequency

AC to high-frequency AC. Wireless charging infrastructure can be categorised based on the operational status of EVs during charging into three groups: 1) static wireless charging (SWC); 2) quasi-dynamic wireless charging (QWC); and 3) dynamic wireless charging (DWC) [116][119].

SWC refers to charging EVs when they are stationary [120], typically installed in public parking areas and residential garages. SWC has a higher efficiency of power transfer than DWC due to improved alignment [121]. Although SWC requires a designated stationary parking area to charge the battery of the EVs. It eliminates the need for human intervention during the automatic charging procedure, which is especially beneficial for individuals with disabilities. The primary technological advantage of SWC over wired EV charging technology is the elimination of shock hazards caused by wired chargers [122]. Amongst the three types of wireless charging technologies, SWC achieves the highest efficiency of 95% due to the enhanced alignment between EV pick-up devices and wireless charging coils [123].

DWC technology means charging the EV when it is in motion [124] [125]. This technology eliminates the need for EVs to stop and wait for charging, thus their travel range can be extended [116]. DWC technology addresses many issues of EVs, including range anxiety and battery cost. Like SWC technology, the power transfer between power supply units and EVs relies on the magnetic coupling effect between the transmitter coils buried underground and the EV pick-up device. A research team at the Korea Advanced Institute of Science and Technology (KAIST) has led the development of DWC technology and has installed a dynamic wireless charging system for passenger buses [126]. An optimisation framework based on the genetic algorithm was proposed in [127] for designing the operation velocity profile of electric buses. [128] proposed a flow-capturing location model for designing the optimal location of wireless charging facilities that could maximise the demand-supply coverage. A comprehensive optimisation approach for designing dynamic wireless charging pads for EVs is presented in [129].

QWC is defined as EVs being charged when moving at low speeds or stopped at stop-and-go positions [130]. Potential implementation locations for QWC include traffic lights, bus stops and taxi parking stands. The KAIST research group has tested a wireless charging system that charges electric buses at lower power levels while in motion and at

high power at bus stops [116], demonstrating the potential of QWC to further improve the range of electric buses. [131] developed a novel user equilibrium model to illustrate the travel choices of electric vehicle drivers when wireless power transmitters are installed. In [131], the trade-off between vehicle speed and travel time is captured because higher speeds make the wireless charging less efficient than lower speeds. If more wireless charging infrastructure is implemented, it could lead to an increase in customers choosing to buy EVs. This, in turn, could subsequently increase the number of dynamic charging EVs on the traffic networks [132]. The impact of different traffic scenarios (motorway, highway, and urban stretch) on wireless charging power for an ordinary EV with 24 kWh battery is compared in [133]; the results reveal that the EVs can be recharged on average at 0.6 kWh/km in the urban stretch and 0.25 kWh/km on the highway. The financial feasibility of DWC system has been examined in [134] for Auckland motorway, offering critical decision support for DWC implementation to stakeholders. [135] assessed the impact of DWC implementation on realistic driving patterns.

In summary, wireless EV charging technologies, including static, quasi-dynamic, and dynamic wireless charging, offer potential solutions to address the challenges associated with wired charging infrastructure. Each type of wireless charging technology has its unique advantages and application scenarios. While SWC is optimal wireless charging solution for stationary charging with the highest efficiency, QWC can be employed at low-speed or stop-and-go positions, and DWC can charge EVs while in motion, extending their range and reducing range anxiety. These innovations in wireless EV charging technology could significantly improve the overall adoption and usability of electric vehicles, contributing to a greener and more sustainable transportation system.

3.3.2 Potential of Bidirectional Wireless Charging

Similar to the V2G concept of plug-in EVs, an emerging technology known as bidirectional wireless power transfer technology will potentially achieve V2G flow remotely between EVs and the power system. [138] reported the development of a large air-gap bidirectional wireless charger without an additional current chopper. [139] and [140] compared V2G power flow based on wired and wireless charging infrastructures. The results show that the connectivity provided by EVs with wireless connection to the grid is higher than that of wired connectivity [136], because the wireless charging

infrastructure could detect the condition of EVs automatically through wireless communication devices [116]. The methodologies that enable long-term, mid-term, and short-term traffic-power network modelling and management have been reviewed in [137]. The design of a bidirectional 20 kW wireless charging system with an air gap of 11 inches is presented in [138]. A heuristic optimisation approach based on a chicken swarm algorithm for designing simply reachable charging stations for EVs is proposed in [139]. The potential of future deployment of bidirectional wireless charging facilities that will enable the EVs to charge and discharge wirelessly in regional road traffic networks is investigated in [140], which reveals that the individual entity building up the wireless charging infrastructures should be responsible for both traffic network and power network, e.g. the government agency and airport designers and operators.

3.3.3 Wireless Charging System for Airport Electric Shuttle Buses

One of the potential application scenarios of wireless charging technology is the charging system of airport ground support vehicles. These vehicles are normally powered by gasolines and diesel engines, which would contribute to the airport ground emissions. According to the goal set up by Flightpath 2050, the elimination of airport ground emission is a high priority of airport operators [1], and the ambitious target towards electrifying airport ground support equipment is attracting widespread interest [141]. In response to the aim for carbon emission reduction in aviation industry, an increasing number of commercial airports have adopted electric vehicle fleets replacing gasoline vehicles to eliminate airfield ground emissions [142]. However, the availability of space on airfields is limited due to the high intensity of airport movement, which makes it difficult for electric ground support fleets to stop and recharge at stationary facilities during busy hours. This frequent plug-in and plug-out activity reduces the efficiency of airfield ground transportation.

Therefore, one of the challenges of electrifying these ground support vehicles is the limitation of space in airfield to install charging infrastructures while the demand of ground support tasks is high [143]. Simultaneously, the airport operation has a dramatically high demand in ground support tasks, which means pre-scheduling for the vehicle charging can be challenging. The wireless power transfer technology will enable the power supply for airport ground support vehicles when they are moving to conduct

tasks through installing wireless power transmitters underneath the airfield [144].

Currently, electric airport ground vehicles used on airfield ground operations are mainly scheduled to charge during off-peak hours [88]. To maintain full day's flight mission demand, significant battery capacities are required on these vehicles, which can result in excessive weight and associated costs. To address the limitations of space and time schedule conflicts and to avoid excessive battery weight and costs, wireless charging systems becomes a promising technology.

Wireless charging systems offer a dynamic approach that allows electric fleets to recharge their batteries while in motion and performing tasks, without requiring them to stop at a stationary position. Importantly, this approach significantly reduces battery weight and improves overall efficiency.

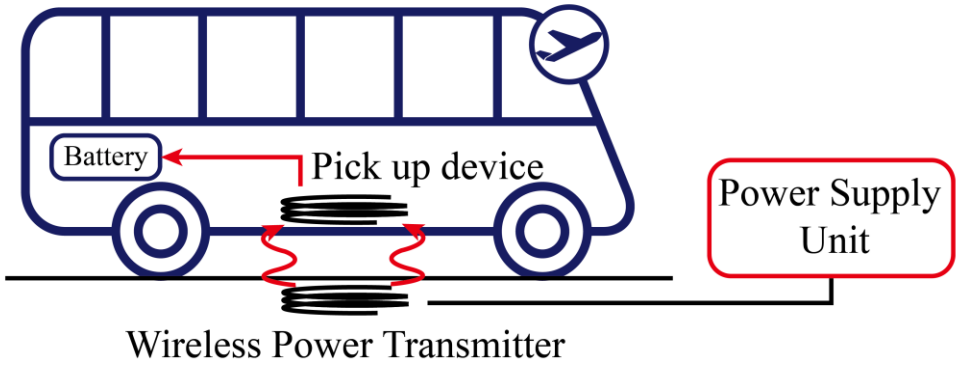

Figure 3-3 Framework of dynamic wireless charging for airport shuttle bus

The technology framework depicted in Figure 3-3 comprises wireless power transmitters (WPT) embedded beneath the ground and a power pick-up device installed on the electric shuttle bus. The WPT coils require a power supply unit (PSU) to convert power from the distribution network. As the electric shuttle bus travels on a road equipped with a power transmitter, the WPTs produce a high-frequency current that generates a magnetic field following Ampere's Law. The magnetic field in turn generates a high-frequency current in the coils of the pick-up device following Faraday's Law. The current is then rectified to charge the battery of the shuttle bus.

The thesis proposes a cutting-edge smart dispatch framework that seamlessly integrates the airport transportation network with the distribution network, employing wireless

charging systems for electric airport shuttle buses, as illustrated in Figure 3-4. At the core of this framework lies the Air Traffic Coordinator, which serves as a central hub for managing and processing crucial information from various sources, including grid-side load flow data, electric shuttle bus location information, and air transport details. By consolidating and analysing these diverse data streams, the Air Traffic Coordinator effectively monitors and optimises the charging policies of the electric shuttle buses. This real-time coordination ensures that the shuttle buses operate at peak efficiency. The implementation of this smart dispatch framework ultimately enhances the overall operational efficiency and sustainability of the airport transportation network, paving the way for a more resilient, eco-friendly, and intelligent transportation ecosystem.

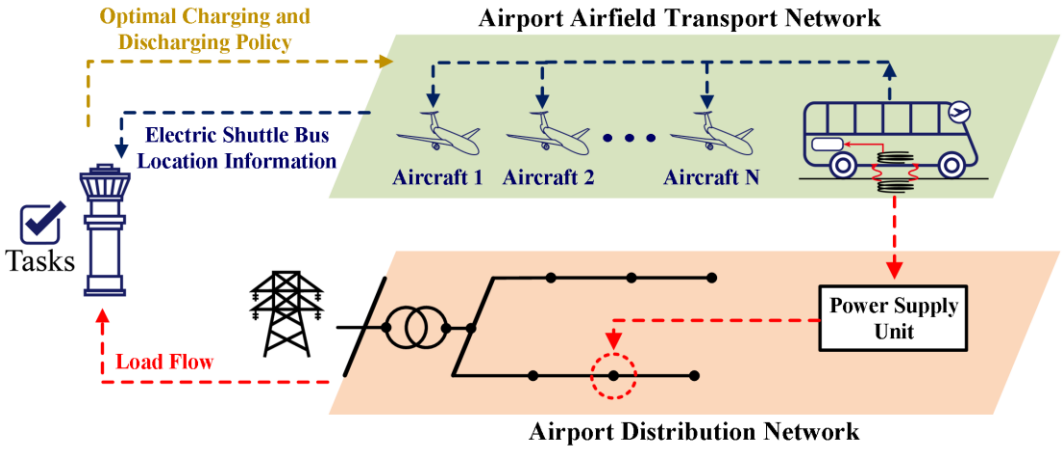

Figure 3-4 Smart dispatch framework for the airport transportation network and distribution network combining by wireless charging systems for airport electric shuttle buses

3.4 Aviation-to-Grid through EA Charging

3.4.1 Nexus between Aviation and Power Systems

Based on the reviewed aviation electrification technologies, there will be more distributed energy resources installed at airports. The aviation industry will be deeply connected with the power grid. As a result, a new nexus between aviation and power systems is emerging. The concept of the nexus between aviation and power systems refers to the fundamental relationship between the two systems, where aviation relies heavily on power systems for its operation, and power systems rely on aviation to a lesser extent as a consumer of electricity. In recent years, the electrification of aviation has led to an increased

dependence on power systems to provide electricity to the emerging fleet of electric aircraft.

The integration of aviation and power systems has become more critical as electrified air transport systems have been developed. This integration is crucial in ensuring the stability and reliability of both systems. As electrified aviation continues to grow, the power system must be capable of meeting the increasing demand for electricity while maintaining a stable supply of energy.

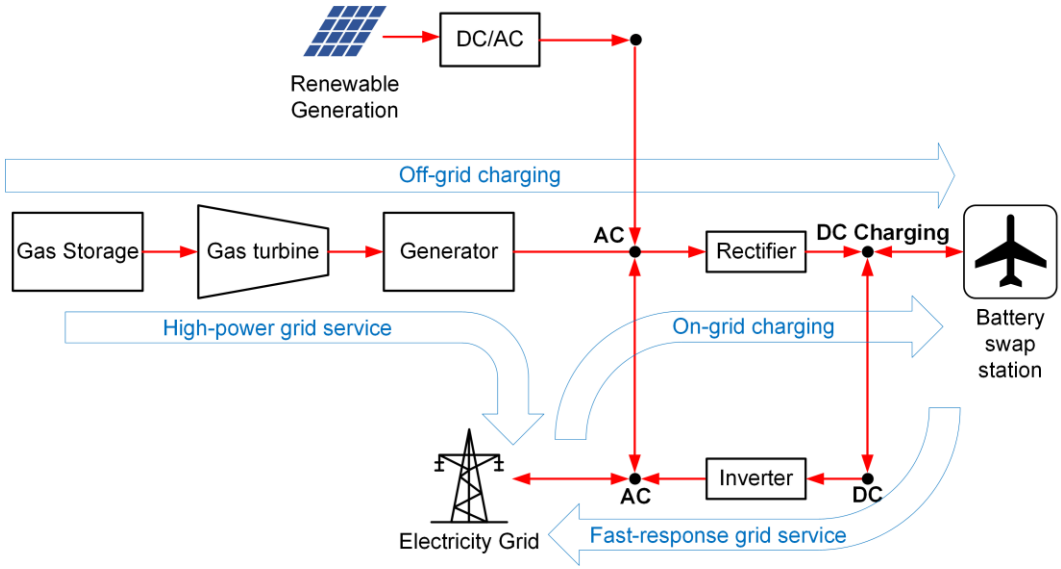

Figure 3-5 The conceptual design of a hybrid and smart EA charging system - A2G

One solution to address this issue is the integration of Aviation-to-Grid (A2G), which can provide flexibility to the electrified air transport system while also supporting the power system's frequency response. The flexibility provided by Aviation-to-Grid allows the electrified air transport system to adjust within an acceptable ramp rate and defined boundary to maintain electricity supply and demand while supporting the power system's frequency response. The conceptual design of the hybrid and smart charging system for A2G system shown in Figure 3-5 presents an innovative approach to integrating renewable energy, energy storage, and conventional power sources for efficient and sustainable airport operations. At the heart of this design, a photovoltaic (PV) system generates solar power, which is then converted from DC to AC using an inverter before being fed into the AC bus. Simultaneously, the battery charging station, which serves as the primary energy storage component, is connected to the busbar and receives power

from multiple sources, including the PV system, an on-site airport gas turbine, and the main electricity grid. This diverse energy mix ensures a reliable and stable power supply for the charging station, allowing it to accommodate fluctuations in demand and resource availability. By harnessing the synergies between renewable and conventional energy sources, the A2G system effectively addresses the unique energy demands of the aviation sector, facilitating smart and sustainable charging solutions that optimise efficiency, reduce environmental impact, and promote a greener future for air transportation.

This integration can lead to effective cost reductions in terms of energy purchase costs and frequency response services in both the power and aviation industries. This integration could potentially facilitate significant cost savings, as it may help reduce both energy purchase costs within aviation industry and expenses related to frequency response services within the power industry. Additionally, it can help achieve a low-carbon energy supply to electrified aviation at affordable costs from the power grid. Therefore, the nexus between aviation and power systems is critical, and the integration of Aviation-to-Grid can provide a solution to address the challenges and issues arising from the electrification of the aviation industry. It is essential to continue researching and developing innovative solutions to integrate the two systems effectively and efficiently to ensure the long-term sustainability and reliability of both industries.

3.4.2 Aviation-to-Grid Concept and Motivation

At present, there exists a notable gap between power systems and electrified air transport with regards to energy users and suppliers, infrastructure, and interoperability to achieve carbon neutrality in both industries. As depicted in Figure 3-6, the electrification of air transport will establish a new “nexus” between power systems and electrified air transport through electrification, creating potentials for a new technology of “Aviation-to-Grid flexibility”. There are various key issues that need to be addressed:

- Electrified aviation must be integrated into ground energy infrastructure and should not burden the future grid.
- Power systems must provide significant volumes of low-carbon electricity to electrified aviation as a new energy user to meet the electricity requirements of electric aircraft.

- The implementation of significant charging infrastructures is necessary. My study on the feasibility of electrifying 10% of domestic flights at Gatwick airport suggests that £50 million will be required for charging infrastructure [168]. There will also be significant costs associated with building additional power generation capacity.

Aviation-to-Grid is defined to include various levels and locations of integration between power system and electrified air transport system, from individual airports as well as national power system operation. Aviation-to-Grid flexibility is proposed as the ability that the electrified air transport can adjust, with an acceptable ramp rate in a defined boundary, to maintain electricity supply and demand in its own system as well as to support the power systems frequency response. Aviation-to-Grid flexibility will be investigated as a key solution for effective costs reduction in terms of energy purchase costs and frequency response services in both power and aviation industries, which will achieve low-carbon energy supply to electrified aviation at affordable costs from power grid.

The main energy resources to provide EA charging consist of grid electricity, micro gas turbines, and solar PV, as shown in Figure 3-6. Gas turbines can provide a reliable and efficient source of energy for charging electric aircraft, while solar PV can provide clean and renewable energy to reduce the carbon footprint of the charging process. However, the intermittency of solar PV and the fluctuating energy demand of electric aircraft require careful management and coordination. One possible mechanism for integrating these energy sources is through a microgrid system. A microgrid is a small-scale, localized power grid that can operate independently or in conjunction with the main power grid. It can incorporate various sources of energy, such as solar PV and gas turbines, and can manage energy storage and distribution. In this way, a microgrid can provide a stable and reliable source of energy to electrified aviation while also managing energy demand and supply.

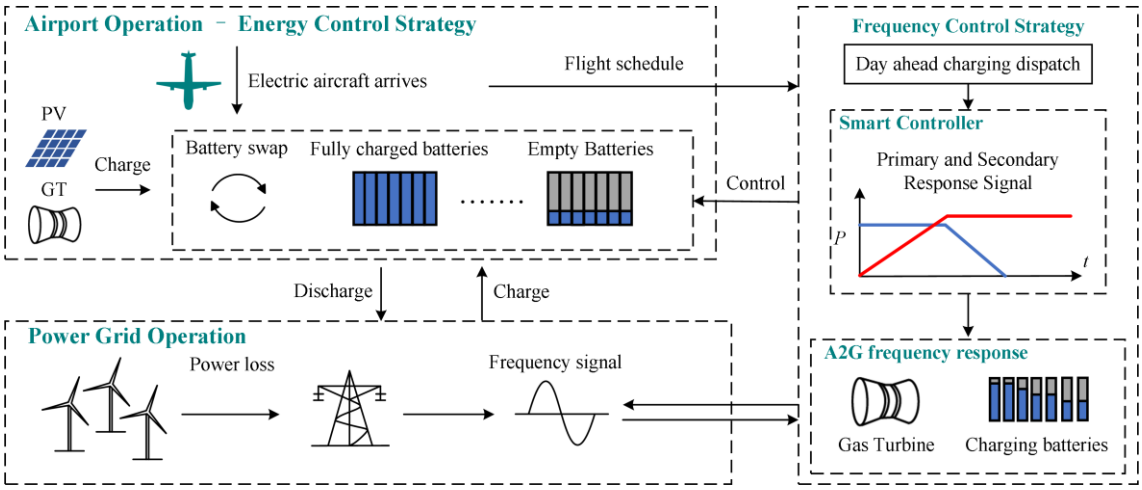

Figure 3-6 The new nexus between electrified air transport and electrical power systems – Electric aircraft charging system with grid frequency response

3.4.3 Deep Reinforcement Learning Applications in Aviation-to-Grid

Another possible mechanism for integrating these energy sources is through a dynamic energy management system. Such a system could incorporate artificial intelligence and machine learning algorithms to optimise energy supply and demand in real-time. For example, the system could adjust energy storage and distribution based on weather patterns and flight schedules and could coordinate with the main power grid to provide frequency response services.

The definition of machine learning is the automated methods that can detect patterns in data and exploit these patterns to achieve some tasks [145]. There are three types of machine learning tasks: supervised learning, unsupervised learning, and reinforcement learning [146]. Reinforcement learning is one of the core topics of machine learning that was invented to handle the sequential decision-making problems. Typically, the reinforcement problem is formalised as an agent that can make decisions based on the observation in an environment to cumulate pre-set rewards, as shown in Figure 3-7. The sequential decision-making problems should be firstly formulated by a Markov Decision Process, which means a discrete time stochastic control process [147].

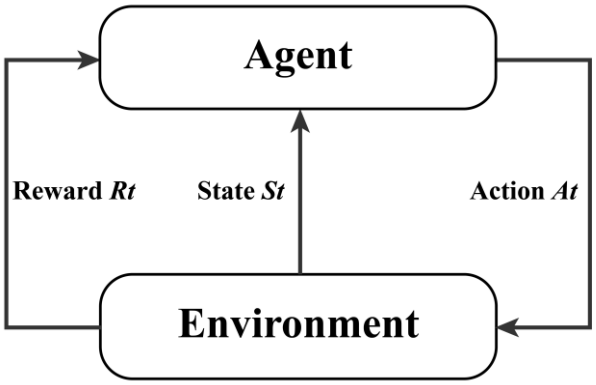

Figure 3-7 Agent and environment of deep reinforcement learning [148]

Deep learning is one of the machine learning approaches based on artificial neural networks, which is capable of supervised, semi-supervised, and unsupervised tasks [149]. By combining reinforcement learning and deep learning, the deep reinforcement learning (DRL) approach has both optimal control ability and data mining ability [148]. These abilities enable DRL to solve stochastic sequential decision-making problems, which are the general forms of energy dispatch problems [150]. In existing studies, DRL has been widely adopted in energy management and power system dispatch problems in existing studies [151]. In [152], a DRL-based controller was designed for managing the SOC of the energy storage system while providing frequency response services to the power system. [158] presents a multi-agent deep reinforcement learning approach for training a multi-area power system frequency controller, which can cooperatively reduce the frequency deviations for all areas by observing local status.[153] proposed a reinforcement learning approach for real-time pricing in EV charging stations. DRL has been widely accepted to be adopted in electrified transport uncertain scheduling for coordinative supporting the power networks. In [154], EVs are dispatched to provide active and reactive power to the distribution networks through DRL algorithms. [155] proposed a DRL-based surrogate modelling approach to enable spatial optimisation of EV flows and the operation of the transport network and power distribution networks. In [156], a hybrid multi-agent DRL for resilience control of EVs to provide ancillary services to the power networks with a high penetration level of renewable generation. In the literature, little research has focused on the application of the DRL-based scheduling approach for battery swap recharging scheduling and frequency response dispatch.

This thesis therefore proposes a novel reinforcement learning dispatch framework. This framework for A2G flexibility is a robust mechanism designed to optimise air transport scheduling in coordination with the power network environment, as shown in Figure 3-8. At the core of this framework lies a deep reinforcement learning process, which facilitates an efficient interplay between the Air Transport Scheduling Agent, and its environment, the Power Network Environment. In this system, the agent continually observes the state of the environment, capturing various parameters such as demand, supply, and grid constraints. It then performs actions, such as dispatching EA battery charging system for serving flights, in response to the observed state. Subsequently, the agent receives feedback in the form of a reward signal that reflects the impact of its actions on the environment. This reward signal enables the agent to learn optimal decision-making strategies over time, aligning air transport operations with the power network's frequency requirements. The iterative nature of the state, action, and reward loop within this deep reinforcement learning dispatch framework allows the Air Transport Scheduling Agent to dynamically adapt to evolving circumstances and achieve seamless integration with the power network environment.

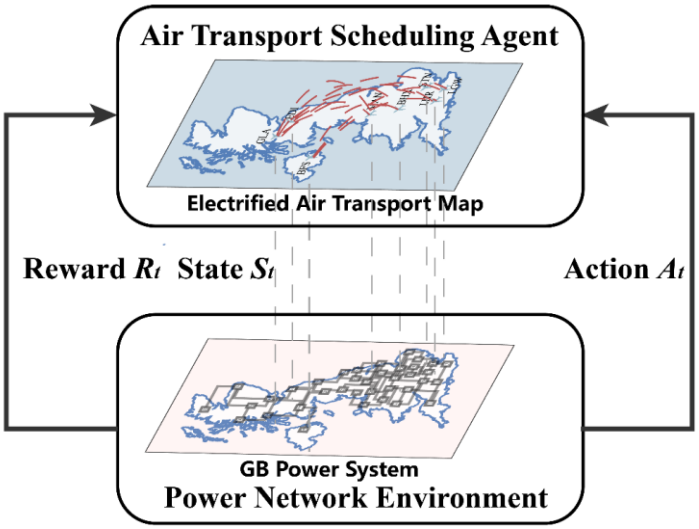

Figure 3-8 Reinforcement learning dispatch framework for A2G flexibility

3.5 Concluding Remarks

In conclusion, this chapter presents a comprehensive exploration of the technology backgrounds for electrified air transport. The chapter covers a broad range of topics, including microgrid architecture with EA and EV scheduling, wireless charging

technologies, Aviation-to-Grid integration, and deep reinforcement learning techniques for dispatching EA charging systems.

Furthermore, the upcoming chapters provide in-depth analyses of the feasibility and effectiveness of the implementations of these technologies, evaluating their potential benefits and drawbacks. These discussions will encompass various aspects, including the impact on power systems, the role of renewable energy sources, infrastructure requirements, and environmental considerations. The findings and insights gleaned from these chapters will contribute to a more comprehensive understanding of the electrified air transport ecosystem and help guide future research, development, and policymaking in this rapidly evolving field.

Chapter 4 The Coordination between Electric Aircraft and Airport Parking of EVs

4.1 Introduction

To achieve the ambitious CO_2 emission mitigation objectives outlined in "Flightpath 2050" and attain net-zero emissions in aviation sector, the adoption of EA has emerged as a promising solution. While there have been numerous prototypes of fully electrically powered aircraft for short-haul commuting air transport, the potential of electrified aviation can only be fully realised with careful planning and design of the ground power systems and associated electric aircraft charging operations, as highlighted in Chapter 2. For this reason, it is crucial to develop a future microgrid energy system for airports that utilises large-scale DERs such as PV and WT to supply clean energy to the airport energy infrastructure, as outlined in [88]. Incorporating these DERs into the airport energy infrastructure not only aligns with the sustainability goals but also enhances the reliability and resilience of microgrid operations. In addition to PVs and WTs, hydrogen system consisting of a hydrogen fuel cell and storage tank with external hydrogen supply are also being considered as a clean distributed generation resource. Integrating these DERs and hydrogen systems into the microgrid energy system will help reduce greenhouse gas emissions and improve energy efficiency.

This chapter presents a comprehensive multi-objective infrastructure planning framework for airport microgrids that incorporates both parking EVs and EA with a focus on the impact of V2G technology. The dispatch problem of the airport microgrid is formulated as a heuristic optimisation problem, which is then solved using the NSGA-II algorithm to identify Pareto optimal solutions. Two different charging strategies for EA, namely plug-in charging and battery swap, are investigated and compared through economic and technological assessments. Additionally, sensitivity analyses are conducted to explore the potential costs associated with increasing the number of EA flights and to evaluate the impact of renewable generation uncertainties. The results show that the proposed framework can effectively manage the coordination of EV and EA charging while improving the flexibility and efficiency of airport microgrid operation. The battery swap strategy for EA charging is found to be more beneficial than the plug-in charging strategy,

as it can reduce peak power demand and operating costs. Furthermore, the V2G technology is found to have a significant impact on the performance of the airport microgrid, enabling further reductions in peak power demand and overall operating costs. The sensitivity analyses reveal that the implementation of additional EAs and fluctuations in renewable power output could result in increased investment costs, highlighting the importance of careful planning and cost analysis when expanding the use of EAs in airport microgrids. The main contribution of this chapter is to investigate the potential for coordinated scheduling of EA and airport parking EV charging demand to improve the efficiency and flexibility of airport microgrid operation. The followings are specific contributions:

- A novel approach for coordinated scheduling of EA and airport parking EV charging demand is proposed. The approach dispatches EV and EA charging demand according to the flight schedule and airport operation conditions. This approach enhances the integration of renewable energy sources and the adoption of EVs, which are essential for achieving sustainability in the aviation industry.
- This study formulates and compares two different scheduling strategies (plug-in and battery swap) for adopting EA battery charging. The economic and airport microgrid operation benefits of these strategies are quantified.
- A multi-objective optimisation framework is developed to manage the airport microgrid adopting EV and EA charging. The framework improves the flexibility of airport microgrid operation by coordinative scheduling for both EV and EA. The impact of V2G on the airport microgrid is also examined.

The rest of this chapter is organised as follows: Section 4.2 introduces the airport microgrid architecture and scheduling approaches for EV and EA charging. Section 4.3 and Section 4.4 mathematically formulates the proposed multi-objective optimisation framework. Section 4.5 presents the case study results and analysis, following the conclusions and summary of this chapter illustrated in Section 4.6.

4.2 Scheduling approach for airport microgrid with EA and EV

The proposed multi-objective infrastructure planning framework for airport microgrid is illustrated in Figure 4-1, which incorporates both EA charging scheduling and

bidirectional charging strategies for EVs. The framework aims to fulfil the airport electric demand of the airport and the charging demand of EA while also reaping benefits from the flexible scheduling of EV and EA. The proposed framework consists of four major steps. Firstly, energy and aviation information databases from airport operators, which includes flight schedules, passenger information (ticket and arrival time), energy consumption, and technology data. Secondly, EV parking lot profiles are generated by linking the flight schedule with the passenger travel patterns. Thirdly, the gathered information is input into the proposed multi-objective model to obtain Pareto fronts and find the compromise optimal solution. Finally, case studies of electrified airport are developed to analyse energy dispatch, EV and EA scheduling, and economic feasibility, and sensitivity analysis on the EA electrification rate.

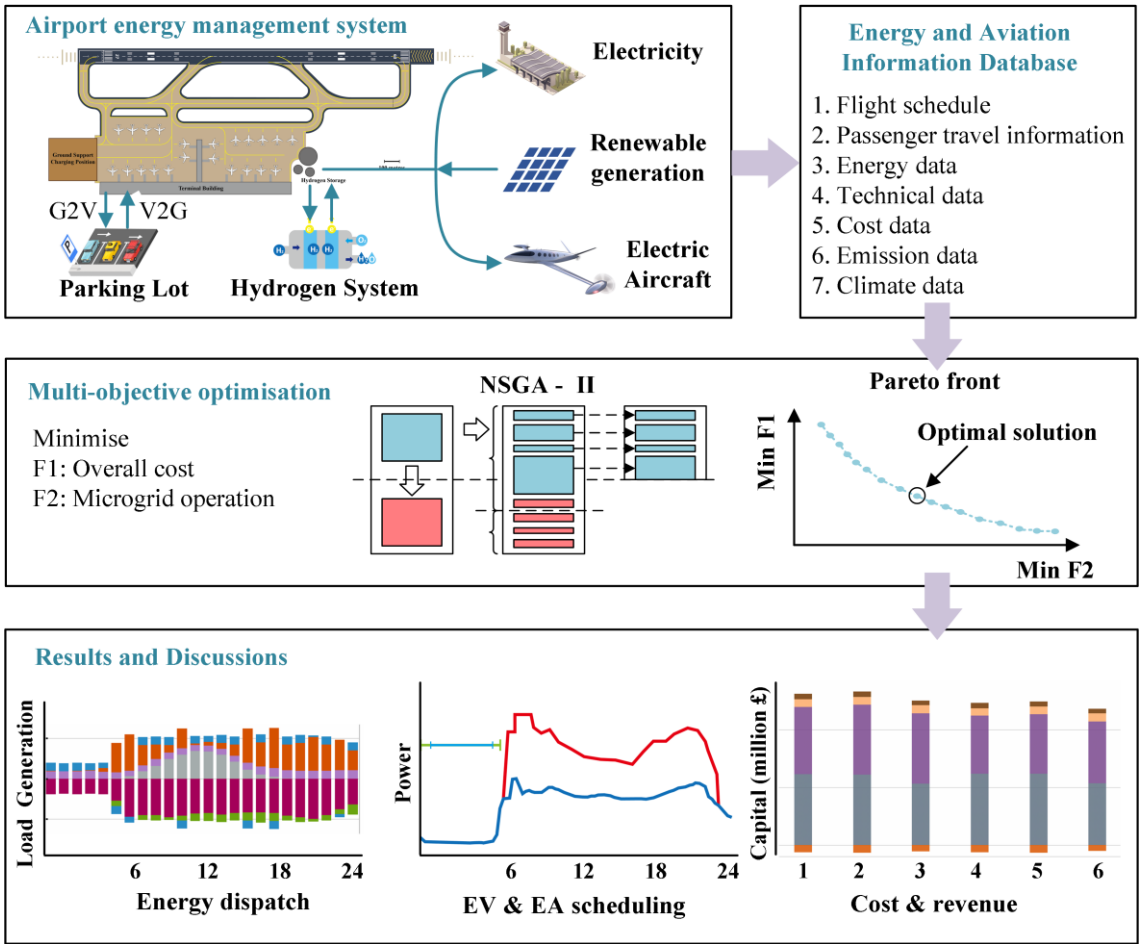

Figure 4-1 Outline of the proposed optimisation framework for airport microgrid

The airport microgrid demand includes the electric load of the airport terminal building, EA charging load, and EV charging load, while the energy supply consists of power grid

electricity supply, airport renewable generations such as PV and WT, and hydrogen systems. By considering these factors, the proposed framework enables efficient and effective management of the airport's energy resources, facilitating the integration of renewable energy sources and the adoption of EVs and EAs for sustainable aviation. The proposed framework also takes into account the flexibility of scheduling EV and EA charging demand, allowing for improved efficiency and cost-effectiveness in the operation of the airport microgrid. The case studies conducted with electrified airports demonstrate the feasibility and potential benefits of the proposed framework, and sensitivity analysis of the EA electrification rate highlights the importance of careful planning and cost analysis when adopting EAs in airport microgrids. Overall, the proposed multi-objective infrastructure planning framework offers a comprehensive and practical approach for managing the energy demand and supply of airport microgrids, promoting sustainable and efficient operations in the aviation industry.

4.2.1 Two EA charging scheduling methods

The “Eviation Alice” is a notable electric aircraft, serving as a reference electric aircraft model due to its impressive technical specifications, which are detailed in Table 4-1. The designed travel distance range of the aircraft is particularly suitable for domestic commuting flight missions. Notably, The “Eviation Alice” is expected to be adopted in airports as early as 2024 [18]. This development is promising news for the aviation industry as it represents a significant step forward in the pursuit of sustainable and environmentally-friendly air transport. As EA technology continues to advance, it is likely that more models will be developed and deployed in the coming years, further reducing the industry's reliance on fossil fuels and contributing to a more sustainable future.

Conventionally, most commuter aircraft can transport 20-50 passengers, with a distance range of less than 1000 km. The “Eviation Alice” will be used to replace conventional commuter aircraft such as SF3 (Saab 340B), as shown in Table 4-1. As the passenger capacity of SF3 is four times higher than the Eviation Alice, it is assumed that four EAs will be utilised to conduct one existing commuter flight mission. To avoid a simultaneous high-power EA charging on the airport microgrid, the flight is rescheduled to evenly distribute one flight mission conducted by conventional aircraft into four flight missions

conducted by EA, as shown in Figure 4-2. Plug-in charge means the EA flights are recharged during the time they are parked at the apron in airports, which is also called turnaround time. Battery swap means the EA batteries are swapped after the EA parking at the apron, then they are recharged at the airport at another time, most likely the time of off-peak electricity demand or price. As a result, additional batteries are required for implementing the EA battery swap.

Table 4-1 The characteristics of electric aircraft and conventional aircraft

Design property	Eviation Alice	SF3
Passenger	9 (+2 crew)	36
Distance Range (nm)	440	977
Battery Energy (kWh)	900	-
Rated charging power (MW)	0.3	-
Fast charging power (MW)	1.26	-
Charging/discharging efficiency	95%	-

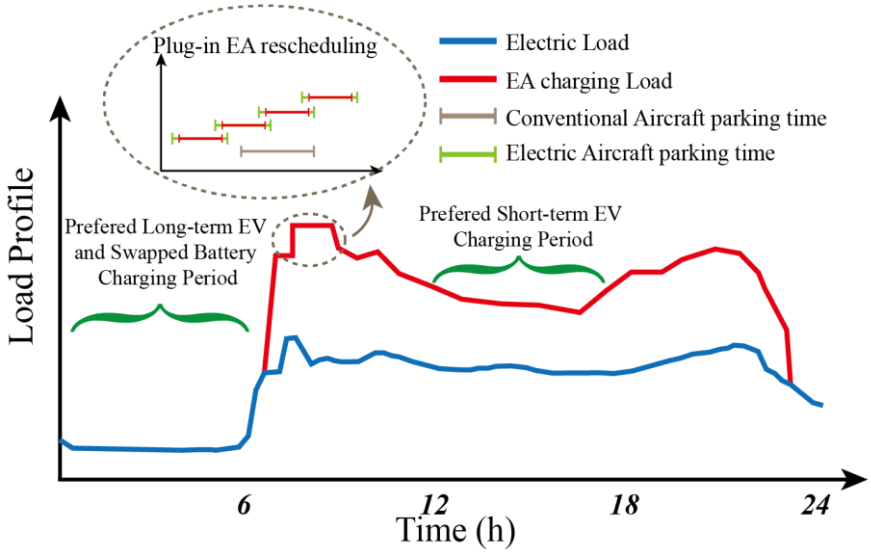

Figure 4-2 Airport electric load and EA EV charging load

To figure out the optimal EA charging solution, the pattern of airport terminal building demand, which is the 'basic' demand, is analysed. There are several general features of energy behaviour in the medium size airport, based on the data metered in [157], the energy consumption loads of airport terminal buildings are shown in Figure 4-2. There is an absolute valley demand time from 0 to 6 o'clock when there is rarely scheduled flight

and passengers in the airport. The valley time should be considered as the preferred EV and swapped battery charging period. As for the plug-in charge, in order to improve the flexibility of EA charging load, EA is rescheduled within 2 hours' range from the original arrival time of the conventional aircraft flight, as shown in the zoom-in figure in Figure 4-2.

4.2.2 Airport EV scheduling

Different from other commercial or residential districts, airports are hubs between ground transport and air transport. As a result, the parking EV charging management is different from most of the districts penetrated with EVs. Firstly, most airports have separate parking lots for short-term and long-term EV parking. In this chapter, passengers who book to-and-from tickets and drive to the airport are defined as long-term parking EV owners. Usually, the long-term parking passengers who choose to travel to and from the airport tend to book tickets in advance with a certain return date which can be linked to the flight schedule. This behaviour benefits the airport operators for gathering and forecasting the airport parking lot demand. These long-term parking EVs with V2G capacity could be aggregated as energy storage. Similar to other commercial areas, there are also short-term parking EVs owned by the airport staff. At Luton Airport, there are 46% of the passengers decided to travel to the airport by their private cars. In order to reduce the congestion of airport parking lots, the airport operators tend to limit the employees who travel to and from work by car to 60% [158]. Table 4-2 provides an overview of the assumptions used in generating EV parking profiles.

Table 4-2 Assumptions for generating EV parking profiles

Parameter	Assumed Value	Ref.
Proportion of to-and-from passengers	50%	-
Proportion of employees driving to work	60%	[163]
Proportion of passengers driving to the airport	30%	-
EV arrival time before flight	2 to 4 hours	[159]
Initial SoC of EVs on arrival	15% to 20%	-

The behaviours of passengers and employees are assumed to be subject to Gaussian distributions and have a dependent relationship with the flight schedules. A set of flights F with their arrival time, departure time, and the number of passengers is defined to represent the flight schedule in Eq. (4.1). The relationship between passenger travel patterns and flight schedules is explored. The proportion of passengers who drive to the airport and book to-and-from tickets are assumed to be 30% and 50% respectively. When the drivers arrive at the airport and park their EVs, the arrival time of the EVs will be like 2 to 4 hours before the scheduled flight departure time. The desired return days and hours are selected according to the following Gaussian distribution, then the closest flight that has an available ticket is booked.

$$F = \{T_{f1}^{arr}, T_{f2}^{arr}, \dots T_{fN}^{arr}; T_{f1}^{dep}, T_{f2}^{dep}, \dots T_{fN}^{dep}; N_{f1}^{pass}, N_{f2}^{pass}, \dots N_{fN}^{pass}\} \quad 4.1$$

$$X_{pass-a} \sim N(2.5,1), X_{pass-a} \sim clip(2,4) \quad 4.2$$

$$X_{pass-d} \sim N(3,1), X_{pass-d} \sim clip(1,10) \quad 4.3$$

$$X_{pass-h} \sim N(12,1), X_{pass-h} \sim clip(6,20) \quad 4.4$$

Meanwhile, the initial SoC of the EVs on arrival is assumed to vary uniformly between 15% to 20%, this means that the initial SOC of arrival EVs are generated with a uniform distribution, as shown in Eq. (4.5).

$$SOC_{init,k}^{EV} \sim random(0.15,0.2) \quad 4.5$$

Finally, a set of EV parking profile E^p is generated according to distribution:

$$E^p = \{T_1^{arr}, T_2^{arr}, \dots T_K^{arr}; T_1^{dep}, T_2^{dep}, \dots T_K^{dep}; SOC_{init,1}^{EV}, SOC_{init,2}^{EV}, \dots SOC_{init,K}^{EV}\} \quad 4.6$$

The daily EV scheduling in the airport parking lot is correlated to the passenger travel plan and flight arrival and departure schedules, which can be modelled as a Monte-Carlo stochastic process. Figure 4-3 shows the parking EV profiles generated from EA flight schedules with stochastic approach.

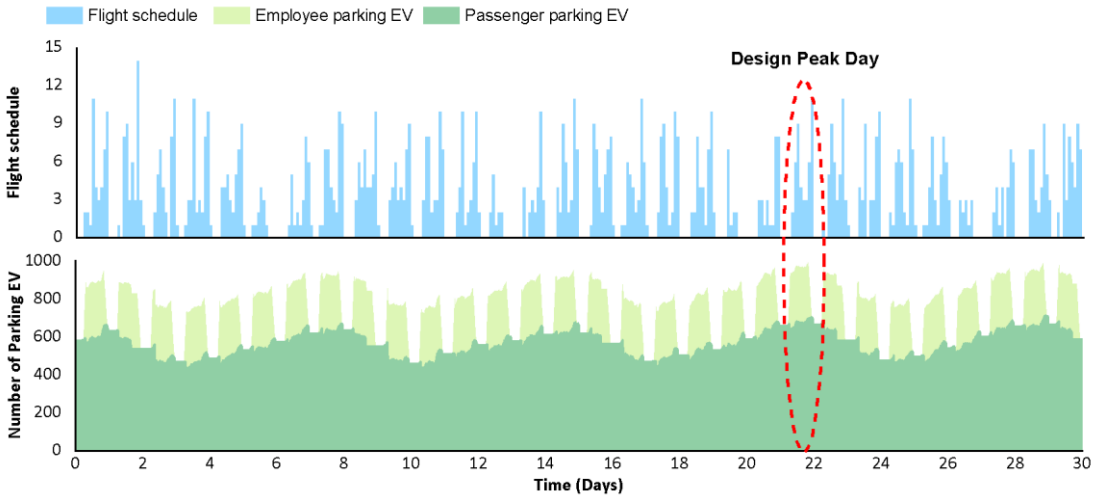

Figure 4-3 Flight schedules and EV parking profiles of the East Midland Airport over one month

The airport facilities are typically designed to meet the traffic demand during a design peak day (DPD) to ensure the airports are designed with adequate capacity to handle demand at extreme peaks [42]. There are various DPD selection methods. In this study, considering the monthly and seasonal impacts on the flight missions, the peak day of the peak month is selected as DPD. According to the proposed data process approach, the flight schedules of the East Midland Airport with EV parking lot profile for one summer season month (30 days) are generated. The flight schedule and parking lot profile with the highest value are utilised as the reference day for flight scheduling in the analysis. The selected DPD from the profiles and the flowchart for the EV profile generation methodology are shown in Figure 4-3 and Figure 4-4, respectively.

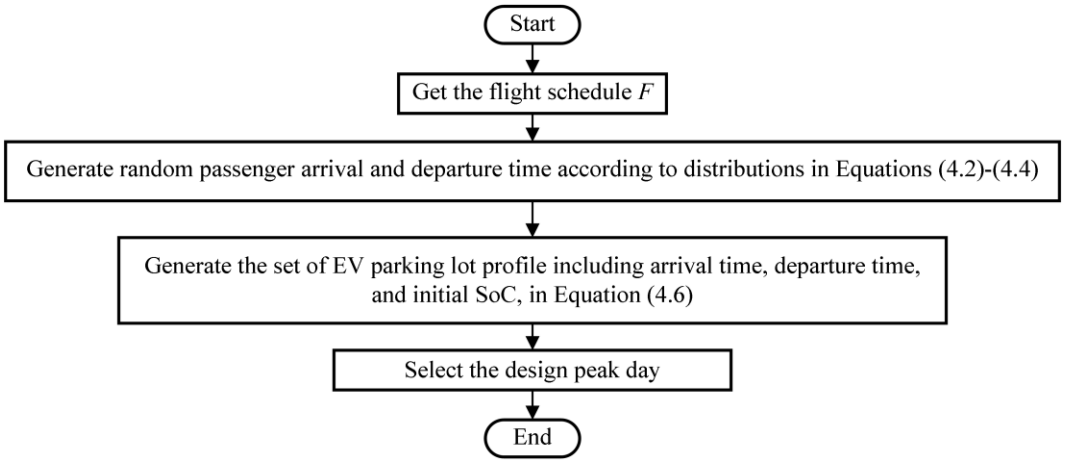

Figure 4-4 The flowchart for the EV profile generation methodology

4.3 Optimisation framework for airport microgrid

4.3.1 Objective functions

In the proposed airport energy management system, two objectives have been considered: the annualised total cost of the system, and the microgrid operation indices.

$$Min\left(f_1 = CAPEX + OPEX + C_{CO_2} + C_{main}\right) \tag{4.7}$$

The capital expenditure (CAPEX) contains the investment cost of installed energy technologies including the hydrogen storage tank, hydrogen fuel cell, transformer, EA charger, PV as well as micro-WT, as shown in Eq. (4.8). The CAPEX is annualised with the capital recovery factor (CRF) as follow:

$$CAPEX = \frac{r \cdot (1+r)^y}{(1+r)^y - 1} \sum_{dev} (CAP_{dev} \cdot \pi_{dev}^{CAP}) \tag{4.8}$$

Where CAP_{dev} represents the installed capacity of the devices and π_{dev}^{CAP} denotes the per unit investment cost of the devices. y denotes the total lifetime of the system; r denotes the discount rate, which is 6% [88].

The operating expense (OPEX) is formulated by the grid electricity purchase cost and the financial compensation for EV owners, as defined:

$$OPEX = \sum_t (\pi_t^e \cdot P_t^{grid} \cdot \varphi^{im} + \pi^{H_2} \cdot m_t^{H_2,p}) + C_{comp} \tag{4.9}$$

where π_t^e and π^{H_2} are the electricity and hydrogen purchasing price, respectively. P_t^{grid} denotes the electricity power imported from the grid. φ^{im} is a binary variable that controls the airport to import electricity from the grid ($\varphi^{im} = 1$) or not ($\varphi^{im} = 0$). $m_t^{H_2,p}$ is the mass of hydrogen purchased by the airport operator.

The emission carbon dioxide (CO_2) emission cost is derived from the power grid:

$$C_{CO_2} = \pi_{CO_2} \cdot \vartheta^{grid} \cdot \sum_t (P_t^{grid} \cdot \varphi^{im}) \tag{4.10}$$

where π_{CO_2} is the penalty fee for CO_2 emission, ϑ^{grid} is the emission factor regarding the grid electricity.

$$C_{main} = \sum_{dev} (CAP_{dev} \cdot \pi_{dev}^{main}) \quad 4.11$$

where π_{dev}^{main} denotes the maintenance cost of the devices.

The financial compensation for EV owners who participate in the V2G process is formulated by the degradation cost of EV batteries:

$$C_{comp} = \frac{C_{batt} \cdot E^{EV} + C_l}{E^{EV} \cdot L_c \cdot DOD} \sum_{t=1}^{T} P_t^{EVdisc} \quad 4.12$$

where C_{batt} is the battery cost per kWh, C_l is the cost of labour for replacing EV batteries, DOD is the depth of discharge, L_c is the life cycle of EV batteries at specific DOD. P_t^{EVdisc} represents the discharging power from airport parking EVs.

The second objective aims to improve the operation stability and renewable consumption of the airport microgrid:

$$Min(f_2 = PAR + RF + (1 - RSCR)) \quad 4.13$$

$$PVR = \frac{Max(P_t^{demand})}{Min(P_t^{demand})} \quad 4.14$$

$$RF = \frac{\sum_{t=1}^{T} P_t^{grid}}{\sum_{t=1}^{T} P_t^{demand}} \quad 4.15$$

$$RSCR = \frac{\sum_{t=1}^{T} (P_t^{renewable})}{\sum_{t=1}^{T} (P_t^{demand})} \quad 4.16$$

where,

- PVR denotes the peak to valley ratio of the airport energy system demand.

- RF denotes the resilience factor, which represents the extent to which the airport energy system demand rely on the electricity imported from the main grid.

- $RSCR$ denotes the renewable generation self-consumption rate.

4.3.2 Constraints

The following constraints must be satisfied during the operation of the airport microgrid.

4.3.2.1 Energy balance constraints

The energy supply and demand in the airport microgrid are balanced at each time interval, as shown in Eq. (4.17).

$$P_t^{grid} + P_t^{PV} + P_t^{WT} + P_t^{fc} + P_t^{EVdisc} = P_t^{E} + P_t^{EVc} + P_t^{EA} \quad 4.17$$

where P_t^{grid} is the imported power from the grid. P_t^{PV}, P_t^{WT}, and P_t^{fc} represent the power generated by PV, micro-WT, and hydrogen fuel cells, respectively. P_t^{EA} is the EA charging power. P_t^{E} is the airport electricity demand. P_t^{EVc} and P_t^{EVdisc} are the charging and discharging power from airport parking EVs, respectively.

4.3.2.2 Renewable generation constraints

The renewable power generation units adopted in the airport microgrid include PV and micro-WT. The power outputs of PV generation can be calculated by Eq. (4.18) [160], which converts solar energy to electricity. This process could be expressed as a function of PV rated power ($P^{PV,rated}$) under 1,000 W/m^2 radiation, solar radiation intensity (r_t), and the temperature of PV panels (T_t).

$$P_t^{PV} = P^{PV,rated} \frac{r_t}{r^{STC}} [1 + k_T(T_t - T_r)] \quad 4.18$$

where P_t^{PV} is the power output of the PV cell at time t. P_{PV}^{max} is the maximum installation capacity of the PV cell under the standard test condition (1,000 W/m^2, 25 ℃). r_t is the light intensity of the PV cell at time t. r^{STC} is the standard test light intensity of the PV cell, equals 1,000 W/m^2. k_T is the power temperature coefficient. T_t is the temperature of the PV cell. T_r is the reference temperature.

The power output of the micro-WT generation depends on the wind speed and the characteristics of the micro-WT, calculated by Eq. (4.19) [161]. The linearized first-order model involves factors including the cut-in velocity $V_{wt,ci}$, the cut-out velocity $V_{wt,co}$, and the rated velocity $V_{wt,rated}$.

$$P_t^{WT} = \begin{cases} 0 & ,0 \le V_{wt,t} \le V_{wt,ci} \\ aV_{wt,t}^3 - bP^{WT,rated} & ,V_{wt,ci} \le V_{wt,t} \le V_{wt,rated} \\ P^{WT,rated} & ,V_{wt,rated} \le V_{wt,t} \le V_{wt,co} \\ 0 & ,V_{wt,co} \le V_{wt,t} \end{cases} \quad 4.19$$

where:

$$a = \frac{P^{WT,rated}}{\left(V_{wt,rated}^3 - V_{wt,ci}^3\right)} \quad 4.20$$

$$b = \frac{V_{wt,ci}^3}{\left(V_{wt,rated}^3 - V_{wt,ci}^3\right)} \quad 4.21$$

$$P^{PV,rated} \leq CAP_{PV} \quad 4.22$$

$$P^{WT,rated} \leq CAP_{WT} \quad 4.23$$

4.3.2.3 Hydrogen energy system constraints

The hydrogen tank stores the hydrogen purchased from the external hydrogen supply that will be used to meet the hydrogen required by fuel cell power generation, as shown in Eq. (4.24) – (4.27). The polymer electrolyte membrane (PEM) fuel cell model is utilised in this research for its reliable performance and commercial availability [162][95]. The power output of this type of hydrogen fuel cell can be expressed as Eq. (4.26).

$$SOC_t^h = SOC_{t-1}^h + \left(m_t^{H_2,p} - m_t^{H_2,fc}\right)/CAP_{H_2 tank} \quad 4.24$$

$$0 \leq SOC_t^h \leq SOC^{h,max}, SOC_0^h = SOC_T^h \quad 4.25$$

$$P_t^{fc} = m_t^{H_2,fc} \cdot \eta^{fc} \cdot LHV^H \quad 4.26$$

$$P_t^{fc} \leq CAP_{H_2 fc} \quad 4.27$$

where SOC_t^h is the equivalent state of charge of the hydrogen storage tank. $m_t^{H_2,p}$ and $m_t^{H_2,fc}$ represent the purchased hydrogen from the external supplier and hydrogen consumed by fuel cell generation, respectively. η^{fc} is the efficiency of hydrogen fuel cells. LHV^H is the lower hearting value of hydrogen, which is 33.33 kWh/kg [163].

4.3.2.4 EA charging constraints

The aircraft behaviours can be described as an event-based model, there are four events for an EA: arrival, start charge, fully charged, and departure. The aircraft is assumed to start charging 10 minutes after arrival and finish charging within 30 minutes. To avoid the charging process causing flight mission delays, the fast charger that has a rated power of 0.63 MW is adopted, and the charging load is modelled as Eq. (4.28) – (4.32).

For the plug-in charge scenario, the EA charging time could be seen as the same as the arrival time. The plug-in EA charging demand is formulated as Eq. (4.28) – (4.29).

$$P_{fi,T_{fi}^{arr}}^{EA} = P_{EA}^{rated} \tag{4.28}$$

$$P_t^{EA} = \sum_{fi} P_{fi,t}^{EA} \tag{4.29}$$

For the battery swap scenario, the EA battery charging is allocated between 1 to 6 am to fill the valley of the airport energy demand. The battery swap EA charging demand is formulated as Eq. (4.30) – (4.32).

$$P_{fi,T_{fi}^{ch}}^{EA} = P_{EA}^{rated} \tag{4.30}$$

$$1 \leq T_{fi}^{ch} \leq 6 \tag{4.31}$$

$$P_t^{EA} = \sum_{fi} P_{fi,t}^{EA} \tag{4.32}$$

where, P_{EA}^{rated} is the rated power of the EA fast charger, T_{fi}^{ch} is the charging time variable of EA.

4.3.2.5 EV charging constraints and setup

The heuristic algorithm is not capable of a high number of variables representing the charging and discharging of every electric vehicle. As a result, the aggregate management strategy is utilised to reduce the dimension of decision variables. As discussed in previous sections, there are two types of control strategies for airport parking EVs: G2V (operate as electric loads) and V2G (operate as energy storage). For the G2V strategy, the EV charging loads are allocated at a specific period of the day before the leaving time of EV owner passengers. For the V2G strategy, the EVs are available for charging and discharging while staying at the airport parking lot.

The EV charging load allocation algorithm was modified from [164] and shown as Algorithm 4.1. In our case, the algorithm has considered that the EV charging power should be allocated within the parking time duration of each EV instead of the whole day. The flowchart for the EV charging load allocation algorithm is shown in Figure 4-5.

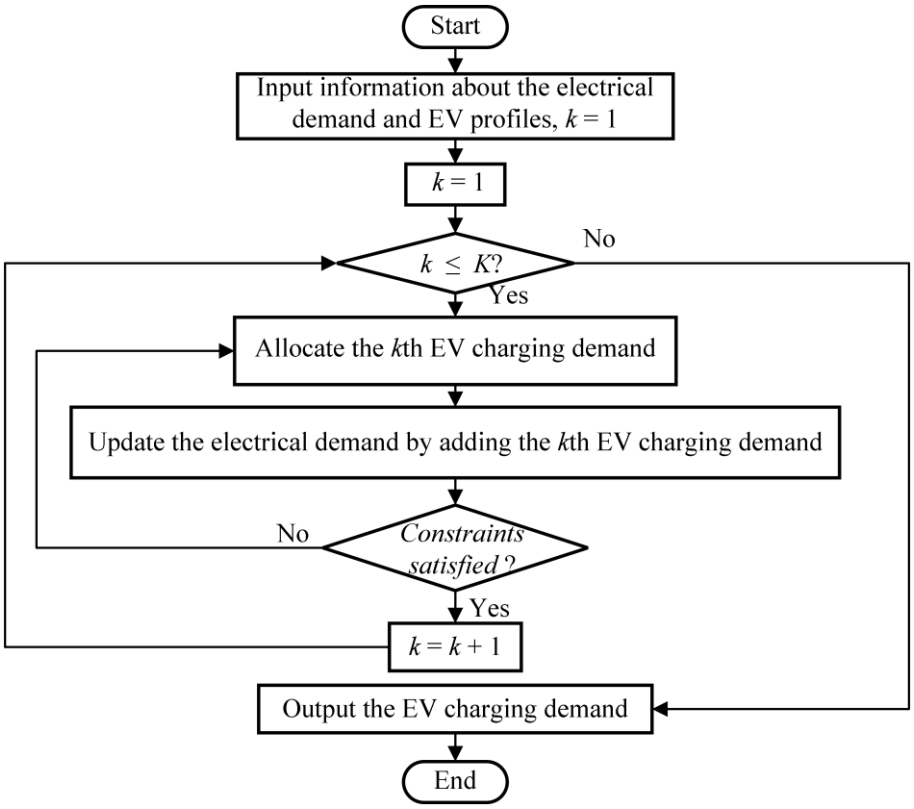

Figure 4-5 The flowchart for the EV charging load allocation algorithm

The following equations are presented as input information for the algorithm.

$$P_t^{netdem} = P_t^E + P_t^{EA} - P_t^{WT} - P_t^{PV} \tag{4.33}$$

$$E_k^{EV,req} = SOC_{init,k}^{EV} \cdot E^{EV} \tag{4.34}$$

$$P_{k,t}^{EV,c} = \begin{cases} P^{EV,max} & \xi - q_{k,t} > P^{EV,max} \\ \xi - q_{k,t} & 0 \le \xi - q_{k,t} \le P^{EV,max} \\ 0 & \xi - q_{k,t} < 0 \end{cases} \tag{4.35}$$

where P_t^{netdem} is the net demand after importing electricity from the grid and hydrogen fuel cell generation. $E_k^{EV,req}$ represents the energy required by kth EV. E^{EV} is the total energy capacity of kth EV batteries. $P_{k,t}^{EV,c}$ and $P^{EV,max}$ are the charging power of kth EV and the rated power of EV charger, respectively.

Algorithm 4.1: EV charging power allocation algorithm [164]

Input: P_t^{netdem}, T_k^{arr}, T_k^{dep}, $SOC_{init,k}^{EV}$, $P^{EV,max}$, $k = 1,2,\dots,K$
Output: $P_t^{EV,c}$
1: Calculate the $E_k^{EV,req}$ according to (4.34)
2: **for** $k = 1,2,\dots,K$ **do**
3: EV_k gets P_t^{netdem} from airport microgrid operator
4: Compute parking period $t_k^p = T_k^{arr}:T_k^{dep}$
5: Compute $q_{k,t} = P_{t_k^p}^{netdem}$
6: define $\xi_{min} = \min(q_{k,t})$ and $\xi_{max} = \max(q_{k,t})$
7: **while** $\xi_{max} - \xi_{min} > \sigma$ **do**
8: $\xi = (\xi_{max} + \xi_{min})/2$
9: Compute $P_{k,t}^{EV,c}$ according to (4.35)
10: **if** $\sum P_{k,t}^{EV,c} > E_k^{EV,req}$ **then**
11: $\xi_{max} = \xi$
12: **elseif** $\sum P_{k,t}^{EV,c} < E_k^{EV,req}$ **then**
13: $\xi_{min} = \xi$
14: **end**
15: EV_k reports new $P_t^{netdem} = P_t^{netdem} + P_{k,t}^{EV,c}$ to operator
16: **end**

In the V2G strategy, the parking EVs are aggregated as flexible energy storage, the following equations describe the charging behaviour of the airport parking EV aggregator.

$$SOC_t^{EV} = SOC_{t-1}^{EV} + (P_t^{EVc} \cdot \eta^{EVc} - P_t^{EVdisc}/\eta^{EVdisc})\Delta t/E^{EV} \quad 4.36$$

$$SOC^{EV,min} \le SOC_t^{EV} \le SOC^{EV,max} \quad 4.37$$

$$0 \le P_t^{EVc} \le P^{EV,max} \quad 4.38$$

$$0 \le P_t^{EVdisc} \le P^{EV,max} \quad 4.39$$

$$SOC_{t_0}^{EV} = SOC_{t_{end}}^{EV} \quad 4.40$$

$$SOC_{t_d}^{EV} \ge SOC^{target} \quad 4.41$$

where, SOC_t^{EV} is the SOC of EV at time *t*, η^{EVc} and η^{EVdisc} are the charging and discharging efficiency of the EV battery respectively, P_t^{EVc} is the rated EV charging power, t_d is the target leaving time of EV owner, E^{EV} is the energy capacity of the EV battery, SOC^{target} is the EV target SOC. $SOC_{t_0}^{EV}$ and $SOC_{t_{end}}^{EV}$ are the initial and final state of charge of the EV aggregator.

4.4 Implementation of multi-objective optimisation

4.4.1 Non-dominant sorting genetic algorithm II (NSGA-II)

The proposed problem is formulated as a heuristic optimisation problem. There are many methods to solve multi-objective problems, and one of the effective algorithms NSGA-II is adopted to solve the proposed problem [165]. The logic flow of the NSGA-II algorithm is described as follows:

(1) Non-dominated sorting and crowding: Classify and confirm the particles' rank, which is used to calculate the distance between particles propagating along fronts. Sort the individuals according to their rank and calculate the crowding distance among particles.

(2) Game selection: Binary tournament is a game strategy that will be used to select two populations to participate in the future crossover and mutation processes. The game selection theory is that particles with a lower (better) rank located in a less crowded zone will be adopted first.

(3) Cross over and mutation: After the crossover and mutation, a new population is created.

(4) Population recombination: At each generation, by evaluating the dominance criterion of all accessible solutions, a combined population with the parent and the current population is constructed to generate non-dominant fronts.

(5) Calculating crowding distance and non-dominated sorting: Repeat non-dominated and crowding distance sorting in the new generation.

(6) New population generation: A new generation is generated from the reproduced population with the same strategy as above.

After the process (1) – (6), a set of potential optimal solutions that represent possible scenarios of energy dispatch is obtained.

$$PF = \{f_1(x), f_2(x), \dots f_i(x)\}, x \in \mathbb{C} \tag{4.42}$$

where $\mathbb{C}$ is the feasible search space, $f_i(x)$ are sets of the Pareto optimal solutions.

4.4.2 Decision making

In multi-objective optimisation, the Pareto optimal front is one approach for representing optimum solutions that satisfy different objectives. After obtaining the Pareto front, the next step is to make a trade-off between the two objectives: annualised total cost of the system and the microgrid operation indices. There is only one solution that could be selected from the Pareto front. TOPSIS has been widely utilised in a wide range as a multiple-attribute decision-making method based on the Euclidean distance of the alternative with respect to the positive ideal solution and negative ideal solution [166]. In this study, the Euclidean-distance-based TOPSIS method is applied to calculate proximity degree and select the final planning solution among Pareto-optimal points.

The two objectives could be normalised by placing all objectives on the same dimension scale between 0 to 1:

$$f_{ij}^{norm} = \frac{f_{ij} - \min\left(f_{ij}\right)}{\max\left(f_{ij}\right) - \min\left(f_{ij}\right)} \tag{4.43}$$

f_{ij} is the values of ith solution of jth objective.

The Euclidean-distance-based TOPSIS approach uses two reference points: "ideal" and "nadir" points representing the best and the worst point to select the best compromising solution. The least Euclidean distance from "ideal" and "nadir" points to non-dominated solutions are marked as ED_{i+} and ED_{i-} respectively.

$$ED_{i+/i-} = \sqrt{\sum_{j=1}^{N_{obj}} \left(f_{ij} - f_{ij}^{ideal/nadir}\right)} \tag{4.44}$$

The smaller value of ED_{i+} implies that the solution is closer to the best decision point. Based on Euclidean distance, the relative closeness index is expressed as (44). The solution with the maximum relative closeness index is recognised as the overall optimal solution.

$$\pi_i = \frac{ED_{i-}}{ED_{i+} + ED_{i-}} \tag{4.45}$$

4.4.3 Overall Algorithm

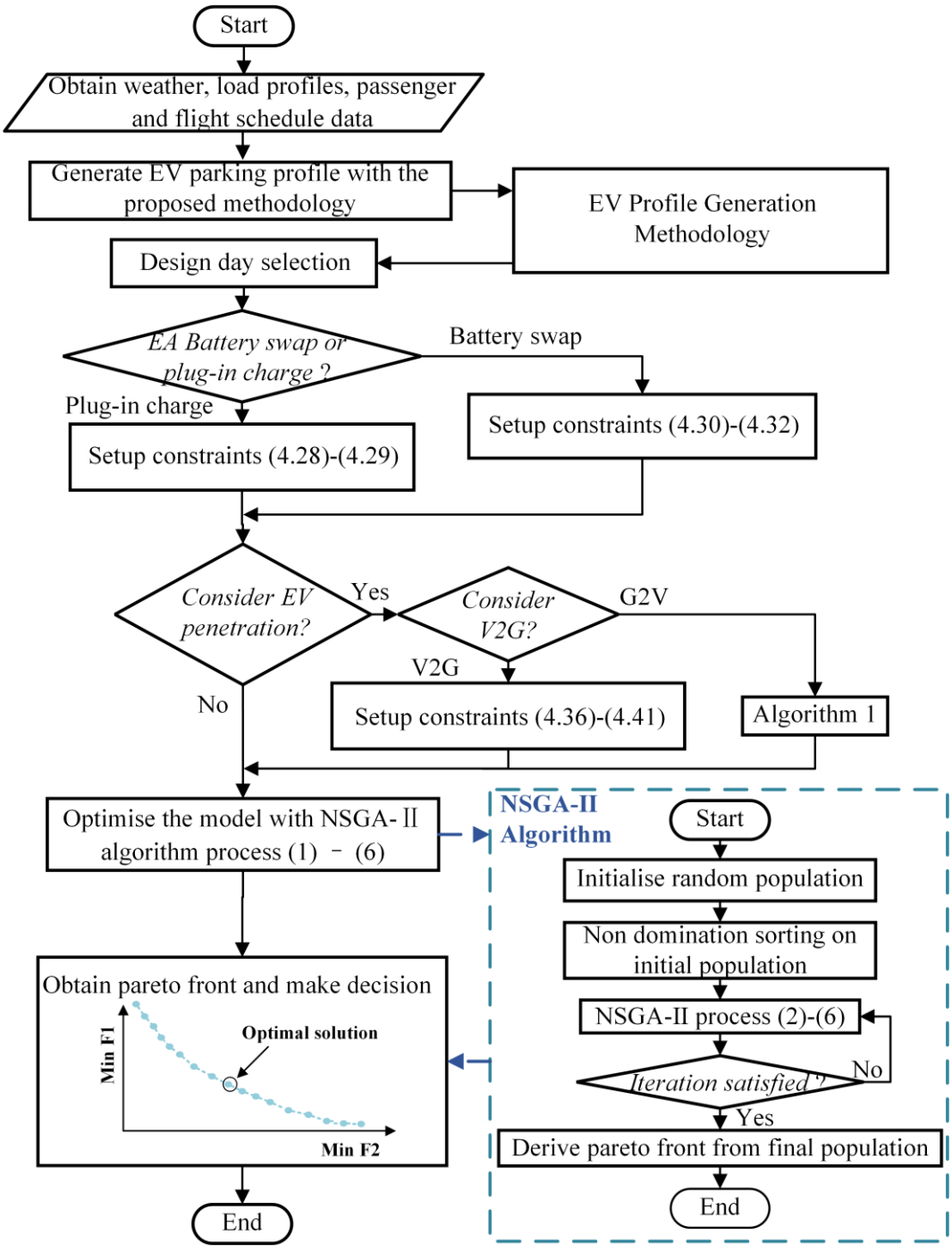

Figure 4-6 Flow chart for overall algorithm

The overall algorithm is illustrated in Figure 4-6. This subsection describes the overall approach to implementing multi-objective optimisation for the airport microgrid integrated with EA and parking EVs. After obtaining the required data, including weather profile, load profile, and flight schedules, the first subprocess is the parking EV profile

generation algorithm, as illustrated in Section 4.2.2. The next step is to set up different constraints for different cases: Eq. (4.28) – (4.29) for plug-in charge cases, Eq. (4.30) – (4.32) for battery swap cases. If the G2V strategy is adopted, the EV charging demand allocation algorithm is implemented to allocate the EV charging demand. Otherwise, the constraints Eq. (4.36) – (4.41) are applied for the V2G strategy. Afterward, all the input and constraints are ready for the implementation of the NSGA-II algorithm. The Pareto front and optimal solution could be derived by solving the proposed algorithm.

4.5 Results and analysis

4.5.1 Overview

In this study, case studies are conducted at the East Midland Airport (IATA code: EMA). To avoid the impact of COVID, the aviation demand data from 2019 is used. Domestic flight schedules from August 1st to 30th August 2019, serve as the basis for generating EA flight schedules and air passenger arrival profiles. It is assumed that 50% of domestic flights to-and-from the East Midland Airport as a hub are electrified. The peak demand for airport terminal building load is assumed to be 10 MW, which is a typical level for a mid-size hub airport [42]. The maximum installation capacities of micro-WT and PV are assumed to be 9 MW and 10 MW, respectively. The initial SOC for arriving EA is assumed to be at 20% in order to simulate an extreme scenario with the highest possible recharging demand. In this research, every megawatt of hydrogen fuel cell requires at least a 500 kg hydrogen storage tank. Economic inputs primarily include investment and maintenance costs for each energy device, as shown in Table 4-3, while energy prices and emission cost parameters are displayed in Table 4-4. Because this work is focusing on the design of airport microgrid, only the maintenance costs of energy supply devices within the microgrid are considered.

Table 4-5 presents the planning parameters for EV battery and compensation costs for EV owners participating in the V2G process. To explore the effect of V2G and various EA scheduling approaches, the following six case studies are investigated: Case 1, EA plug-in charge without Parking EV; Case 2, EA plug-in charge with G2V; Case 3, EA plug-in charge with V2G; Case 4, EA battery swap without Parking EV; Case 5, EA battery swap with G2V; Case 6, EA battery swap with V2G. These case studies aim to

provide insights into the effects of various charging and energy management strategies on airport microgrid infrastructure planning. The proposed airport microgrid multi-objective infrastructure planning framework and the NSGA-II algorithm are coded in MATLAB 2021a on a PC with AMD Ryzen 5 3500XCPU @ 3.6 GHz and 16 GB of RAM. The population size and the number of iterations are set as 200 and 2000, respectively.

Table 4-3 Economic parameters of devices [57], [88]

Device	Installation cost	Maintenance cost (per year)
PV	2245 £/kW	28.7 £/kW
micro-WT	1451 £/kW	37.5 £/kW
Transformer	25,000 £/MVA	-
EA Chargers	10,000 £/each	-
EV Chargers	1,300 £/each	-
Fuel Cell	501.64 £/kWh	11.57 £/kW
Hydrogen tank	1341 £/kg	15.65 £/kW

Table 4-4 Economic parameters

Parameter	Time	value
Electricity price [167]	0:00-7:00, 21:00-24:00	0.1£/kWh
	7:00-21:00	0.2 £/kWh
CO_2 Emission cost	-	20 £/t
Hydrogen price	-	5 £/kg
Electricity Carbon factor	-	0.257 kg/kWh

Table 4-5 EV Planning Parameters [168]

Parameter	Value	Parameter	Value
EV Battery Cost	300 £/kWh	EV Battery Capacity	25 kWh
Labour Cost of Replacing Battery	240 £	Charging/Discharging Efficiency of EV	92%
Battery Life cycle	5000	Maximum SOC	90%
DOD	80%	Minimum SOC	20%

4.5.2 Microgrid energy dispatch

Figure 4-7 Energy dispatch results of the airport microgrid. (a) EA plug-in charge case without EV, (b) EA plug-in charge case with G2V, (c) EA plug-in charge case with V2G, (d) EV battery swap case without EV, (e) EV battery swap case with G2V, (f) EV battery swap case with V2G

This section investigates the impacts of different EA charging scheduling strategies and G2V/V2G on airport microgrid energy dispatch. The energy dispatch results for all six cases are presented in Figure 4-7. As demonstrated, the load characteristics of EA plug-in charge cases and battery swap cases differ, with the load curves of EA battery swap cases appearing more flattened than EA plug-in charge cases. By incorporating battery swap technology into EA charging scheduling, a more balanced and smoother electric load pattern in airport microgrid can be achieved. Approximately half of the airport loads, including EV and EA charging, are supplied by renewable power generation in the selected design day. However, due to the limited installation capacity of the PV and micro-WT generation, the microgrid must request power from the main grid. When the EA charging load exceeds microgrid generation limits, the hydrogen fuel cell system operates to support the system and achieve power balance by generating electricity from the hydrogen storage tank.

Meanwhile, parking EVs can serve as an alternative stable distributed energy storage during daytime hours. As shown in Figure 4-7 (c) and (f), hydrogen fuel cell system generation operates less with the existence of V2G for both EA plug-in charge and battery swap cases. This demonstrates that V2G from parking EVs and the hydrogen fuel cell system work together to satisfy the total demand of the airport microgrid, thereby improving its resilience. The hydrogen fuel cell system also tends to generate electricity when renewable generation is not at its peak. Parking EVs prefer to charge during renewable generation and valley of other demands, as this improves the resilience factor and renewable self-consumption rate.

Table 4-6 Optimal microgrid operation indices for all 6 cases

EA Charging Strategy	EV Charging Strategy	Indices			Sum.	Avg.
		PVR	RF	RSCR		
Plug-in Charge	w/o EV	2.88	0.51	0.38	4.01	3.89
	with G2V	2.92	0.42	0.37	3.97	
	with V2G	2.45	0.58	0.35	3.68	
Battery Swap	w/o EV	1.55	0.45	0.38	2.62	2.55
	with G2V	1.65	0.42	0.37	2.7	
	with V2G	1.13	0.54	0.35	2.32	

In generally, the EA battery swap scenario appears more flattened than the plug-in scenario, regardless of whether EVs are involved. This indicates that adopting the EA battery swap strategy is more beneficial for airport peak load shaving and valley filling than V2G from airport parking EVs, due to the difference in their capacity. Table 4-6 presents the optimal microgrid operation indices for all six cases. Among all cases, the PVR is significantly reduced in EA battery swap cases, suggesting that the energy consumption of the microgrid has less fluctuation during the day. The average microgrid operation indices of EA battery swap cases (which is 2.55) are smaller than that of EA plug-in charge cases (which is 3.89). As observed from Table 4-6, V2G can help improve the PVR and RF, meaning that flexible EV charging and discharging can help reduce the gap between peak and valley demand and enhance the microgrid resilience.

4.5.3 EV and EA scheduling

This section examines the results of EA charging scheduling and the interactions between EV and EA. Figure 4-8 clearly demonstrates that EA battery swap scenarios necessitate a greater number of chargers compared to EA plug-in charge scenarios.

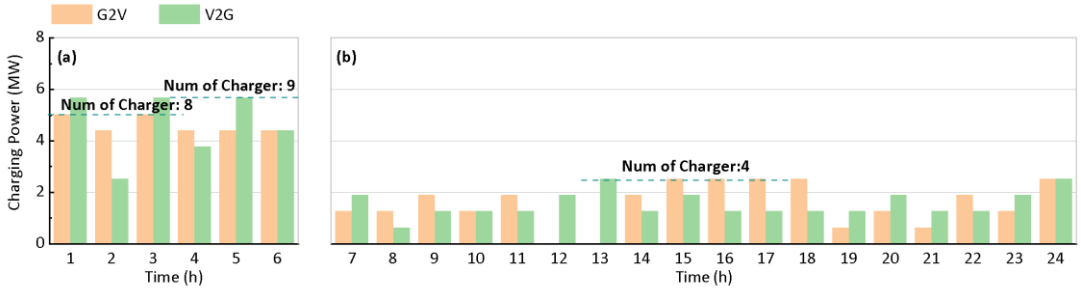

Figure 4-8 The EA charging schedules for four cases (a) EA battery swap cases with G2V and with V2G, (b) EA plug-in charge cases with G2V and with V2G

As shown in Figure 4-8 (a), the demand for EA charging in EA battery swap cases is more evenly distributed, rather than experiencing uneven fluctuation. This is an optimal solution for minimising the total number of required chargers. In EA plug-in charge scenarios, the EA charging demand for both V2G and G2V cases exhibit distinct characteristics. The EA charging demand in the V2G case is more consistent than in the G2V case as the V2G process contributes to a more balanced energy price throughout the day. The peak EA charging demand in the G2V case occurs between 3 – 6 pm, coinciding with renewable resource electricity generation. This suggests that the charging schedule

of the G2V case is more reliant on renewable energy. As a result, the previous evening peak (7 – 8 pm) in the G2V cases shifts to an earlier time for enhanced energy price and efficiency.

In contrast, the V2G cases still have noon (12 pm) and evening (8 pm) peaks. These findings indicate that if airport operators choose to maintain the daily flight schedules similar to that conducted by conventional aircraft, V2G technology could offer more benefits in terms of the airport microgrid scheduling performance. Overall, this analysis indicate that the EA battery swap approach provides a more evenly distributed demand, minimizing the total number of chargers needed. Meanwhile, the EA plug-in charge scenarios display unique characteristics based on the V2G and G2V cases, with V2G offering a more balanced energy price throughout the day.

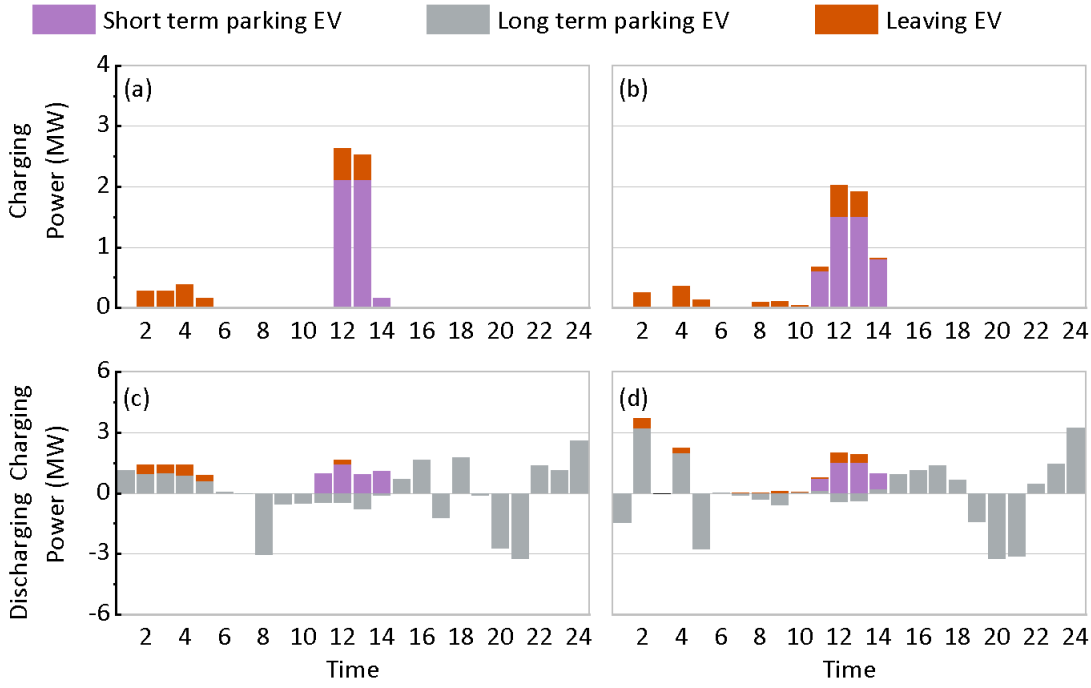

Figure 4-9 EV charging and discharging schedules. (a) Case 2: EA plug-in charge case with G2V, (b) Case 4: EA battery swap case with G2V, (c) Case 3: EA plug-in charge case with V2G, (d) Case 6: EA battery swap case with V2G

The EV charging and discharging scheduling results can be seen in Figure 4-9. A comparison of the charging demand for departing EVs (long-term parking EVs leaving today) in EA plug-in charge cases (Figure 4-9 (a) and (c)) and EA battery swap cases (Figure 4-9 (b) and (d)) reveals a distinct difference: more departing EVs tend to charge

during daytime hours in the battery swap case. This is because the charging demand for swapped EA batteries fills the valley between 0 to 6 am, eliminating the need for EVs to charge during this period to balance the total demand of the airport microgrid.

Another observation is that the charging demands for departing EVs consistently peak around the noon (12 – 1 pm) in all cases, coinciding with the highest level of renewable energy generation. Regarding short-term parking EVs, they tend to charge primarily between 10 to 2 pm in all cases to consume excess renewable energy generation.

Figure 4-9 (c) and (d) show that the EVs are more likely to charge during off-peak hours (10 pm – 12 am and 12 to 4 am) and renewable generation peak time (10 am to 2 pm), then provide surplus energy during the morning peak (8 to 10 am) and evening peak (4-8 pm). This illustrates the V2G function logic effectively. In Case 3 (EA plug-in charge case), EVs tend to charge continuously during the early morning hours (12 – 5 am) because they are responsible for flattening the demand by filling the valley. Conversely, in Case 4 (EA battery swap case), EVs are free to charge and discharge to support EA swapped battery charging during the same period.

4.5.4 Economic assessment

This section discusses the economic assessment of the optimal solutions for the six investigated cases. Figure 4-10 shows that the costs of G2V cases (Case 2 and Case 5) are the highest within their respective scenarios (EA plug-in charge or battery swap). Simultaneously, Case 3 (EA plug-in charge case with V2G) has the lowest cost among all EA battery swap cases.

The implementation of V2G technology significantly reduces both the CAPEX and OPEX of EA plug-in charge cases: Case 3 achieves a 6.1% reduction in CAPEX and a 16.9% reduction in OPEX compared to Case 2. In contrast, the reductions in EA battery swap cases are less pronounced, with only 2.8% decrease in CAPEX and 15.9% decrease in OPEX. It is important to note that V2G increases the emission cost for both EA plug-in charge and battery swap by 43.9% and 35.6% respectively. This could be attributed to the fact that EVs with V2G capacity typically charge when electricity demand is low and discharge during peak times. This pattern could potentially lead to additional emissions due to increased use of grid electricity. Emission Cost is lowest in Case 5 (EA battery

swap with G2V) at 17.159 thousand pounds, followed by Case 2 (EA plug-in charge with G2V) at 17.211 thousand pounds, indicating that incorporating G2V in both plug-in charging and battery swapping scenarios can effectively reduce emissions. Case 3 (EA plug-in charge with V2G) and Case 6 (EA battery swap with V2G) have higher emission costs, 24.774 thousand pounds and 23.274 thousand pounds, respectively, which implies that V2G integration may lead to increased emissions. Case 1 (EA plug-in charge without Parking EV) and Case 4 (EA battery swap without Parking EV) show intermediate values of 20.162 thousand pounds and 17.839 thousand pounds, respectively, suggesting that Parking EVs may have an impact on emission reduction. Maintenance Costs are quite similar across all cases, with a range between 8.215 thousand pounds and 8.221 thousand pounds, indicating that the choice of charging strategy (plug-in charge or battery swap) and the integration of G2V or V2G services have minimal impact on maintenance costs in the airport microgrid.

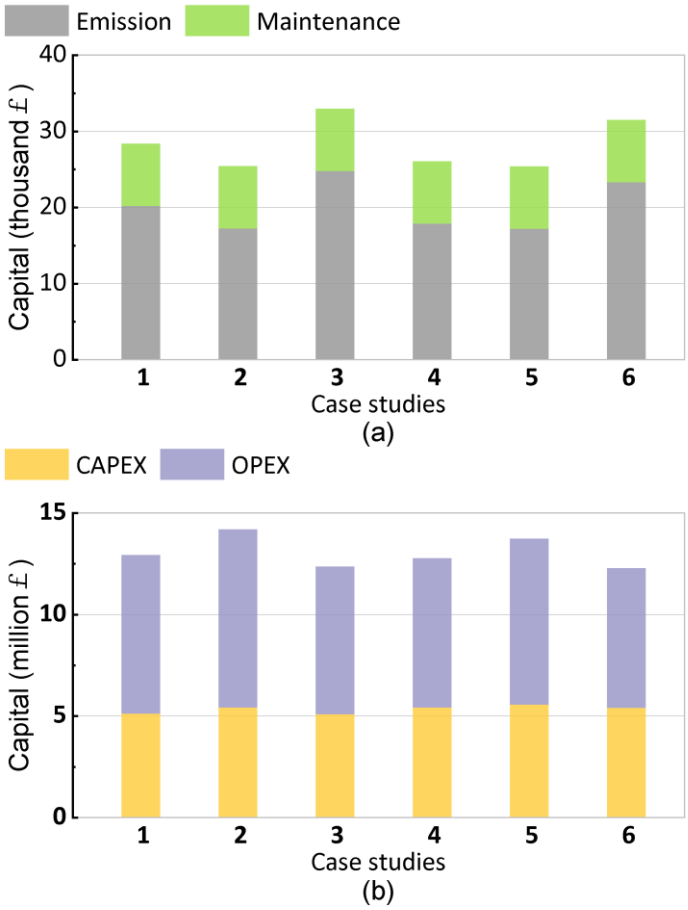

Figure 4-10 Optimal annualised costs for the 6 cases. (a) Emission and Maintenance Costs, (b) CAPEX and OPEX.

In conclusion, incorporating G2V strategies in both plug-in charging and battery swapping scenarios can help reduce emissions effectively, while V2G integration may lead to increased emissions. Maintenance costs are not significantly affected by the choice of charging strategy or the integration of G2V or V2G services.

The overall cost of EA battery swap with the V2G case falls between the other two EA battery swap cases. Although the improvement may not be substantial, V2G can still be considered an economically viable option when taking microgrid performance enhancement into account.

4.5.5 Microgrid energy technologies installed capacity

This section focuses on the installation capacity of airport microgrid energy technologies. Figure 4-11 displays the changes in installed hydrogen fuel cell capacities across the six cases, with two objectives: optimal cost (Objective f_1) and optimal operation (Objective f_2). As evident in Figure 4-11, when the focus shifts towards optimal microgrid operation, the installed hydrogen fuel cell capacity increases from approximately 1 MW to around 9 MW. This highlights the significance of the hydrogen system for the airport microgrid operation performance. However, the high cost of hydrogen fuel cell systems means they are only considered for large-scale installation (8 to 10 MW) when microgrid operational performance becomes a more critical objective.

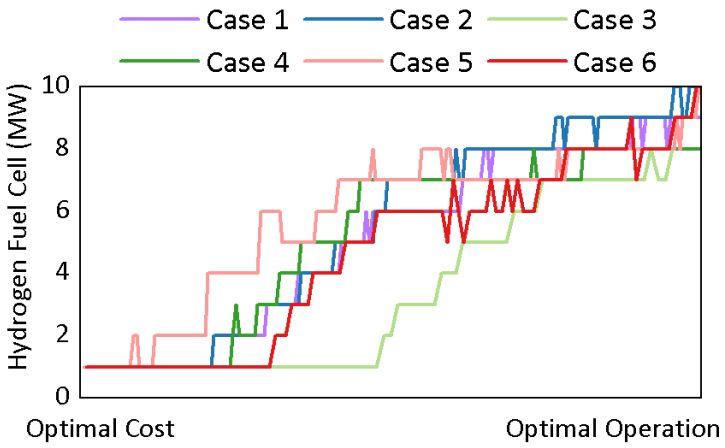

Figure 4-11 Installed capacity of hydrogen fuel cell varying with two objectives in 6 cases

The importance of the hydrogen system varies across different cases; it is less significant in cases with V2G (Case 3 and Case 6), as also corroborated in section 4.5.2. For G2V

cases (Case 2 and Case 5), the hydrogen fuel cell system is of paramount importance, as without V2G resources to improve overall microgrid performance, it becomes the only means to achieve enhanced stability and resilience.

Table 4-7 presents the optimal installed capacity of microgrid installation for all six cases, revealing a trend where the adoption of V2G technology results in reduced requirement for hydrogen fuel cell systems.

Table 4-7 Optimal microgrid technology installation capacity for all cases

Infrastructure	Unit	Plug-in charge			Battery swap		
		w/o EV	with G2V	with V2G	w/o EV	with G2V	with V2G
PV	MW	10	10	10	10	10	10
micro-WT	MW	9	9	9	9	9	9
Fuel Cell	MW	4	7	2	6	7	4
Transformer	MVA	9	9	10	9	8	9
Charger number	Quantity	4	4	4	8	8	9

4.5.6 Pareto Fronts and Microgrid Scoring

Figure 4-12 illustrates the trade-off between microgrid operation indices and costs for all six investigated cases. Due to the high investment cost of EV charging, the costs for both G2V cases (Case 2 and Case 5) are higher than those without EVs (Case 1 and Case 4). Additionally, the microgrid operation performance of cases without EVs is superior to G2V cases, as the G2V strategy only adds a burden to the airport demand.

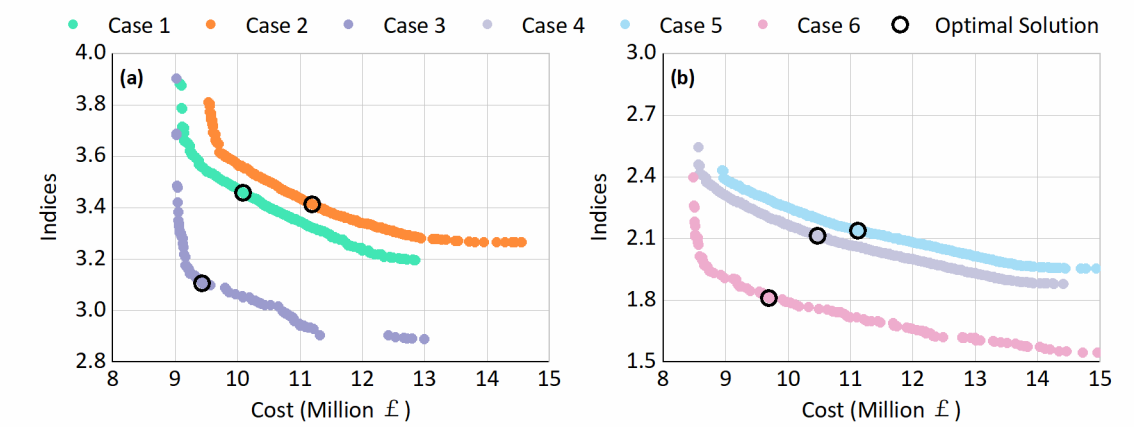

Figure 4-12 Pareto fronts of different cases

However, in both scenarios, V2G cases achieves better operational performance with lower costs compared to G2V cases. The difference between EA plug-in charge and battery swap scenarios can be analysed by comparing Figure 4-12 (a) and (b). EA battery swap cases exhibit better microgrid operation performance, while V2G helps improve the performance of EA plug-in charge cases.

4.5.7 EA implementation level sensitivity analysis

The level of EA implementation could potentially impact the operational and economic performance of airport microgrids. A sensitivity analysis has been conducted, exploring the effects of increasing the percentage of flights replaced by EAs from 50% (benchmark) to 100%. Figure 4-13 presents the trade-off between airport microgrid operation and economic performance, with varying EA implementation levels.

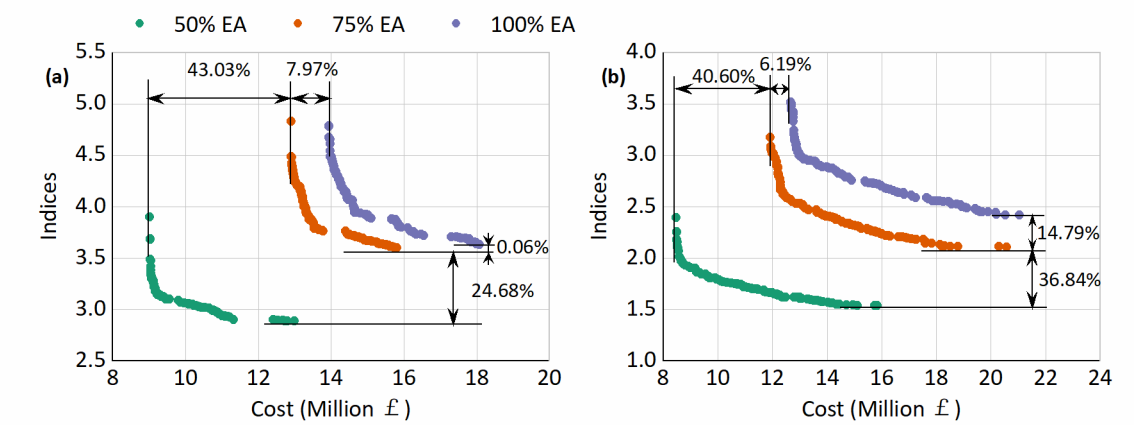

Figure 4-13 Pareto fronts of sensitivity analysis of EA implementation level. (a) EA plug-in charge cases, (b) EA battery swap cases

In general, EA battery swap cases consistently outperform plug-in charge cases across all EA implementation level. Moreover, both objective values in EA plug-in charge cases increase more significantly as the EA implementation level rises, compared to EA battery swap cases. This is because plug-in charge cases have less flexibility to reduce costs and improve operational performance.

Additionally, there is a considerable gap in airport microgrid performance indices between the reference case (50% EA implementation) and the other two implementation levels. This occurs because the EA charging power in cases with 75% EA implementation has substantially exceeded the original electric load of the airport terminal building,

resulting in uneven airport microgrid operation. This insight suggests that airport operators should consider constructing a separate microgrid to accommodate higher EA charging demand if the EA implementation level exceeds 50%.

4.5.8 Renewable generation uncertainty sensitivity analysis

Seasonal fluctuations in renewable generation can influence planning results for airport microgrids. To address the uncertainties associated with PV and micro-WT generation, a sensitivity analysis on seasonal renewable generation has been performed. Scenarios for three design days with low, medium, and high renewable generation profiles are explored. The renewable generation profiles are depicted in Figure 4-14.

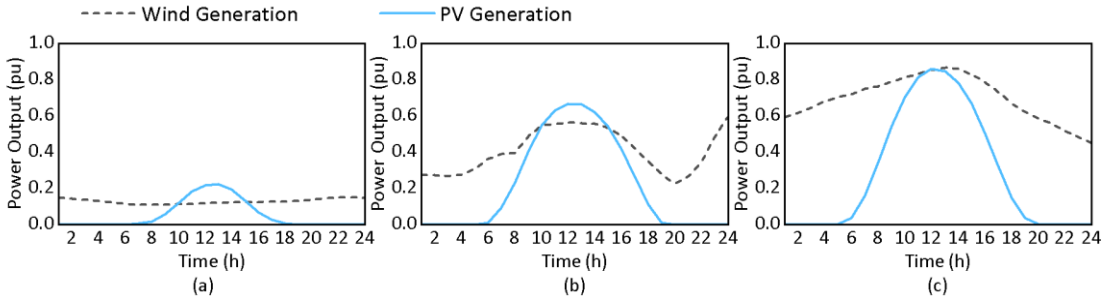

Figure 4-14 Three renewable generation scenarios. (a) low renewable generation, (b) medium renewable generation, (c) high renewable generation

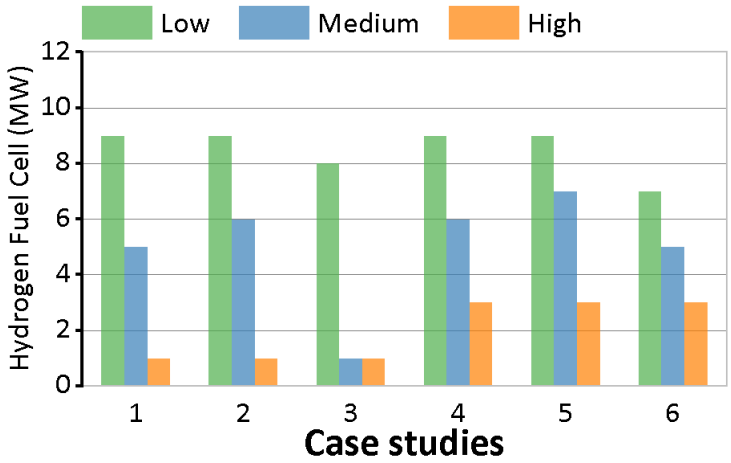

Figure 4-15 Hydrogen fuel cell capacities in different renewable generation scenarios

Figure 4-15 displays the optimal installation capacities of hydrogen fuel cells for three design days and six cases. The designed fuel cell capacities for EA plug-in charge cases (Case 1, 2, and 3) are more sensitive than those for EA battery swap cases (Case 4, 5, and 6). This is because the demand for EA plug-in charge cases is more concentrated during

the daytime when PV generates electricity, while the demand for EA battery swap is more evenly distributed throughout the day. With higher renewable generation power, the required capacities of hydrogen fuel cells decrease from 7 - 9 MW to 3MW for EA battery swap cases, and from 8 - 9 MW to 1 MW for EA plug-in charge cases.

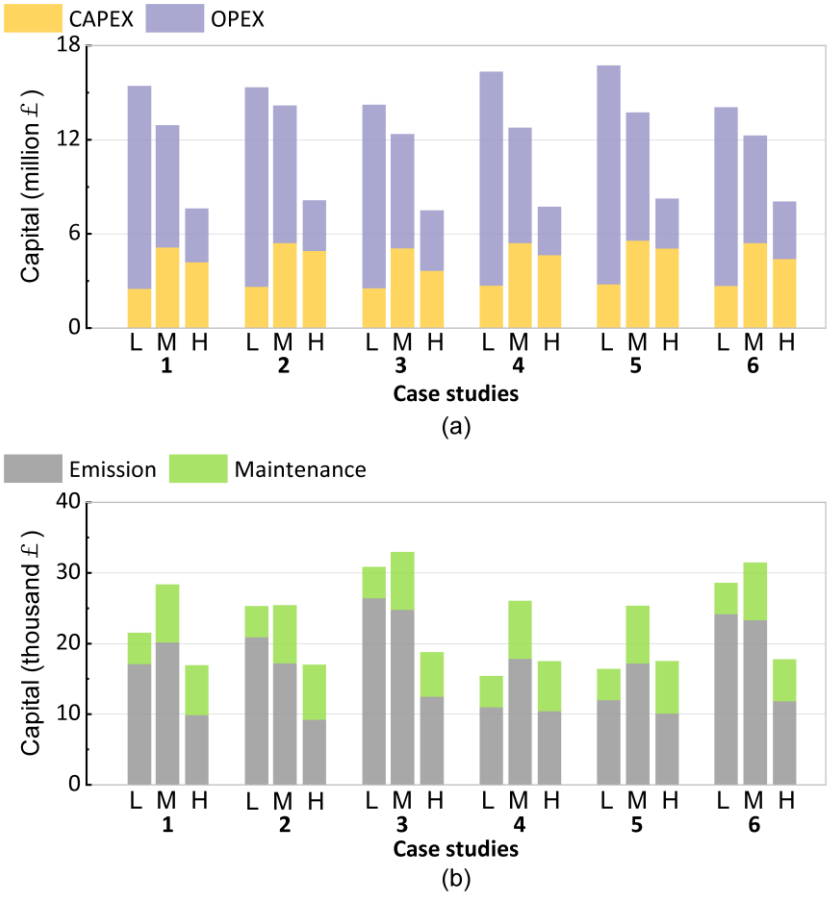

Figure 4-16 Optimal annualised costs under different renewable generation scenarios. (a) CAPEX and OPEX, (b) Emission and Maintenance Costs. L: low renewable generation, M: medium renewable generation, H: high renewable generation

Figure 4-16 presents the annualised costs for the six cases under three design days. For low renewable generation scenarios, less renewable generation power is expected, and the CAPEX is as low as around £2.5 million because no renewable generation unit is deployed. Under the low renewable generation situation, renewable resources are less economical for airport microgrid operation, and OPEX will be 50.5% to 87.8% higher than risk-neutral strategies. For high renewable generation scenarios, the CAPEX will be 5.5% to 25.6% lower than in medium renewable generation scenarios, while the OPEX will reduce dramatically by 47.4% to 61.7%, as most of the demand will be covered by

renewable generation resources. Under the low renewable generation scenario, Case 4 (EA battery swap without Parking EV) and Case 5 (EA battery swap with G2V) yield the lowest emission costs, indicating that battery swap systems are more beneficial when renewable generation is low. For the medium renewable generation scenario, Case 2 (EA plug-in charge with G2V) presents the lowest emission cost, suggesting that plug-in charging combined with G2V is optimal when renewable generation is moderate. In the high renewable generation scenario, Case 2 (EA plug-in charge with G2V) still performs well with the lowest emission costs, followed closely by Case 5 (EA battery swap with G2V).

4.6 Conclusions

This chapter presents a multi-objective infrastructure planning framework that aims to accommodate both parking EVs and EAs in the airport microgrid. The proposed framework includes two scheduling strategies for EA charging, namely, the EA plug-in charge strategy and the EA battery swap strategy. The trade-off objectives of economic and operational performance are optimised to evaluate the advantages and disadvantages of these strategies. With the proposed framework, the airport can economically accommodate EAs and operate safely.

The results of the study demonstrate that the adoption of the V2G strategy can improve the airport microgrid's performance in terms of economics and operation, compared to the G2V and without EV cases. The V2G service of the airport parking EVs can support the energy management of the airport microgrid with EA charging. Additionally, the parking EV is essential for reducing the total cost of future electrified aviation, which is a crucial consideration for airport operators.

The study also reveals that the EA battery swap strategy performs better than the EA plug-in charge strategy in terms of microgrid operation performance, regardless of whether EVs are involved or not, especially in the peak-to-valley ratio (PVR) and resilience factor (RF). Moreover, the difficulty of airport microgrid operation increases sharply with an increase in EA implementation level. Hence, it is essential to consider adopting an independent microgrid to support a higher EA implementation level.

Lastly, to handle the uncertainties of renewable generation and risks involved in the

planning and operation of the airport, a higher capacity of the hydrogen fuel cell is required to reduce the negative impact on the microgrid.

Overall, the findings of this study provide valuable insights that will help airport operators make informed decisions on how to achieve aviation electrification while optimizing the performance of the airport microgrid.

Chapter 5 Infrastructure Design for Airport Shuttle Bus Electrification

5.1 Introduction

Ground support vehicles at airfields are typically powered by fossil fuels, which contribute to air pollution and greenhouse gas emissions. To address this issue, there is a growing trend towards electrifying ground vehicles. However, implementing stationary charging facilities can be challenging due to limited movement space and time schedules at airports. Therefore, dynamic wireless charging technology has emerged as a promising solution to enable the stable electrification of airfield transport network. This chapter focuses on the implementation of wireless charging facilities for electric shuttle buses at commercial airports. To handle the large number of decision variables and constraints involved in the optimisation process, a multi-objective Non-dominated Sorting Genetic Algorithm-III (NSGA-III) and mixed integer linear programming (MILP) algorithm are employed. The traffic data for the airport shuttle buses is simulated using a multi-agent-based model (MABM).

The proposed system aims to integrate the airport ground support network with the power grid network in order to achieve sustainable aviation goals. To assess the techno-economic potential of wireless charging technologies, this chapter presents a bi-level optimisation framework is presented to determine the optimal design of the proposed wireless charging system. The framework is applied to three case studies, which demonstrate the feasibility of wireless charging technology for electric shuttle buses at airports. The analysis includes a thorough evaluation of the techno-economic factors, taking into account the costs of equipment, installation, and operation, as well as the environmental benefits of reducing emissions.

The chapter makes three significant contributions:

- A multi-agent-based model based on Anylogic software is proposed for simulating the airfield shuttle bus transport network. This model generates detailed position and energy consumption profiles of the shuttle buses, providing valuable information for optimising the wireless charging system. The use of this

model allows for a more accurate assessment of the energy requirements and operational characteristics of the electric shuttle buses, which is essential for designing an effective wireless charging system.

- A bi-level optimisation framework is developed that combines NSGA-III algorithm and MILP algorithm to solve the optimal planning problem for the wireless charging system. This framework enables the simultaneous optimisation of both the wireless charging infrastructure and the charging and discharging behaviours of airfield shuttle bus fleet. The use of a bi-level optimisation approach allows for a more comprehensive assessment of the trade-offs between various system design parameters, such as the number and location of PSU, the capacity of the batteries, and the charging strategy.
- The chapter conducts a techno-economic assessment of four different airport shuttle bus power systems: conventional diesel fuel, stationary wired charging, and wireless charging. This analysis investigates the potential cost reduction (including capital and operational expenses). The results of this assessment demonstrate the significant potential benefits of implementing wireless charging systems, which can reduce both costs and emissions.

This chapter is structured as follows: The multi-agent-based model framework for airport airfield traffic network simulation is proposed in Section 5.2. In Section 5.3, the mathematical formulation of the bi-level optimisation framework that is developed from the NSGA-III algorithm and MILP algorithm is presented. Case studies based on a realistic commercial airport (London City Airport) are presented in Section 5.4 and finally conclusions are summarised in Section 5.5.

5.2 Multi-Agent based Airport Transport Network Simulation

The airport transport network is a complex system involving the transportation of various vehicles and frequent communication between different individuals. Multi-agent-based modelling (MABM) is a computational approach that provides a framework for simulating and studying the interactions between multiple agents in a dynamic environment [169]. In this chapter, a multi-agent-based model is proposed to investigate the corporative behaviour of three agents involved in airport ground transportation dispatching.

The proposed multi-agent airport transport simulation system includes three agents: flight agent, air traffic coordinator agent, and shuttle bus agent, as shown in Figure 5-1. The flight agent is responsible for providing information about the arrival and departure of flights, which is essential for coordinating the movement of the shuttle buses. The air traffic coordinator agent is responsible for managing the air traffic at the airport and ensuring the safety of the flights. The shuttle bus agent is responsible for dispatching and managing the electric shuttle buses, including their routes and schedules.

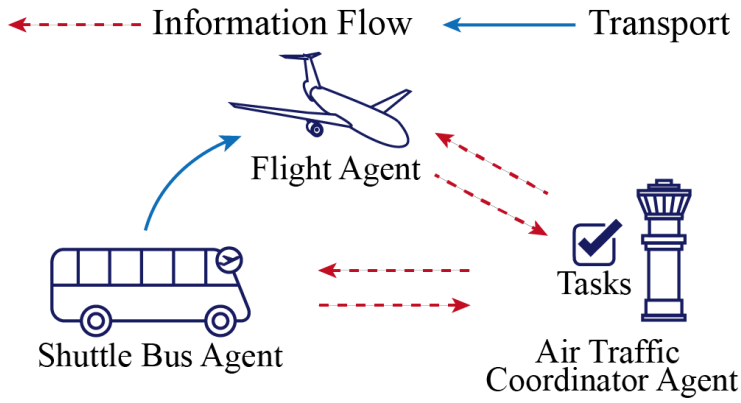

Figure 5-1 Multi-agent based airport transportation network simulation

5.2.1 Flight agent

The flight agent is responsible for representing the aircraft that requires boarding and disembarking services, which are conducted by airport shuttle buses. The population of flight agents and the time they enter the simulation environment are based on the realistic flight demand and schedules at the airport.

When an aircraft arrives at the airport, its ground service time and departure time are determined. The flight agent sends a service request to the air traffic coordinator agent, indicating the expected time of boarding and disembarking of the passengers. Upon receiving the request, the air traffic coordinator agent coordinates with the aggregator of shuttle bus agent to allocate the appropriate electric shuttle buses to the aircraft.

Once the shuttle bus arrives, the passengers disembark from the aircraft and travel to the terminal building by shuttle bus. The shuttle bus agent ensures that the electric shuttle buses are dispatched in a timely manner and follow the designated routes to transport the passengers.

When the flight is scheduled to departure in 15minutes, the flight agent sends another request for shuttle bus transportation to transport the passengers from the terminal building to the remote gates. The shuttle bus agent responds by dispatching the appropriate electric shuttle buses to transport the passengers.

By simulating the interactions between the flight agent and other agents in the multi-agent-based model, the proposed simulation system can provide a more accurate representation of the ground transportation system at the airport. The model generates detailed position and energy consumption profiles of the electric shuttle buses, which are used as input data for the wireless charging optimisation framework. The results of the simulation provide insights into the performance of the airport ground transportation system and help to identify potential areas for improvement.

5.2.2 Shuttle bus agent

As outlined in previous section, the shuttle buses play a critical role in transporting passengers to and from the aircraft parking at the remote gates. When not engaged in a transport task, the shuttle buses are aggregated into a fleet and managed by the "Aggregator". The air traffic coordinator agent communicates task messages to the Aggregator when shuttle bus services are requested to transport passengers.

The shuttle bus agent is responsible for recording position information and energy consumption profiles of each shuttle bus. Energy consumption profiles are calculated based on the length of operation, which is determined by the transport tasks assigned by the air traffic coordinator agent, as shown in Eq. (5.1). Upon completing an assigned task, the shuttle bus returns to the Aggregator and becomes available for the next task. The shuttle bus agent ensures efficient and effective use of shuttle buses for timely passenger transportation.

$$E_{s,t}^{bus} = E_{s,t-1}^{bus} - (1 - u_{s,t}^{bus}) \cdot v_{s,t}^{bus} \cdot f^{rate} \tag{5.1}$$

where $E_{s,t}^{bus}$ is the stored energy in the battery of sth shuttle bus at time t. $u_{s,t}^{bus}$ is the operation status factor of shuttle buses, 1 stands for operating, 0 stands for idling. $v_{s,t}^{bus}$ represents velocity of shuttle buses. f^{rate} is the energy consumption rate.

5.2.3 Air traffic coordinator agent

The air traffic coordinator agent is the central coordinator for the air transport management system. It plays a crucial role in receiving the service requirement message from the flight agents and assigning specific shuttle buses to conduct the services. Unlike other agents, the air traffic coordinator agent holds all the information about air transport movements, including the spatial information and operation status of shuttle buses, gate and departure time of flights. It ensures effective communication and coordination between different agents by acting as the dispatcher.

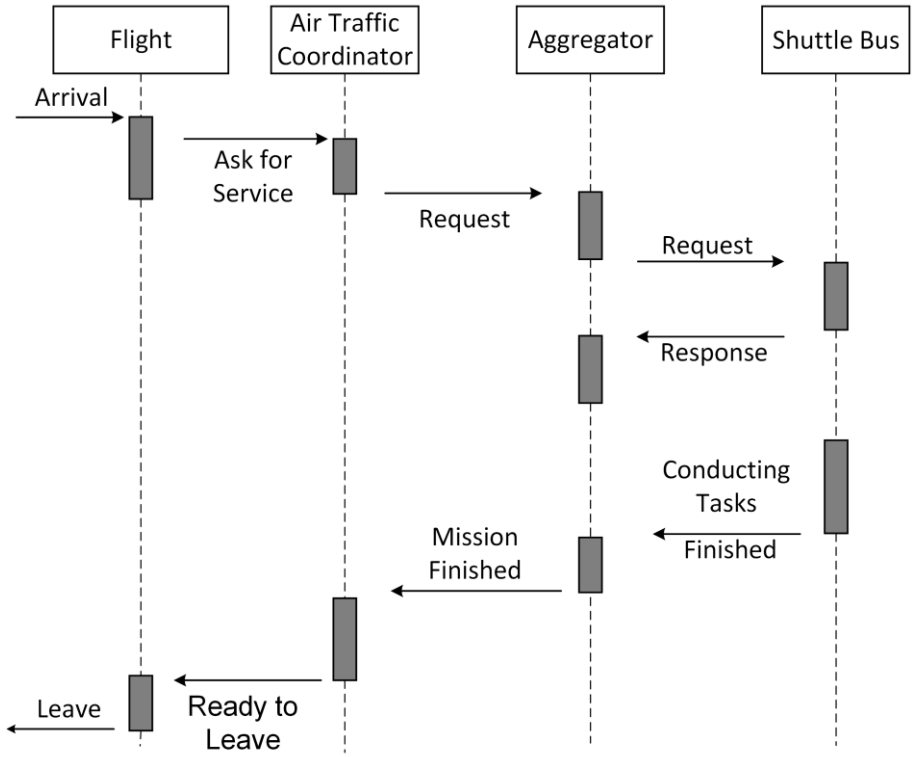

Figure 5-2 MABM communications between flight agent, air traffic coordinator agent, aggregator, and shuttle bus agent

When flight agents communicate and share information with the air traffic coordinator agent, it creates a task request for shuttle bus agents. The task is a discrete event that allocates the appropriate vehicle agents to serve various aircraft based on the information gathered by the other agents. The air traffic coordinator agent records the position information for parameter $L_{s,t}$ of shuttle buses, which is a critical profile generated from the proposed MABM simulation. The interactions between different agents in the airport

transport network are shown in Figure 5-2, where the air traffic coordinator agent communicates with other agents to ensure efficient and effective transportation services for passengers.

5.3 Bi-level Optimisation Framework Formulation

After conducting the MABM simulation presented in Section 5.2, the position information and energy consumption profiles of shuttle buses are obtained. In order to optimise the charging and discharging behaviours as well as WPT installation solutions, a large number of requirements need to be met. To handle the complexity of the problem, the WPT installation problem is formulated as a bi-level optimisation framework, as shown in Figure 5-3.

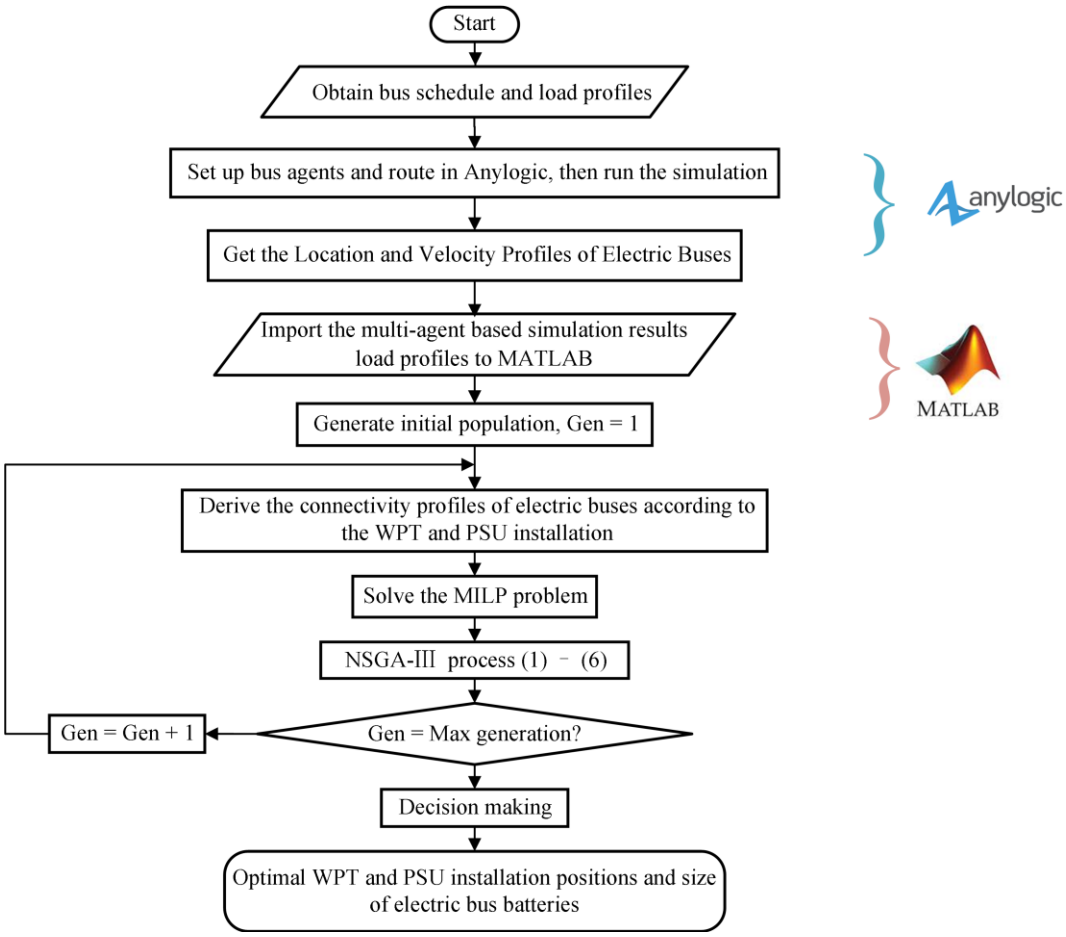

Figure 5-3 Flowchart of the overall algorithm

The primary level of the framework utilises the Non-dominated Sorting Genetic Algorithm-III (NSGA-III) to determine the optimal WPT and PSU installation positions.

These positions are then passed to the secondary level problem, which optimises the charging and discharging behaviours of the electric shuttle buses based on the WPT and PSU installation decisions. The secondary level problem is formulated as MILP model, which takes into account a variety of constraints and decision variables to determine the optimal charging and discharging behaviours. Overall, this bi-level optimisation framework provides a comprehensive approach to optimising the design and operation of the proposed wireless charging system.

5.3.1 NSGA-III Infrastructure Design

The proposed primary infrastructure design problem was solved using the effective multi-objective heuristic algorithm known as the NSGA optimisation algorithm [170], which is described in this section. Following the NSGA-II algorithm, the NSGA-III algorithm uses a reference-point-based technique presented in [171] to enhance performance while addressing multi-objective problems. The selection operator, which was created for maintaining variety among population members by updating reference points, is the only distinction between the NSGA-III algorithm and the NSGA-II algorithm. The NSGA-III optimisation technique was used to produce a number of pareto front solutions. The reference points are selected using the Das and Denis approach [172] prior to running the NSGA-III algorithm. The trade-off between two or more objectives is displayed by the pareto front. The decision-making process is the same as described in Section 4.4.2.

The NSGA-III algorithm is a multi-objective optimisation algorithm that is widely used in solving optimisation problems. The logic flow of the NSGA-III algorithm is composed of several steps. First, the algorithm begins with a population of particles that are randomly generated. Then, the algorithm sorts the particles and validates their rank to establish how far apart they are from one another as they move along fronts. The crowding distance between particles is calculated after sorting people by rank. This process is known as random non-dominated sorting and crowding.

Next, the algorithm uses game selection, which is a gaming approach for selecting two populations to participate in upcoming crossover and mutation operations. The game selection theory states that particles in a less congested zone and with a lower (better) rank are adopted first. After selecting the particles for crossover and mutation, a new population is created. The population recombination process follows, where a combined

population with the parent and current populations is formed at each generation to develop non-dominant fronts. The dominance criterion of all feasible solutions is assessed to achieve population recombination.

The NSGA-III algorithm's sorting and selection procedure occurs in the new generation. The sorting approach involves three steps: normalizing the objective functions of the population into numbers within the range 0 to 1, associating each individual of the population to a reference point, and performing niche preservation operation by counting the number of members of the population that are associated with reference points, and exclude the reference points that there is no member associated. Then apply non-dominated sorting approach.

Finally, the replicated population is used to create a new generation using the same methodology as previously. The NSGA-III algorithm is a powerful tool that can be used to solve many optimisation problems, including those with multiple objectives. The aforementioned steps result in the generation of a set of probable optimal solutions that represent distinct energy dispatch scenarios.

$$\mathrm{PF} = \{y_1(x), y_2(x), \dots y_r(x)\}, x \in \mathbb{Q} \tag{5.2}$$

where $\mathbb{Q}$ is the feasible search space, $y_r(x)$ are sets of pareto optimal solutions, r is the number of population.

The installation locations of WPT and PSU are determined by binary variables Θ^{wpt} and Θ^{psu} at the primary level. While there is no limit on the number of WPTs that can be installed, only one PSU is installed in order to connect all WPTs to the network.

$$\Theta^{wpt} = \{wpt_1, wpt_2, \dots wpt_w\}, w \in \mathbb{R} \tag{5.3}$$

$$\Theta^{psu} = \{psu_1, psu_2, \dots psu_m\}, \mathrm{m} \in \mathbb{N} \tag{5.4}$$

$$\sum_z p_z = 1 \tag{5.5}$$

where $\mathbb{R}$ and $\mathbb{N}$ denote collections of routes that are potentially being installed with WPT and network nodes being installed with PSU respectively.

By incorporating the position information of shuttle buses $L_{s,t}$ obtained from MABM simulation, the connectivity information of shuttle buses can be determined. Specifically,

a matrix $C_{s,t}$ containing full of binary parameters is created to represent whether each shuttle bus is connected to the network at each time interval. For example, if a WPT is installed along a route wpt_w, all positions in $L_{s,t}$ that correspond to wpt_w are set to 1 in the corresponding positions of $C_{s,t}$.

The NSGA algorithm implements power flow during each evaluation cycle to prevent network constraint violations. Backward forward sweep (BFS) algorithm [173] [174], a precise and effective voltage dependent power flow algorithm, is used to solve the ac power flow. This step ensures that the proposed solution meets the power system constraints and regulations. The power flow analysis evaluates the distribution network's ability to accommodate the charging load and determines if there are any violations of the network's voltage drop limits. By incorporating power flow compliance analysis, the proposed solution ensures that the charging operations of the electric shuttle buses do not violate the stability constraints of the distribution network.

(1) Backward sweep

Backward sweep technique is the BFS algorithm's first stage. In this stage, the voltage $V_{i,t}^{o}$ is assumed for o-th iteration, and the Kirchhoff's current law (KCL) is used to determine the current at each bus. The following formulas are used to calculate the bus current $I_{i,t}^{o}$ for o-th iteration and apparent power $S_{i,t}$:

$$I_{i,t}^{o} = \left(\frac{S_{i,t}}{V_{i,t}^{o}}\right)^{*} \tag{5.6}$$

$$S_{i,t} = P_{i,t} + jQ_{i,t} = \left(P_{i,t}^{G} + jQ_{i,t}^{G}\right) - \left(P_{i,t}^{L} + P_{i,t}^{ES} + jQ_{i,t}^{L}\right) \tag{5.7}$$

where $P_{i,t}$ and $Q_{i,t}$ represent the real and reactive power at bus i, $P_{i,t}^{G}$ and $Q_{i,t}^{G}$ denote the real and reactive generation power output at bus i, $P_{i,t}^{L}$ and $Q_{i,t}^{L}$ are the real and reactive power consumption of conventional loads, $P_{i,t}^{ES}$ is the aggregate charging/discharging power of the WPT system.

Then the branch current $I_{ij,t}^{o}$ is calculated by summing in the backward direction from the end node j to the root node p, which is given by:

$$I_{ij,t}^{o} = I_{j,t}^{o} + \sum_{p} I_{jp,t}^{o}, p \in \Psi_{j} \tag{5.8}$$

where Ψ_j is the set of all buses that are adjacent to bus j downwards.

(2) Forward sweep

Based on Kirchhoff's Voltage Law, the forward sweep procedure looks for a voltage decrease from the upstream bus to the downstream bus (KVL).

$$V_{j,t}^{o} = V_{i,t}^{o} - Z_{ij} I_{ij,t}^{o} \tag{5.9}$$

where $V_{i,t}^{o}$ and $V_{j,t}^{o}$ represent the voltage at bus i and bus j. Z_{ij} is the impedance of the branch ij.

(3) Voltage tolerance

The voltage difference between the current step and the step before it, minus the tolerance parameter σ ($\sigma = 10^{-4}$ in this research), is the iteration convergence condition.

$$\Delta V_{i,t}^{o} = V_{i,t}^{o} - V_{i,t}^{o-1} \tag{5.10}$$

$$\begin{cases} \left|Re\left(\Delta V_{i,t}^{o}\right)\right| \le \sigma \\ \left|Im\left(\Delta V_{i,t}^{o}\right)\right| \le \sigma \\ \left|\Delta V_{i,t}^{o}\right| \le \sigma \end{cases} \tag{5.11}$$

When the iteration is terminated, the voltage $V_{i,t}$ and current $I_{i,t}$ at each node equal the final converged value of $V_{i,t}^{o}$ and $I_{i,t}^{o}$, respectively.

The apparent power of each branch $S_{br,t}$ should be within the limitation:

$$S_{br,t} = \sqrt{{P_{br,t}}^2 + {Q_{br,t}}^2} \le S_{br}^{max} \tag{5.12}$$

$$P_{br,t} = \sum_{ij} P_{ij,t}^{G} - \sum_{ij} P_{ij,t}^{L} \tag{5.13}$$

$$Q_{br,t} = \sum_{ij} Q_{ij,t}^{G} - \sum_{ij} Q_{ij,t}^{L} \tag{5.14}$$

The following constraints are node voltage constraints and feeder thermal limits.

$$(1-\varepsilon)V_0 \le V_{i,t} \le (1-\varepsilon)V_0 \tag{5.15}$$

$$I_{ij,t} \le I_{ij}^{max} \tag{5.16}$$

The power loss of the network can be calculated by the equation:

$$P_t^{loss} = \sum_{i,t} R_{ij} \left[\frac{|V_{i,t} - V_{j,t}|}{Z_{ij}} \right]^2 \quad 5.17$$

The proposed primary optimisation framework is designed to address the challenges of wireless charging technology for electric shuttle bus deployment at airports. The framework is based on a bi-level optimisation approach with two conflict objective functions. The first objective aims to minimise the battery costs, including both capital and operation and maintenance (O&M) costs for batteries.

To achieve the first objective, the framework considers the cost of the batteries, including the initial cost of purchasing and installing the batteries, as well as the ongoing O&M costs, such as electricity purchasing and infrastructure maintenance costs. The optimisation algorithm is designed to identify the optimal battery capacity and the number of batteries required to meet the operational requirements of the electric shuttle buses, as shown in Eq. (5.18).

The second objective seeks to minimise the infrastructure installation costs for wireless power charging points (CAPEX) and the energy consumption cost of shuttle buses (OPEX), including the power loss of the network, as shown in Eq. (5.19). Both battery costs and the CAPEX are annualised with the CRF, which is calculated with Eq. (5.21).

$$Min\ Obj_1 = \frac{r \cdot (1+r)^y}{(1+r)^y - 1} \cdot C_{batt} \cdot E^{max} \quad 5.18$$

$$Min\ Obj_2 = CAPEX + OPEX \quad 5.19$$

$$CAPEX = \frac{r \cdot (1+r)^y}{(1+r)^y - 1} \sum_{dev} (CAP_{dev} \cdot \pi_{dev}) \quad 5.20$$

$$OPEX = d \cdot \left(\sum_t \left(\left(\pi_t^e + \pi_{CO_2} \cdot \vartheta^{grid} \right) \cdot \left(P_t^{grid} + P_t^{loss} \right) \right) + \pi^p \max\left(P_t^g \right) \right) \quad 5.21$$

where E^{max} represents the capacity of EV batteries. C_{batt} is the purchasing price for battery per kWh. The subscript dev denotes the installed devices, CAP_{dev} is the installed capacity of device dev, r is the discount rate, y is the number of years in lifetime, d is the number of representative days. π_t^e is the time-of-use electricity price, π_{dev} is the capital cost of device dev. P_t^{grid} is the imported grid electricity, π_{CO_2} is the penalty fee

for CO_2 emissions. ϑ^{grid} denotes the emission factor of the grid electricity. π^p is the demand charges for the peak electricity demand.

The primary decision variables, which include installation positions of WPT and PSU, will be passed on to the secondary level for optimisation of charging and discharging dispatch.

5.3.2 MILP-based Wireless Charging Management

Due to the large number of decision variables and constraints involved in the problem, the secondary layer problem was formulated using mixed integer linear programming problem as a heuristic algorithm was insufficient to handle the complexity. MILP formulation is better suited for solving such complex problems and ensures efficiency in the optimisation process.

The MILP problem is solved for each evaluation of the population generated in the NSGA-III algorithm. The objective of the MILP problem is to obtain an optimal charging / discharging dispatch profile for electric shuttle buses, given the current WPT and PSU installation choices of each individual in the NSGA-III algorithm. By formulating and solving the MILP problem for each individual, the NSGA-III algorithm is able to generate a diverse population of solutions that effectively represent the trade-offs between conflicting objectives.

The charging constraints for electric shuttle buses are derived from their transportation profiles, which consists of two main components: the energy consumption profile $E_{s,t}^{cons}$ and the connectivity profile $C_{s,t}$. The energy consumption profile describes the amount of energy consumed by the shuttle buses at each time slot during its operation, while the connectivity profile represents the availability for wireless charging at different location and times.

To manage the charging and discharging process, two binary variables are used: $u_{s,t}^{ch}$ controls the charging behaviour, and $u_{s,t}^{disc}$ controls the discharging behaviour. These variables are designed to optimise the charging and discharging operations of the shuttle bus fleet, while ensuring that the charging constraints are met.

$$u_{s,t}^{ch} + u_{r,t}^{disc} \leq 1 \qquad 5.22$$

$$P_{s,t}^{ch} = u_{s,t}^{ch} \cdot P^{rated} \quad 5.23$$

$$P_{s,t}^{disc} = u_{s,t}^{disc} \cdot P^{rated} \quad 5.24$$

The connectivity between electric shuttle buses and WPTs is represented by a matrix $C_{s,t}$. Specifically, if the s-th electric shuttle bus is connected to a WPT at time t, the corresponding value in the matrix $C_{s,t}$ is set to 1; otherwise, it is set to 0.

To ensure the safe and efficient operation of the WPT systems, a power limit is imposed on the connectivity between electric shuttle buses and WPTs. The power limit is expressed as the following equation:

$$P_{s,t}^{disc}, P_{s,t}^{ch} \leq C_{s,t} \cdot P^{rated} \quad 5.25$$

The amount of energy stored in each shuttle buses is expressed as follows:

$$E_{s,t}^{bus} = E_{s,t-1}^{bus} + \eta^{wch} \cdot P_{s,t}^{ch} - P_{s,t}^{disc}/\eta^{wch} - E_{s,t-1}^{cons} \quad 5.26$$

$$E_{s,0}^{bus} = E_{s,T}^{bus} \quad 5.27$$

$$0.2 \cdot E^{max} \leq E_{s,t}^{batt} \leq E^{max} \quad 5.28$$

where η^{wch} represents the efficiency for wireless charging.

The total charging power required by the shuttle buses is formulated as follows:

$$P_t^{ES} = \sum_s \left(P_{s,t}^{ch} - P_{s,t}^{disc}\right) \quad 5.29$$

Once the MILP problem is solved, the total charging power of electric shuttle buses is returned to the NSGA-III algorithm for power flow compliance analysis.

5.3.3 Secondary objective function

The objective of the secondary level problem is to minimise the overall cost associated with the electric shuttle bus system. This cost includes the annualised cost of the batteries installed in the electric shuttle buses, as well as the annual cost of purchasing electricity for charging the batteries. The problem seeks to find an optimal solution with minimum costs while meeting the charging constraints and other operational requirements.

$$Min \left(CRF \cdot C_{batt} \cdot N_{ev} \cdot E^{max} + d \cdot \sum_t \pi_t^e \cdot P_t^{ES} \right) \quad 5.30$$

where C_{batt} is the battery purchasing cost, N_{ev} is the number of EVs.

5.4 Case studies

To demonstrate how the proposed approach can be applied in real-world scenarios, a comprehensive case study is investigated on London City Airport (IATA code: LCY). LCY is a regional airport located in London, England, with a standard linear terminal building. The flight demand at LCY airport on a typical day is shown in Figure 5-5.In this study, the airfield transport network and power network topologies of LCY airport are analysed, which are presented in Figure 5-4. The power network consists of nine nodes (N1 – N9), which are located at contact gates in the terminal building. Additionally, there are 24 gate positions (G1 – G24) and 18 shuttle bus transport routes (R1 – R18) throughout the airport. It is worth noting that in this study, the power network supplying LCY airport was assumed to be an IEEE 9-bus radial distribution network, with each node located at one contact gate at the terminal building. The chosen distribution network may not accurately represent a common distribution network in Great Britain. However, it has been selected in this context specifically for testing the proposed optimisation framework.

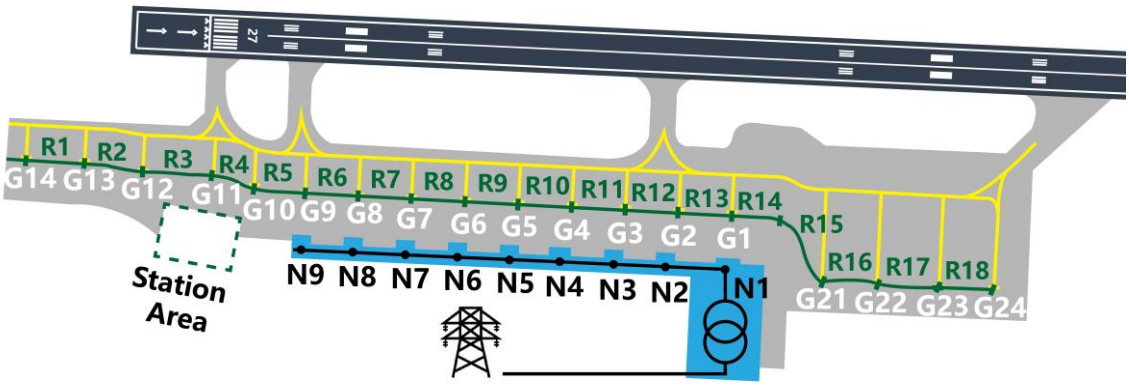

Figure 5-4 The airport ground transportation network and the IEEE 9-bus radial distribution network framework in London City Airport (LCY)

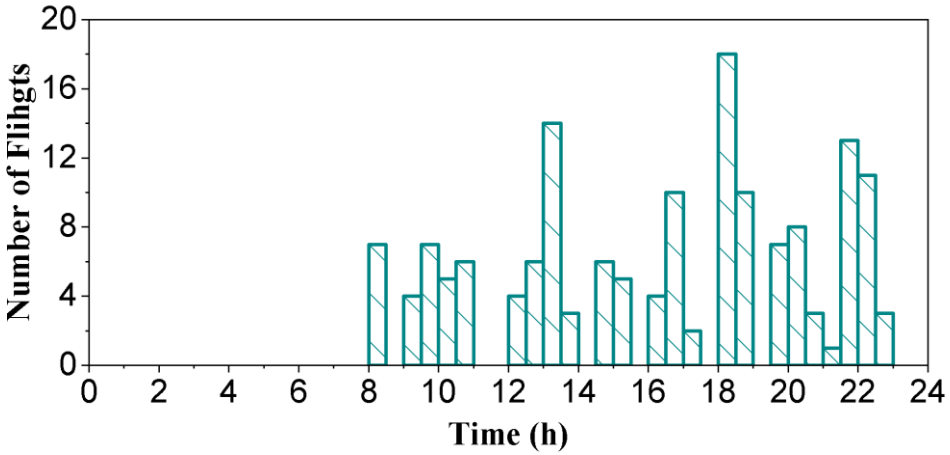

Figure 5-5 The flight demand at LCY airport on 31st March 2019 on a half-hourly basis

The candidate installation positions of WPT and PSU were identified at all power network nodes and shuttle bus transport routes. The total number of shuttle buses is assumed to be 60 (the minimum number of shuttle buses that can fulfil the flight service demand without causing any delay according to the proposed multi-agent-based simulations). The energy consumption rate for diesel of the shuttle bus was 0.32 L/km, while the energy consumption rate for electricity was 1.27 kWh/km, which were obtained from [175]. The speed of shuttle buses was assumed to be 15 miles per hour for the shuttle buses.

To assess the economic parameters and energy factors associated with the proposed approach, Table 5-1 and Table 5-3 were used, respectively. The simulation was conducted on one of the busiest days (31st March) in 2019, taking into account the flight demand at LCY airport, as shown in Figure 5-5. This enabled a comprehensive analysis of the effectiveness of the proposed approach.

There are two benchmark scenarios: Case 1: no electrification, all shuttle buses are using diesel; Case 2: EV wired charging; and two investigated scenarios: Case 3: EV wireless charging.

1) Case 1: no electrification is implemented, and all shuttle buses continue to use conventional diesel fuel.
2) Case 2: Electric shuttle buses are introduced, and wired charging is used at the stationary charging facilities located at node 9 of the distribution network, as shown in Table 5-2 and Figure 5-4. The assumption is that all electric shuttle buses are equipped with batteries that are fully charged at the beginning of the day,

which can meet the power requirements of the day's flight service missions. A regular AC charger with a rated power of 50 kW is used to charge the buses during the off-peak period from 0:00 to 6:00 when the airport is not in operation. Under this scenario, it is assumed that the airport shuttle buses will only be recharged during off-peak hours, with no charging occurring during daytime operations. This scenario requires a battery energy capacity of 174.5 kWh and a total of 33 chargers.

3) Case 3: Electric shuttle buses are charged wirelessly through installed unidirectional WPT and PSU.

The modelling and simulations are conducted on a PC equipped with AMD Ryzen 5 3500X 3.6 GHz processor and 16 GB RAM. The MABM simulation is implemented in Anylogic software, and the bi-level optimisation framework is developed in the MATLAB 2021a environment and solved with Gurobi solver and YALMIP software. The MABM simulation takes 1 minute 12 seconds to complete. The optimisation times for Case 3 is 25 minutes.

The electricity pricing mechanism used in this study is the time-of-use (TOU) pricing, which varies throughout the day [167]. The electricity prices are set at £0.07 per kWh during off-peak hours (00:00-07:00), £0.15 per kWh during mid-peak hours (10:30-16:00 and 21:00-24:00), and £0.2 per kWh during peak hours (07:00-10:30 and 16:00-21:00), with an additional demand charge of £0.2 per kW per day. The demand charge is calculated based on the maximum power demand during the operation.

Table 5-1 Economic parameters of technologies [144]

Device	Installation cost	Maintenance cost	Cases
WPT	89,264 £/mile	892 £/mile per year	3, 4
PSU	10,000 £/each	100 £/year	3, 4
Pickup device	5000 £/each	-	3, 4
EV 50 kW Chargers	2,500 £/each	250 £/10 years	2

Table 5-2 Line and load data of the IEEE 9 bus radial test system

	Bus Number								
	1	2	3	4	5	6	7	8	9
P (kW)	1840	980	1790	1598	1610	780	1150	980	1640
Q (kVar)	460	340	446	1840	600	110	60	130	200
i bus	0	1	2	3	4	5	6	7	8
j bus	1	2	3	4	5	6	7	8	9
$R_{i,j}$ (Ω)	0.123	0.014	0.746	0.698	1.983	0.905	2.055	4.795	5.343
$X_{i,j}$ (Ω)	0.413	0.605	1.205	0.608	1.728	0.789	1.164	2.716	3.026

Table 5-3 Energy prices/factors of airport power system

Parameter	value	Ref
Fuel price	1.3 £/kg	[176]
CO_2 Emission factor of diesel fuel	2.68 kg/L	[177]
CO_2 Emission factor of electricity	0.257 kg/kWh	[178]
CO_2 Emission cost	75 £/t	[179]

5.4.1 Pareto fronts

Figure 5-6 displays the resulting non-dominated Pareto front solutions for Case 3. The solution shows annualised CAPEX and OPEX ranging from 0.360 to 0.395 million pounds, while the battery cost range from 0.014 to 0.046 million pounds.

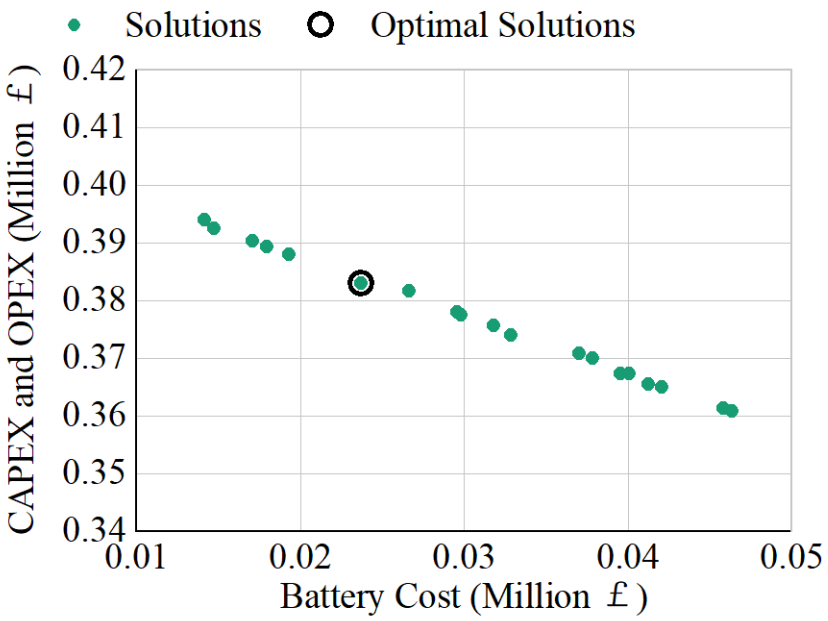

Figure 5-6 Pareto front for Case 3

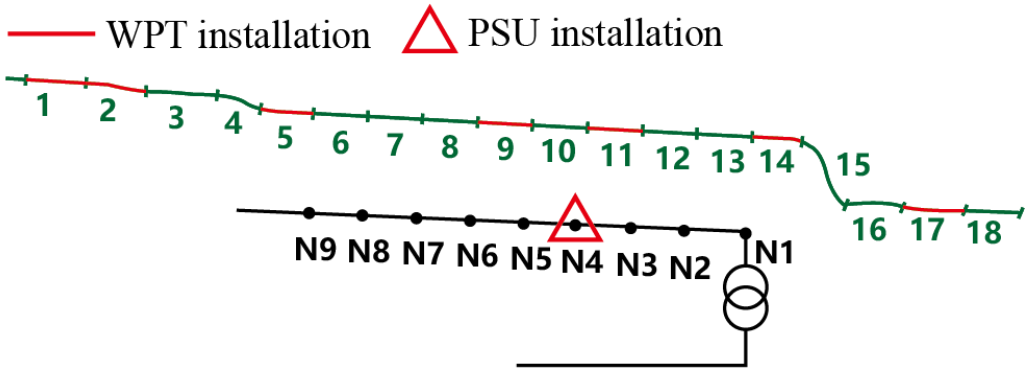

Figure 5-7 WPT and PSU installation positions for wireless charging (Case 3)

Figure 5-7 shows the optimal installation positions of WPT for Case 3. In this case, there are seven routes equipped with WPT, and the distance between the PSU and the closest WPT is approximately 68 metres and the PSU is installed on node 4.

5.4.2 Charging power and aggregate stored energy

Figure 5-8 and Figure 5-9 illustrate the electric shuttle bus charging power dispatch and aggregate stored energy in the shuttle bus fleet. Figure 5-9 (a) reveals that the electric shuttle buses recharge during early morning hours (1 to 5 am) when there is no flight demand, as the fleet is in use during the daytime. As a result, large batteries are required

to ensure that daytime energy consumption is met, as shown in Figure 5-8. On the other hand, the demand for wireless charging of electric buses is evenly distributed during the daytime, as demonstrated in Figure 5-9 (b).

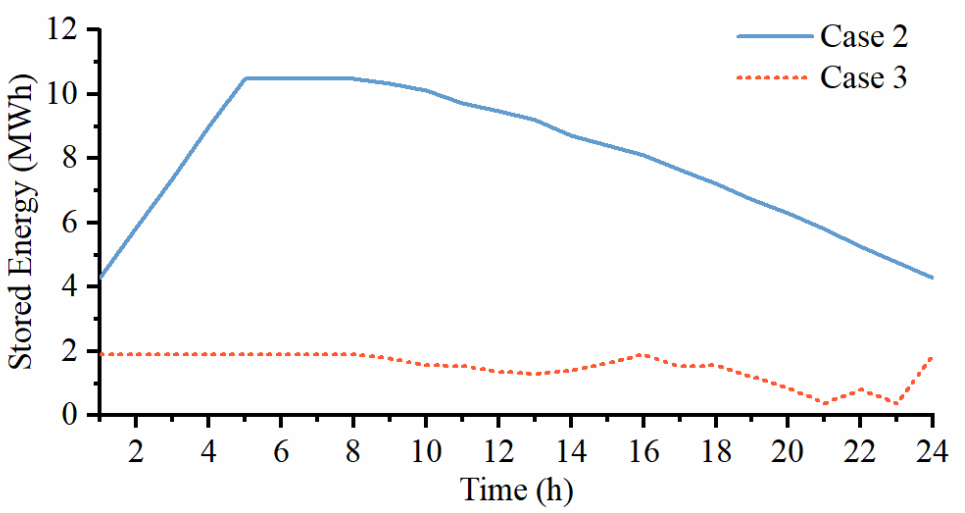

Figure 5-8 Aggregate energy storage of all electric shuttle buses for Case 2 and Case 3

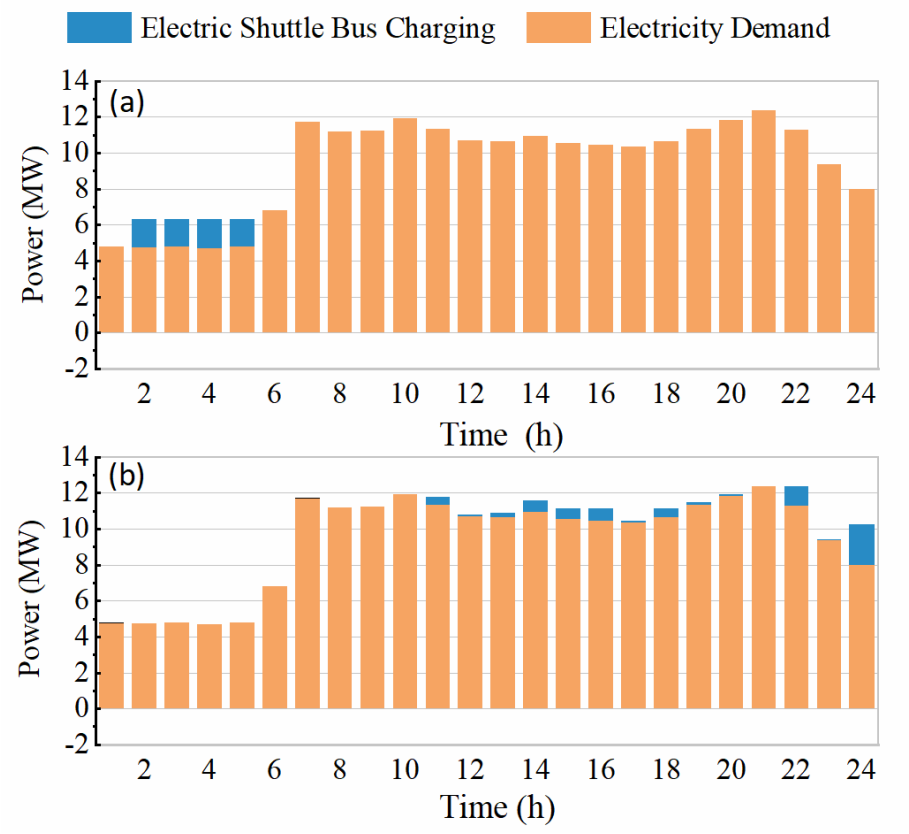

Figure 5-9 Charging and discharging power dispatch results for (a) Case 2 and (b) Case 3

Table 5-4 provides a comparison of the demand profile characteristics of Cases 2, and Case 3. The findings indicate that wireless charging technology, used in Case 3, had similar peak and average demand values as wired charging technology, used in Case 2. This suggests that wireless charging can provide the same level of power output and charging capacity as wired charging while eliminating the need for physical connections between the vehicle and the charger.

Table 5-4 Comparison of demand characteristics between three cases

Cases	Peak demand (MW)	Average demand (MW)	Peak hour	Annual electricity charges	
				TOU charge (million £)	Demand charge (million £)
2	12.37	9.69	21:00	6.37	0.12
3	12.37	9.72	21:00	6.47	0.11

5.4.3 Economic analysis

The figure presented in Figure 5-10 shows the total annualised cost results for the three cases. Among the electrification cases (Cases 2 - 3), the conventional diesel shuttle buses (Case 1) have significantly higher costs, mainly due to the high fuel price. The plug-in charging option (Case 2) has a higher cost because of the larger battery size, but the electricity cost is lower due to lower night-time electricity prices.

Moreover, it is worth mentioning that the emission cost of Case 1 is significantly higher than that of the electrification cases (Cases 2 - 3). Specifically, the emission cost of Case 1 is 159%, and 132% higher than that of Case 2, and Case 3, respectively. This indicates that the emission tax could be a vital factor that encourages airport designers and operators to consider electrifying their shuttle fleets to avoid high carbon tax in the future.

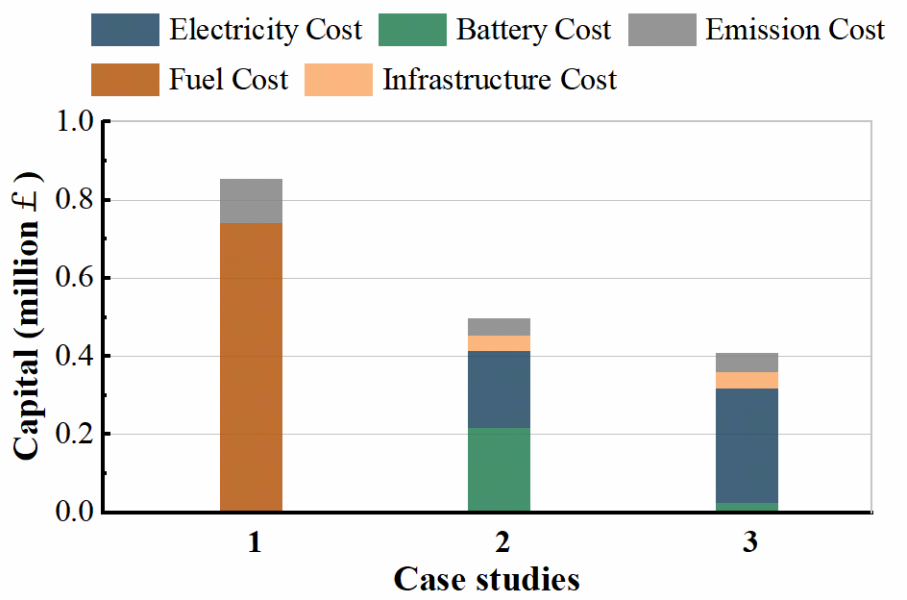

Figure 5-10 Annualised costs of all three cases

5.5 Conclusions

In this chapter, a bi-level optimisation framework is proposed for the allocation of WPT and PSUs in the airfield traffic network and distribution power network of a commercial airport. The framework aims to address the challenge of electrifying airport ground vehicles while ensuring that the distribution network can accommodate the additional demand. Four case studies are presented to demonstrate the techno-economic feasibility of using wireless charging technology for airport electric shuttle buses.

The economic analysis shows that the annualised operation cost of conventional diesel shuttle buses is much higher than that of electric shuttle buses, making electrification a promising option. Wireless charging technology allows for smaller batteries to be used in electric shuttle buses while still achieving the same performance.

In summary, the results suggest that future airport designers and operators are likely to adopt electrification of ground vehicles in the airside of the airport, with wireless charging technology being an attractive option for economic reasons. The benefits of this approach are demonstrated through a realistic example.

Future research could explore the potential of cooperation between electric ground support vehicles, airport parking EVs, and future adopted electric aircraft. Additionally, the feasibility of wireless charging technology on road traffic and ordinary electric

vehicles could be investigated. Overall, this chapter highlights the potential of wireless charging technology to revolutionize airport ground vehicle electrification, paving the way for a greener and more sustainable aviation industry.

Chapter 6 Power Grid Ancillary Services through Aviation-to-Grid Flexibility

6.1 Introduction

This chapter proposes a novel concept of 'Aviation-to-Grid (A2G)' flexibility that utilises EA battery charging to provide frequency reserve services to the power grid. Smart battery swap-based EA charging system is developed, utilising PV, gas turbine, and grid electricity. An hourly energy dispatch strategy is proposed based on the mixed integer linear programming, which is designed to meet the demand for electrified aviation charging while simultaneously providing A2G frequency response to the power grid. The A2G flexibility concept addresses the challenges of high-power and highly-scheduled EA charging, while also exploring new flexibility provisions from EA charging. By utilising EA battery charging system to provide frequency response for frequency regulation. A2G frequency response services can be enhanced even further by coordinating with airport gas turbines which are primarily used to provide off-grid and high-power charging to the swappable EA batteries. To validate the feasibility and effectiveness of the proposed A2G flexibility concept, case studies were conducted in 8 major UK airports. These case studies considered seasonal flight schedules and power system operation scenarios.

The main contributions of this chapter are:

- An EA charging system is developed to handle highly-scheduled charging patterns that are driven from the electrified air transport. The developed charging system is able to accommodate high-power charging in a short flight turnaround time at airports.
- A novel A2G concept that uses EA charging as a new energy resource to provide flexibility to the power grid. Coordinated energy control solutions of EA batteries and gas turbines will provide combined primary and secondary frequency responses to grid disturbance. This approach enables the integration of electrified air transport into the power system, while also providing a reliable and sustainable source of frequency response to the grid.

The rest of this chapter is structured as follows: The infrastructure of the EA charging system is proposed in Section 6.2. In Section 6.3, the mathematical formulation of the Aviation-to-Grid frequency response framework is presented. Case studies based on 8 UK major commercial airports are presented in Section 6.4 and finally conclusions are summarised in Section 6.5.

6.2 Electric Aircraft Charging Systems

The research in this chapter focuses on the UK air transport sector and the GB power system. In the UK, there are 40 commercial airports with a high volume of domestic and international flights. However, due to the significant investment required in electric charging infrastructure, it is assumed that the top 8 busiest UK airports are electrified. In addition, in these airports, only domestic flights are considered to be electrified due to battery energy density and range anxiety of EA.

To further support this research, the annual air traffic data for UK airports was obtained from the UK Civil Aviation Authority (CAA) [180]. Based on this data, it was found that the top 8 UK airports serve around 37% of the total number of UK domestic air passengers. Therefore, focusing on these airports provides a significant opportunity to explore the potential of utilising EA charging as a flexible resource to support the power grid, while meeting the demand for electrified air transport in the UK.

Based on the analysis in Chapter 3, there are two technical approaches to recharge the EA batteries. The first approach is to implement fast chargers, which aims to recharge EA batteries during the ground handling process for the flight similar to the fuel refilling. However, flight schedule data from London Heathrow Airport shows that domestic flights typically park at the gate position for only 30 to 50 minutes [181], which is a limited time period to recharge the EA batteries for medium-range aircraft with high-power chargers (50 MW level chargers for the proposed EA). There are significant technical barriers to develop the chargers for EA, such as power capacity, overheating, battery degradation, and the network constraints.

As an alternative, the battery swap approach is proposed, where all EA batteries can be recharged on the ground for a flexible time period and then swapped to the arrival aircraft during the ground handling process [29]. The battery swap is chosen as the suitable

technology for integrating into existing airport operation management in our case studies, as it avoids the need for 50 MW level chargers with long battery charging time, which would delay the flight journey.

Aviation is a highly scheduled transportation monde that allows airport operators to manage the arrival and departure times of aircraft and fit the battery swap process in between. The battery swap process is conducted together with the ordinary cargo loading and unloading processes, taking around 30 minutes after the EA has parked at the apron with all passengers de-boarded [29]. Therefore, an analysis of the charging schedule is required for the economic dispatch of the airport charging system for battery swap process. This ensures that the battery swap process can be effectively integrated into the airport's operation management, providing a reliable and efficient solution for EA batteries.

Based on our analysis in this study, a significant amount of daily energy consumption, amounting to 8.7 GWh daily, is required for EA charging in the top 8 UK airports. Such high energy demands cannot be fully met by grid-level energy supply alone. Therefore, a more comprehensive airport energy system that includes gas turbines, PV and microgrid is proposed.

Specifically, the proposed integrated energy system allows for 50% off-grid charging using the airport gas turbines and microgrid, which can help relieve the grid-level energy requirements. Additionally, 15% of charging energy can be supplied by renewable energy sources. By combining these energy sources with grid-level power supply, a robust airport microgrid can be created by combining these energy sources with grid-level power supply, which can be coordinated to provide super-fast charging to meet the demands of busy flight schedules.

The airport microgrid with combined gas turbine, PV as well as grid-level power supply allows for a more flexible and reliable charging system for electric aircraft. By utilising a combination of energy sources, we can ensure that the energy demands for charging are met, while also reducing the reliance on the grid and increasing the use of renewable energy. This energy system can also help mitigate the challenges of high-power charging and battery range anxiety, allowing for a more efficient and effective electrification of air transport in the UK.

6.2.1 Flight schedule driven charging requirement

Over the past decade, aircraft designers have developed more than 50 all-electric conceptual, experimental, and commercial aircraft. While the current highest battery specific energy level of around 250 Wh/kg is insufficient to power a middle-size all-electric aircraft, research indicates that the battery specific energy has the potential to reach 800 Wh/kg by the mid of the century [5]. Based on the research [3], an 800 Wh/kg battery would enable all-electric A320 to carry a 28 MWh battery and transport 180 passengers over a range of 500 nm, which would cover the regional and domestic flight missions in the UK. As a result, the commercial all-electric aircraft is anticipated to enter into service for the UK domestic air transport by 2050 [5]. In this chapter, the novel concept of A2G flexibility is investigated using an all-electric aircraft with a battery specific energy of 800Wh/kg, a 500 nautical-mile design range, and 180 passenger capacity, as designed in [3]. Table 6-1 lists technical assumptions of all-electric A320 including the aircraft battery and charging. The following sections present case studies that investigate the interaction between electrified air transport and the power grid, with the all-electric A320 aircraft used as a reference.

Table 6-1 The parameters of the all-electric aircraft A320 [3]

Design property	All-electric aircraft
Passenger	180
Distance Range (km/nm)	926/500
Battery Energy (MWh)	28
Nominal charging and discharging power (MW)	5
Charging/discharging efficiency (%)	97

To meet the peak charging demand of the EA, a detailed analysis of the flight schedules is conducted. The peak charging hours are determined based on the number of chargers available at the airport. After analysing the flight schedules, it is observed that there are very few flights during 00:00 to 07:00. Therefore, to ensure that the EA batteries are fully charged batteries for the entire day's flights, it is planned to recharge 30% of daily energy requirement of all EA batteries during that time period. To facilitate this, the initial number of swappable batteries are set equal to the number of arrival flight at the peak of

the flight schedule in each airport. The number of chargers required can be calculated using a formula that takes into account the energy capacity of the battery and the charging time required, as shown following.

$$N_c = \frac{\beta_e \times E_{batt}^{EA}}{P^{charger} \cdot T_{night}} \quad 6.1$$

where N_c is the number of battery chargers at each airport, β_e is the coefficient of the required energy for charging EA batteries during the 7 hours night period, $P^{charger}$ is the rated power of each battery charger, E_{batt}^{EA} is the total energy required by the EA batteries of daily scheduled flights, T_{night} is the night charging period defined from 00:00 to 07:00.

The capacity of the transformer is determined based on the maximum power required to charge the EA on the busiest day of flight schedule. The number of daily domestic flights travelling to and from these 8 major UK airports are shown in Table 6-2. This ensures that the transformer for each airport can handle the peak charging demand without causing any overloading issues or system failures.

Table 6-2 8 major UK airports with number of daily flights

Airport	IATA code	Num. of daily flights*
London Heathrow	LHR	240-260
Edinburgh	EDI	230-240
Glasgow	GLA	160-170
Manchester	MAN	100-120
Birmingham International	BHX	70-80
Belfast International	BFS	50-80
London Gatwick	LGW	50-60
London Stansted	STN	40-50

** The number of flights listed in this table specifically pertains to those travelling between the selected airports and does not represent the total number of all flights.*

In addition, to ensure reliable energy operation, the installed capacity of airport gas turbine is assumed to be equal to the capacity of the grid transformer. This means that if one of these energy devices experiences an outage or failure, the other can still supply power to meet the peak charging demand of the EA. This approach follows the 'N-1'

criteria, which means that the system can still operate with a single contingency event, ensuring a high level of resilience in case of any unforeseen circumstances.

6.2.2 PV capacity and output profile

The estimation for the maximum PV installation capacity considers the land availability at each individual airport. This study focuses on identifying the ideal locations for PV installation, such as car park canopies and building rooftops, which can vary in capacity based on the type of PV module technology and mounting systems used. However, as the main focus of this research is on the EA charging system, the calculation of PV capacity will only be based on the initial and high-level estimation of the area of canopy and building rooftop.

To estimate the PV installation capacity, the worldwide standard of PV land size over installed capacity is used as a reference, which is 1 MW per 2 hectares (5 acres) [182]. This standard will be applied to estimate the PV capacity in airport areas. Additionally, the 2019 PV generation profiles of relevant cities where the airports are located are calculated based on this model. The PV panels are installed horizontally, which means the installation tilt is 0°. This represents an extreme scenario where the PV panels are installed without any tilt angle.

The results of the PV installation capacity for the top 8 UK airports are summarised in Appendix A. The estimation considers the land availability and location of the airport and may vary depending on the specific details of each airport's layout and infrastructure.

The power output profile of airport PV generation has been calculated using the Global Solar Energy Estimator (GSEE) model [183] , which is a widely used and reliable model in the field of solar energy. This model takes into account the irradiance data of the PV panels and the estimated maximum PV installation capacity for the airport.

6.2.3 Gas turbine operation parameters

The power output of the gas turbine can be calculated as Eq. (6.2).

$$P_t^{GT} = \eta^{GT} \cdot G_t^{GT} \tag{6.2}$$

where P_t^{GT} is the power output of the gas turbine at time *t*. η^{GT} is the efficiency of the gas turbine. G_t^{GT} is the gas input at time *t*.

To enable switch-on and switch-off control for gas turbine scheduling, the gas turbine sate flow model [184] is utilised. This model includes three operation statuses of gas turbine that considers switch control and is formulated using Equations (6.3-6.7). The model also introduces state binary variables, including the operation state variable v_t^{GT}, starting up integer variable y_t^{GT}, and shutting down integer variable z_t^{GT}. The transition between these variables is formulated using a set of equations that describe the physical constraints and operating limits of the gas turbine, including ramp-up and ramp-down limits.

$$y_t^{GT} - z_t^{GT} = v_t^{GT} - v_{t-1}^{GT} \tag{6.3}$$

$$y_t^{GT} + z_t^{GT} \leq 1 \tag{6.4}$$

$$\lambda_{GT,min} \cdot P_{GT}^{max} \cdot v_t^{GT} \leq P_t^{GT} \leq \lambda_{GT,max} \cdot P_{GT}^{max} \cdot v_t^{GT} \tag{6.5}$$

$$RD \cdot v_{t-1}^{GT} \leq P_t^{GT} - P_{t-1}^{GT} \leq RU \cdot v_t^{GT} \tag{6.6}$$

$$UT \cdot y_t^{GT} \leq \sum_{l=\mathrm{t}}^{\mathrm{t}+UT} v_t^{GT} \leq DT \cdot (1 - z_t^{GT}) \tag{6.7}$$

The operation boundaries of the gas turbine are critical factors to be considered in optimising the energy dispatch. To this end, the constraints (6.5) and (6.6) are formulated to define the upper and lower limits and the ramp-up and ramp-down limits of the gas turbine's power output. These constraints are essential to ensure that the gas turbine operates within a safe and efficient range while providing the required power output. Additionally, the start-up time of gas turbine is taken into consideration by incorporating Equation (6.7). The parameters of the gas turbines can be found in [81]. By considering these constraints and parameters, the gas turbine scheduling can be optimised to ensure that the power output is both safe and efficient, making it a valuable tool for integrating renewable energy sources into the energy grid.

6.2.4 Battery swap state flow model

The process of battery swap process for EA is a complex task that can be represented mathematically as a job-shop problem [34]. To describe this process, a state flow model has been developed and used in this study, based on existing literature. The model used represent the EA battery swap process is formulated using Equations (6.8-6.14) that capture the key variables and constraints involved in the process.

$$\sum_{i}^{T_c}\left(n_{c,t}^{i}+n_{w,t}^{i}\right)+n_{f,t}=N_b \tag{6.8}$$

$$n_{dc,t}^{i}+n_{dw,t}^{i}=n_{d,t-T_{bs}}^{i} \tag{6.9}$$

$$n_{c,t}^{i}=n_{c,t-1}^{i-1}+n_{dc,t-1}^{i-1}+n_{wc,t}^{i} \tag{6.10}$$

$$n_{w,t}^{i}=n_{w,t-1}^{i-1}+n_{dw,t-1}^{i-1}-n_{wc,t}^{i} \tag{6.11}$$

$$n_{f,t}=n_{f,t-1}+n_{c,t}^{T_c}-\sum_{i}^{T_c}\left(n_{d,t}^{i}\right) \tag{6.12}$$

$$\sum_{i}^{T_c}\left(n_{c,t}^{i}\right)\leq N_c \tag{6.13}$$

$$n_{c,1}^{i}=n_{c,T}^{i},n_{w,1}^{i}=n_{w,T}^{i},n_{f,1}=n_{f,T} \tag{6.14}$$

Eq. (6.8) describes the balance of the total number of batteries N_b, which remains constant in three charging states including charging $n_{c,t}^{i}$, fully charged $n_{f,t}$ and empty $n_{w,t}^{i}$. The battery swapping process is governed by the constraint represented by Equation (6.9). this equation defines the process of dividing depleted batteries into two groups: the direct charge group $n_{dc,t}^{i}$, and the waiting for charge group $n_{dw,t}^{i}$ after the time T_{bs} spent on battery swapping. The number of charging and waiting batteries can be calculated using Equations (6.10) and (6.11), respectively. Additionally, $n_{wc,t}^{i}$ represents the number of batteries transferred from the waiting to the charging state at time *t*.

The number of fully charged batteries is calculated by summing up the number of fully charged batteries and subtracting the depleted (swapped) batteries $\sum_{i}^{T_c}\left(n_{d,t}^{i}\right)$. The daily repetitive operation pattern of the airport battery swapping process ensures that the number of batteries with SoC in each state remains equal between the beginning and end of the day, as formulated in Equations (6.12-6.14). Notably, all the variables in Eq. (6.8)-(6.14) that represent the numbers of batteries are integer.

6.2.5 Electrical power balance

To calculate the total charging demand of EA battery accurately, it is necessary to consider both the number of charging batteries and the rated power of the battery chargers. This information can be used to determine the total amount of power required to charge all the batteries in a given time period. By taking into account both of these factors, a

more accurate estimation of the total charging demand can be formulated as Equation (6.15), enabling better planning and management of the airport's energy resources.

$$P_t^{EAc} = \sum_i^{T_c} \left(n_{c,t}^i\right) \cdot P^{charger} \cdot \eta^{EAc} \quad 6.15$$

where P_t^{EAc} is the charging power output of EA battery chargers. η^{EAc} is the charging efficiency of EA batteries.

To ensure a stable and reliable energy supply, the power generated from the grid, gas turbines, and PV panels must be balanced with the EA charging demand. This balancing process represented by Equation (6.16) is crucial to prevent overloading the system, which can result in power outages or damage to the equipment.

$$P_t^{grid} + P_t^{PV} + P_t^{GT} = P_t^{EAc} \quad 6.16$$

where P_t^{grid} is the power import from the grid, P_t^{PV} is the power generated by PV, P_t^{GT} is the power generated by the gas turbine.

To ensure the reliable and safe operation of the airport energy system, it is important to ensure that the power output of each energy source is within its capacity. This is achieved by imposing constraint (6.17) on the power output of the grid, gas turbines, and PV panels.

$$0 \leq P_t^{unit} \leq P^{unit,max}, \ \ unit = PV, grid, GT \quad 6.17$$

6.3 Aviation-to-Grid Frequency Response

The EA charging system is designed to not only provide power for the EA charging, but also offer primary and secondary frequency response to the power grid. The system utilises the batteries of the electric aircraft and the airport gas turbine to provide this response. A control strategy is developed to manage the dispatching of the EA batteries and gas turbines by monitoring the real-time system frequency. A frequency response control is also established to mitigate frequency deviation. The charging scheme for the EA will be scheduled on an hourly basis, based on the flight schedule, along with the battery swap process. Utilising the EA charging system for frequency response through this innovative approach can provide a fast and high-power A2G frequency response.

This approach has the potential to significantly reduce the risk of power outages that may be caused by a frequency drop.

6.3.1 Objective function of EA charging system operation with A2G frequency response

In order to determine the optimal charging schedule for the EA at the airport, a MILP optimisation problem is formulated. The main objective of this optimisation is to minimise the overall energy operation costs of the airport EA charging system. The costs include the electricity purchase cost from the grid, the gas supply cost for the airport gas turbine, and the revenue earned from providing frequency response services to the power grid. By solving this MILP optimisation problem, a charging schedule is derived, which ensures the EA batteries are fully charged and available for flight operations while minimising the overall energy operation costs of the airport. The optimised charging schedule also enables the airport to reserve for the frequency response services to the power grid, which can generate additional revenue for the airport.

To calculate the frequency response revenue, Eq. (6.18-6.19) is used. These equations take into account the energy costs, the amount of power that the airport can provide for frequency response, and the market price for frequency response services.

$$Obj = min\left(\sum_{s=1}^{2} d_s\left(OC_s - R_{A2G,s}\right)\right) \tag{6.18}$$

$$OC_s = \sum_{t=1}^{T}\left(P_{s,t}^{grid} \cdot \pi_t^e + G_{s,t}^{GT} \cdot \pi_g\right) \cdot \Delta t \tag{6.19}$$

where OC_s is the operation costs of EA charging system. π_t^e is the time-of-use electricity price. π_g is the gas price. d_s is the number of days in one season (230 days for summer, 135 days for winter).

To ensure grid stability, a mechanism named “Firm Frequency Response” is triggered when the grid frequency drops below a certain threshold of 49.7Hz [185]. In this mechanism, the charging batteries of the EA charging systems will reverse their charging state to discharging, providing double the volume of frequency response to their rated power. All batteries are required to sustain their output for 30 seconds, as mandated by primary response, after which the batteries will linearly reduce their power output at the

rate of 0.5 MW/s in order to prevent instantaneous power imbalance [31][32]. The A2G frequency response system comprises both gas turbines and EA batteries, and it is illustrated in Figure 6-1, which displays the primary and secondary frequency response control for both of these components.

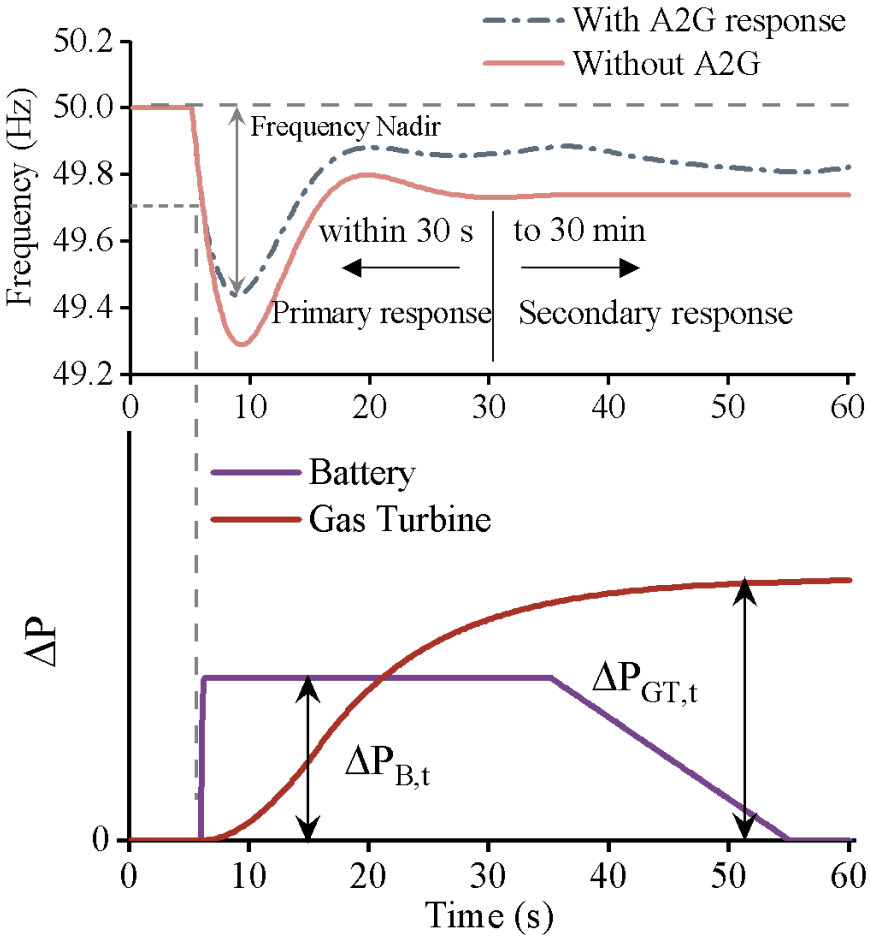

Figure 6-1 Primary and secondary frequency response control for gas turbines and EA batteries

Since primary response only requires the batteries to discharge for 30 seconds, the SoC of the batteries is estimated to decrease by less than 5%, which will not have any significant impact on the scheduled flight operations. It is worth noting that the batteries' discharging state will not go beyond the minimum SoC limit, which is set at 20% to ensure the batteries' longevity.

The gas turbine plays an important role in the frequency control of the power system. It is capable of participating in both primary and secondary frequency control as long as the

operation reserve of gas turbine is available [188]. The primary frequency control requires the gas turbine to automatically increase or decrease its power output within a certain timescale when a grid frequency event occurs. [195]

The secondary response is provided by the gas turbines to sustain the system frequency for a longer period of time, usually around 30 minutes. The total primary response power and secondary reserve energy provided by the gas turbines can be calculated by Eq. (6.20-6.23). By participating in the frequency response, the gas turbines can generate additional revenue, which is considered as one component of the objective function of the MILP optimisation problem. This revenue can help to offset the costs of electricity purchase from the grid and gas supply, leading to a more economically sustainable charging system.

$$\Delta P_{B,t}^{res} = 2 \cdot P_t^{EAc} \tag{6.20}$$

$$0 \leq \Delta P_{GT,t}^{res} \leq \varphi^{res} \cdot P_{GT}^{max} \cdot v_t^{GT} \tag{6.21}$$

$$\Delta P_{A2G,t} = \Delta P_{B,t}^{res} + \Delta P_{GT,t}^{res} \tag{6.22}$$

$$E_{A2G,t} = \Delta P_{GT,t}^{res} \cdot T_s \tag{6.23}$$

where φ^{res} denotes maximum reserve power proportion of gas turbines, $\Delta P_{B,t}^{res}$ is the response power from the EA batteries. $\Delta P_{A2G,t}$ is the A2G primary response power. $E_{A2G,t}$ is the A2G secondary reserve energy, $\Delta P_{GT,t}^{res}$ is the response power from gas turbines. T_s is the response time of gas turbine, which is 30 minutes.

The contract between the airport EA charging systems and the GB National Grid for Firm Frequency Response will specify a revenue settlement every half hour, regardless of whether there is an actual frequency event or not. The primary and secondary response reserve revenue will be paid by a fixed tariff rate, which is similar to an insurance premium [189]. The frequency response revenue is calculated using the formula shown in Eq. (6.24), which takes into account the duration and amount of power delivered by the EA charging system to the grid during a frequency event. The revenue earned through participating in frequency response programs incentivises the airport operators to maintain a reliable and stable grid, while also promoting the integration of renewable energy sources and reducing carbon emissions from aviation sectors.

$$R_{A2G,S} = \sum_{t=1}^{T} \left(\Delta P_{A2G,t} \cdot p_{pri} + E_{sec,s,t} \cdot p_{sec}\right) \cdot \Delta t \tag{6.24}$$

where $R_{A2G,s}$ is the daily A2G frequency response revenue in summer or winter season. p_{pri} and p_{sec} are the primary and secondary frequency response revenue respectively.

6.3.2 A2G frequency response integration to power system

After the MILP optimisation problem is solved, the results of A2G frequency response powers ($\Delta P_{B,t}^{res}$ and $\Delta P_{GT,t}^{res}$) are input into the frequency response simulation model to obtain the frequency response results. The simplified Great Britain (GB) power system with inertia estimation [77] was used to analyse the frequency response from the EA charging system, as depicted in Figure 6-2.

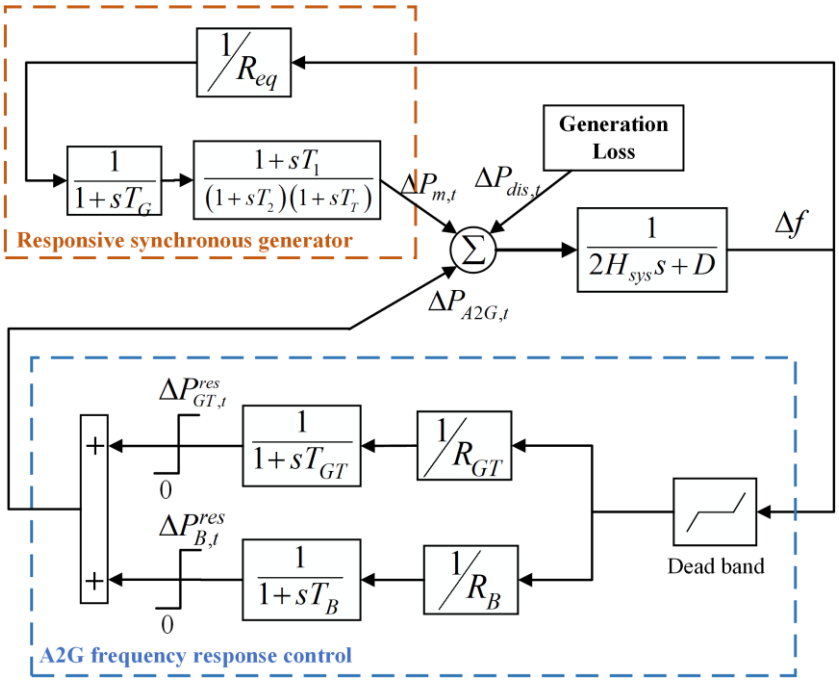

Figure 6-2 Simplified GB power system model with the A2G frequency response control [77]

This system model includes various parameters, such as power system demand level, damping constant, and power system inertia constant, which are specified in [190]. The time evolution of system frequency deviation can be mathematically represented by a first-order ordinary differential equation in Equation (6.25) [77].

$$2H_{sys}\frac{\partial \Delta f_t}{\partial t} + D * P_t^D * \Delta f_t = \Delta P_{m,t} - \Delta P_{dis,t} + \Delta P_{A2G,t} \qquad 6.25$$

where Δf_t is the frequency deviation at time t, P_t^D (MW) is the power system demand

level, and $\Delta P_{dis,t}$ is the generation power loss, $\Delta P_{m,t}$ is the response power from synchronous generators. The H_{sys} (MW/Hz) is the power system inertia constant, which represents the total stored kinetic energy in the synchronous generators of the power system.

The synchronous generators are modelled by a governor droop block, a governor actuator block, and a turbine block. T_G is the typical governor actuator time constant of 0.2s. A transient droop compensation is introduced between the governor and the turbine which is a lead-lag transfer function with time constants T_1 and T_2 at 2s and 12s respectively. The turbine model is characterized by a time constant T_T of 0.3s, which represents the mechanical power output following the governor action. D (%/Hz) is a single damping constant which represents the damping provided by the frequency-dependent loads. These parameters capture the characteristics of different governors and turbines in response to a frequency change, which can be derived from a frequency deviation event caused by power imbalance [190]. The responsive synchronous generators are represented by the closed-loop transfer functions Eq. (6.26-6.27).

$$G_g(s) = \frac{1}{1 + s \cdot T_G} \tag{6.26}$$

$$G_T(s) = \frac{1 + s \cdot T_1}{1 + s \cdot T_2 T_T + s^2 \cdot (T_2 + T_T)} \tag{6.27}$$

The primary and secondary responses of the gas turbines and EA batteries are coordinated through the adoption of droop control, wherein they will operate at a fixed frequency deviation and output power level according to the results obtained by solving MILP problem. Upon sensing a system frequency below 49.7 Hz, the reserve power from the system will be discharged to address the power system frequency drop issue. The dynamic behaviour of the system can be described by a set of first-order Equations (6.28-6.29) that capture the time evolution of the system's frequency and power output levels.

$$\frac{\partial \Delta P_t^{unit}}{\partial t} = \frac{1}{T_{unit}} \left(-\frac{\Delta f_t}{R_{unit}} - \Delta P_t^{unit} \right) \ , (unit = B, GT) \tag{6.28}$$

$$\Delta P_{A2G,t} = \sum\nolimits_{unit} \Delta P_t^{unit} \ , (unit = B, GT) \tag{6.29}$$

where $\Delta P_{unit,t}$ is the response power output from the units (EA batteries and gas turbines).

T_{unit} and R_{unit} are the time delay constant and the droop constant for the EA batteries and gas turbines to inject response power to grid.

6.4 Results and Discussion

6.4.1 Case studies with input data and assumptions

The sizing of EA charging systems, as shown in Figure 6-2, is crucial to ensure the efficient operation of the system. To achieve this, the A2G frequency response control system and the simplified GB power system are modelled on the Simulink platform of MATLAB 2019b. The EA charging scheduling problem is solved by the MILP algorithm with CPLEX solver, which can provide an optimal solution for the given inputs.

The modelling process is conducted on a PC with Intel Core i5-8500 CPU @ 3.00 GHz and 8 GB RAM. As discussed in the previous section, the flight schedules vary with seasonal effect. In the case studies, two weeks' flight schedules in summer peak month (May) and winter peak month (November) are investigated, as shown in Appendix B. The flight schedule in 2050 is forecasted by scaling up from the base year 2019, and the effect of COVID was also considered, as shown in Appendix C.

In this chapter, the inertia of the GB power system is based on the long-term inertia forecast of a typical value 100 GVA·s in 2050 across both summer and winter for the simplification purpose [191]. T_B is assumed to be 35 ms that is similar to the normal EV charging case [192]. T_{GT} is set at 10s according to reference [193]. The maximum reserve power proportion of gas turbines is assumed to be 15%. The droop constants of the EA batteries and gas turbines are assumed to be 2.5% and 5% respectively. The sizing of EA charging system is shown in Table 6-3.

The national demand profiles on typical summer and winter days are utilised in the case studies. The total power system demands are 41.6 GW as the winter maximum demand and 21.2 GW as the summer minimum demand, respectively. In order to maintain consistency with the power loss event of 2019, the national demand profiles from the same year are utilised in this analysis. The simulated generator loss is assumed to be 1,800 MW, which is equivalent to the largest generators loss at Sizewell nuclear power station in the UK. The power loss is assumed to happen repeatedly in every 30 minutes interval for test.

Table 6-3 Sizing of EA charging equipment and airport energy resources

Airport	Grid (MVA)	PV (MW)	GT (MW)	Num. of Batteries	Num. of Chargers
LHR	180	50	180	260	36
EDI	170	17	170	240	34
GLA	120	7	120	170	24
MAN	85	17	85	120	17
BHX	60	21	60	80	12
BFS	60	11	60	80	12
LGW	45	43	45	60	9
STN	35	19	35	50	7

For airport energy purchase from grid, the gas price is stable at 0.038 £/kWh, while the TOU pricing mechanism of electricity price is introduced as £0.07 (00:00-07:00), £0.15 (10:30-16:00 and 21:00-24:00), and £0.2 (07:00-10:30 and 16:00-21:00) per kWh. The primary A2G frequency will receive a stable capacity revenue which is assumed to be 8 £/MW per 30 min, while the secondary response power will receive a payment for reserved energy (10 £/MWh per 30 min). The national demand profiles on a typical summer and winter day in 2019 are utilised in the case studies as shown in Figure 6-3.

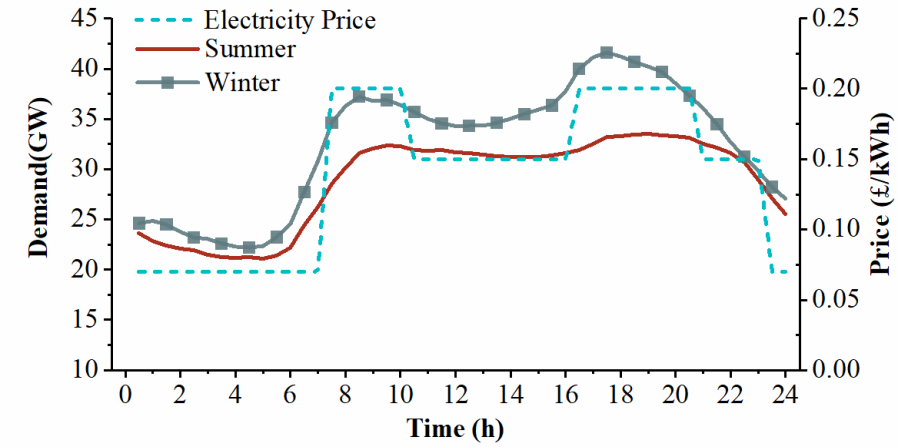

Figure 6-3 UK national demand in summer and winter typical days with TOU electricity price

6.4.2 Energy dispatch results of EA charging system

Figure 6-4 shows the hourly EA charging supply and demand driven by the power generation dispatch with defined flight schedules. The results indicate that the EA charging demand patterns are different to the flight schedules due to the battery swap with optimal energy dispatch that enables the charging demand flexibility in the airport operation. In terms of power generation, the power drawn from the grid is significantly high during the night from 00:00 to 07:00, while gas turbines supply the most EA charging demand during the daytime and in the evening. This is because the electricity price is cheaper during the night which incentivises the EA charging system to purchase electricity from grid to fully change batteries for the oncoming flight missions.

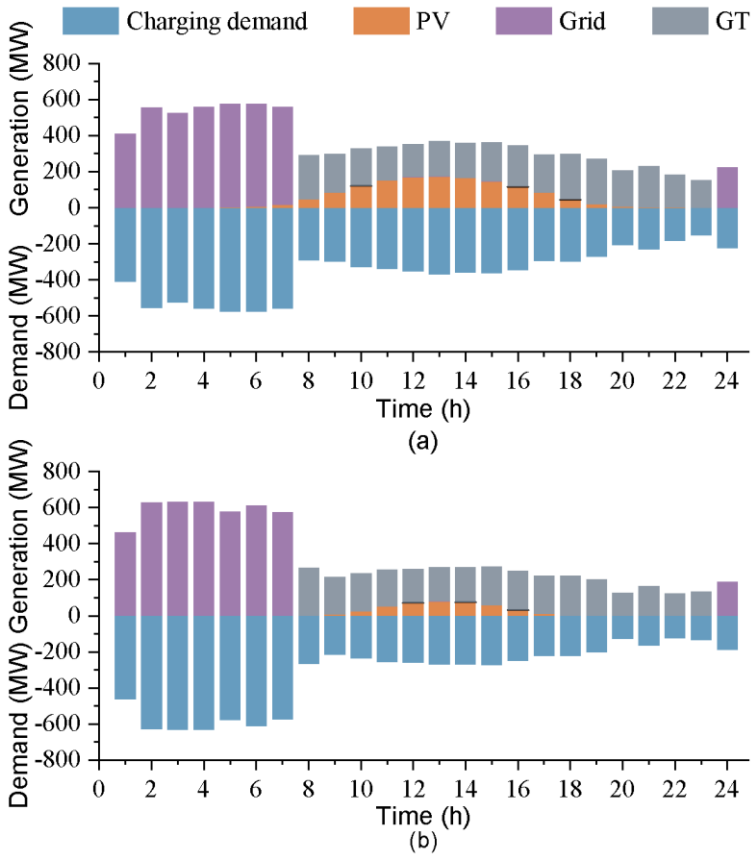

Figure 6-4 Energy dispatch results of the 8 UK airports. (a) Summer, (b) Winter.

The advantage of this EA charging arrangement is to compensate the national power system demand profiles across the 8 UK airports, where the overnight national demand valley can be filled by EA charging, while the day and evening demand peak can be self-dispatched by airport gas turbines. To maximise the PV generation, the EA charging

system dispatches the maximum available PV generation during the daytime, which ensures the 100% utilisation of renewable PV generation. Due to the seasonal effect of solar energy source in particular the output reduction over winter period, gas turbines are operating at a higher level in the winter daytime.

6.4.3 A2G frequency response results

The A2G frequency control mechanism is triggered when a frequency deviation such as power generation loss occurs. Figure 6-5 presents a comparison of the frequency deviation profiles with and without A2G frequency response in response to a 1,800 MW generation loss on the GB power system at 06:00 and 23:00 in summer and winter, respectively.

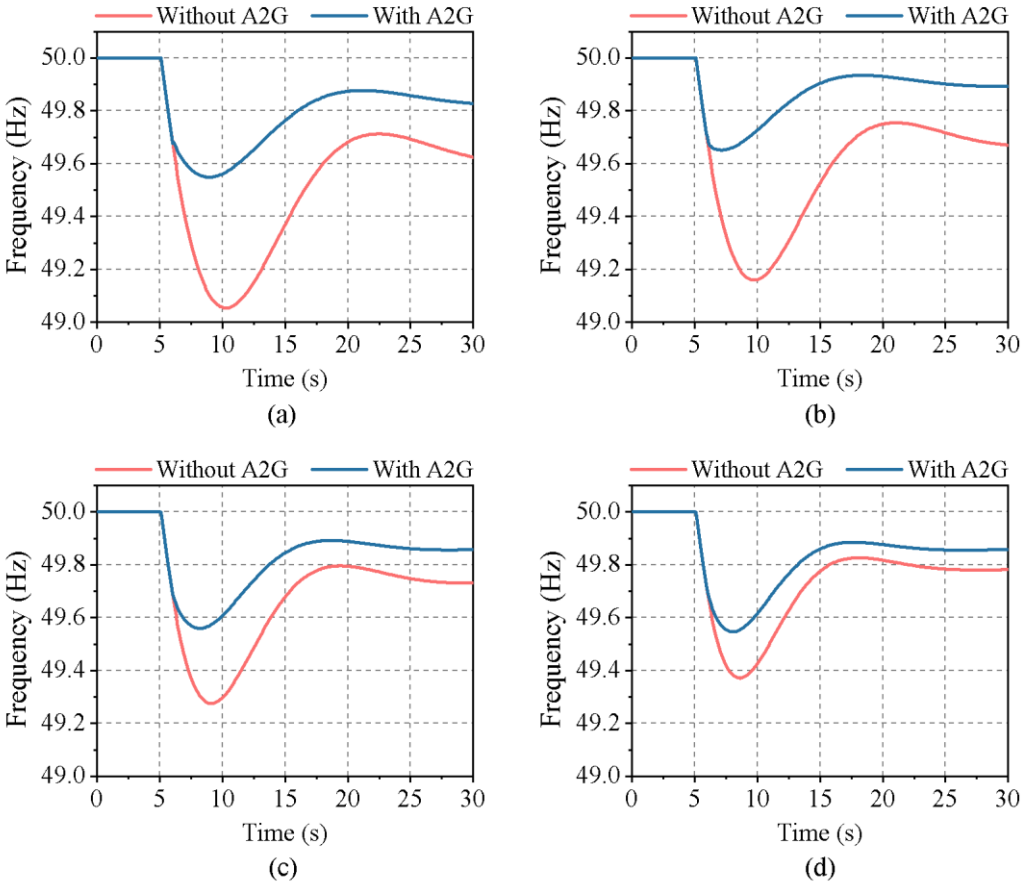

Figure 6-5 Frequency drop in different cases with and without A2G response (1,800MW loss): (a) Summer 06:00 am, (b) Winter 06:00 am, (c) Summer 23:00 pm, (d) Winter 23:00 pm

The results reveal that A2G frequency response is most effective at 06:00 in summer (Figure 6-5 a), where it prevents the frequency nadir from dropping to 49.05 Hz and increases it to 49.55 Hz compared to non-A2G response. This is because A2G can provide high response power during a period of no flight schedules, coupled with low system inertia during the summer minimum demand period. On the other hand, A2G provides the least effective frequency response at 23:00 in winter (Figure 6-5 d) due to peak flight schedules. At this time, the EA charging system prioritizes its reserve power to meet aviation requirements rather than grid frequency response. The study also highlights the effectiveness of EA batteries and gas turbines in providing frequency response services. At 06:00 (Figure 6-5 a-b), the primary frequency response is mainly provided by EA batteries, while at 23:00 (Figure 6-5 c-d), gas turbines provide the frequency response. The results show that gas turbines are three times less effective than EA batteries in restoring frequency nadir due to slower response times.

Figure 6-6 (e) and (f) show a series of frequency nadirs – the minimum post-contingency frequency after the system suffers a loss of 1,800 MW generation in every 30 minutes interval with and without A2G frequency response. Comparing with and without A2G scenario, the half-hourly frequency nadir improved significantly by approximately 0.4 Hz during the night and 0.2 Hz in the day. The effectiveness of A2G frequency response in improving frequency nadir is dependent on the power system inertia, and A2G becomes more effective in the summer and 00:00-07:00 period due to the weak system inertia. When the frequency event occurs, the charging batteries not only stop charging but also being able to fully discharge the power back to the grid. This makes the "double effect" of frequency response capacity. Therefore, the night frequency nadir improved twice as much as daytime due to the EA batteries which are fully available to provide frequency response 00:00-07:00 when no flights are scheduled. During the daytime the frequency response is mainly provided by gas turbines. In a realistic power system operation scenario, the frequency contingency events will not happen repeatedly at such a short interval. As a result, this study always assumes that each frequency events in a half-hourly interval are independent and there is sufficient power reserve capacity to restore the frequency before the next contingency event. Overall, the average frequency nadir can be improved by 0.31 Hz in summer, and 0.23 Hz in winter due to the A2G frequency response services. Most importantly, the number of Infrequent Infeed Loss Risk (defined

as below 49.5 Hz [186]) can be reduced by 83.33% in summer and 68.75% in winter, which significantly reduce the likelihood of significant frequency deviations with A2G frequency response services.

6.4.4 Response power and energy from A2G system

The amount of response power available from A2G frequency response through EA batteries and airport gas turbines is calculated, and the results are shown at every half an hour for a summer and winter day in Figure 6-6 (a-b).

There are 900 to 1,200 MW response power capacity from 00:00 to 06:30 when there is no flight, and 300 to 900 MW capacity when the EA requires charging power. The higher power response capacity during night is caused by the full amount of EA batteries that are available at airports overnight. In the peak flight scheduling periods of 20:00 - 22:00 in summer and 19:00 - 21:00 in winter, the majority of EA batteries are used to meet aviation requirements, therefore less power response capacity is observed. Such response power capacity has a strong impact by the EA charging schedules. To discuss the response power capacity from different sources, the EA batteries provide 100% of response power capacity overnight and around 80% - 90% capacity during the day, gas turbines can only provide around 10% to 20% response power capacity from 07:00 to 23:00. This is because the response power of gas turbines for frequency control can only provide response power when the turbines are dispatched. Overnight due to the low electricity price, the charging power is mainly from the external power grid with no gas turbines dispatchable overnight to provide response power capacity. For the rest of time, the A2G system provides a combined response power from EA batteries and gas turbines.

The response energy provided by EA batteries and gas turbines is calculated in Figure 6-6 (c) and (d). Gas turbines can provide more than 30 MWh response energy on most occasions, with peak response energy of 35 MWh in both summer and winter. However, the EA batteries can only provide response energy around 10 to 15 MWh (overnight) and 5 to 10 MWh (daytime). The reason for gas turbine to provide much higher response energy is due to the sustained power output of gas turbine over a longer period of 30 minutes comparing with the constrained response time of only 30 seconds for EA batteries. The response energy provided by gas turbines is up to four times higher than EA batteries.

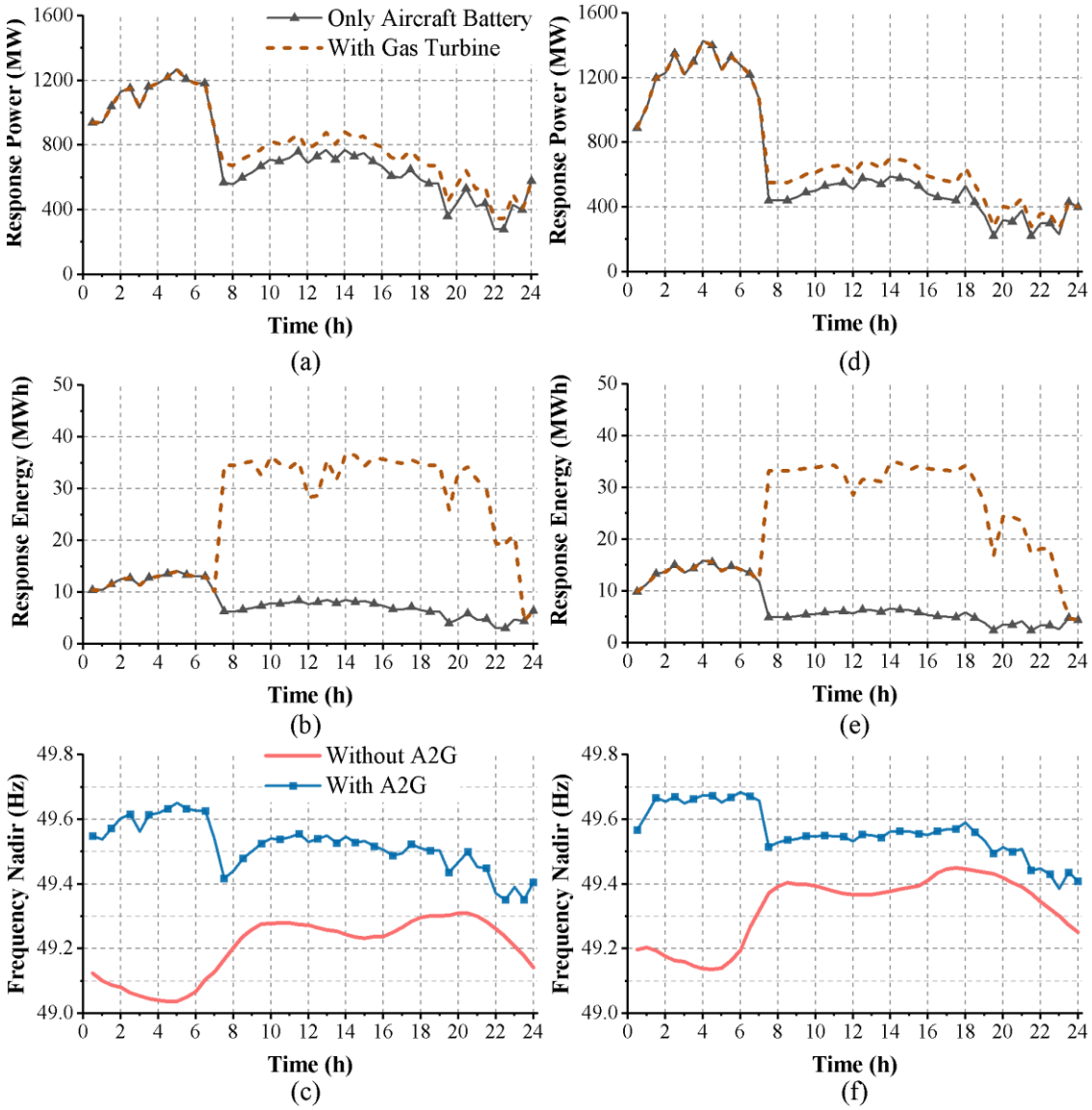

Figure 6-6 Frequency response power and energy from the EA batteries and gas turbine. (a) response power (summer), (b) response power (winter), (c) response energy (summer), (d) response energy (winter), (e) Frequency nadir (summer), (f) Frequency nadir (winter)

6.4.5 Response revenue and charging costs

The annual EA charging costs with A2G frequency response revenue are shown in Figure 6-7. The EA charging costs consist of two main parts: the grid electricity purchase and the gas turbine energy consumption, which are based on the electricity and gas prices provided. The calculated EA charging costs across 8 UK airports demonstrate a balanced

expenditure on electricity and gas usage for all airport size with flight schedule variation. The annual frequency response revenue is calculated in Eq. (6.24). In average, the frequency response revenue can off-set 19.8% to 30% of charging costs across 8 UK airports. The total revenue generated from A2G frequency response services is estimated at £46.58 million.

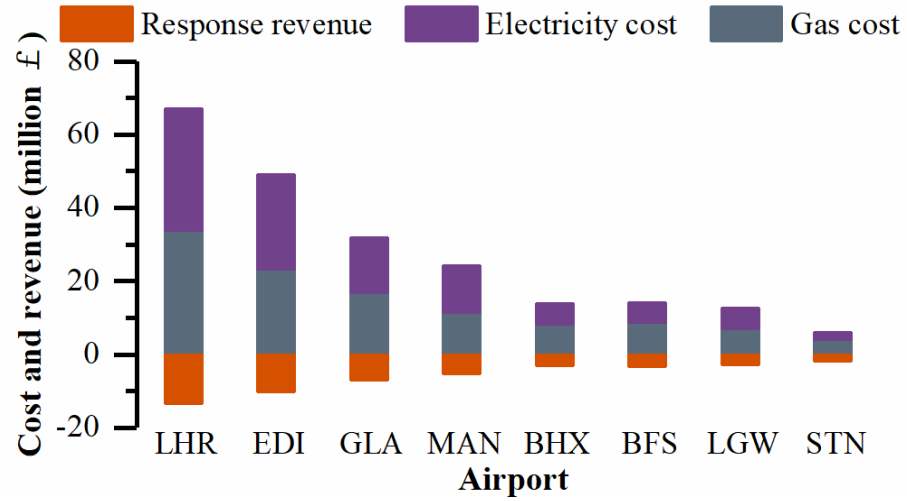

Figure 6-7 Annual EA charging costs and A2G frequency response revenue for 8 UK airports

6.4.6 Sensitivity analysis of A2G generation capacity

A sensitivity analysis has been conducted to investigate the impacts of generation capacity on the energy dispatch of the EA charging system, as well as the associated A2G frequency response power and energy. Two additional scenarios are considered: Scenario 2 with half the gas turbine capacity and Scenario 3 with half the grid transformer capacity.

Figure 6-8 presents a comparison of the energy dispatch simulation results for these two scenarios with the base case. In scenario 2 (illustrated in Figure 6-8 b), with a 50% reduction in gas turbine capacity, a portion of the daily EA charging demand shifts to the overnight period, where it is supplied by grid electricity. As a result, the gas turbine generation profile becomes flattened and constrained by the decreased capacity.

In scenario 3 (depicted in Figure 6-8 c), with a 50% reduction in grid transformer capacity, the grid electricity is insufficient to meet the EA charging demand overnight. This situation necessitates the scheduling of the gas turbine to fulfil approximately 30% of the charging demand. Additionally, the gas turbine is required to generate more power during

daytime hours to offset the energy deficit resulting from the insufficient EA charging overnight.

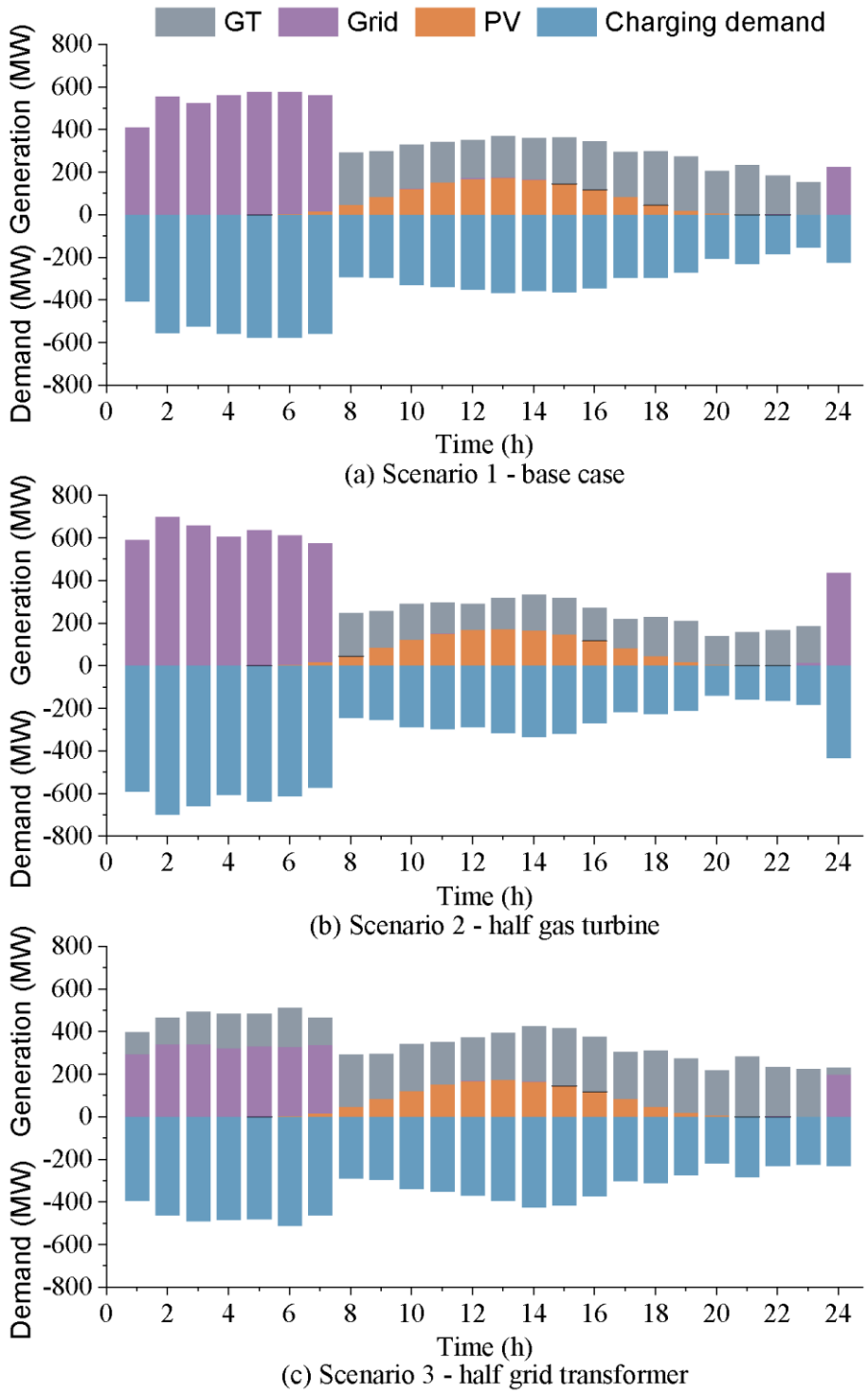

Figure 6-8 Energy dispatch and EA charging demand with reduced generation capacities

Figure 6-9 presents the response power and energy provided by the 50% reduced capacity of gas turbine or grid transformer, along with the frequency nadir simulation results subject to half-hourly power loss events.

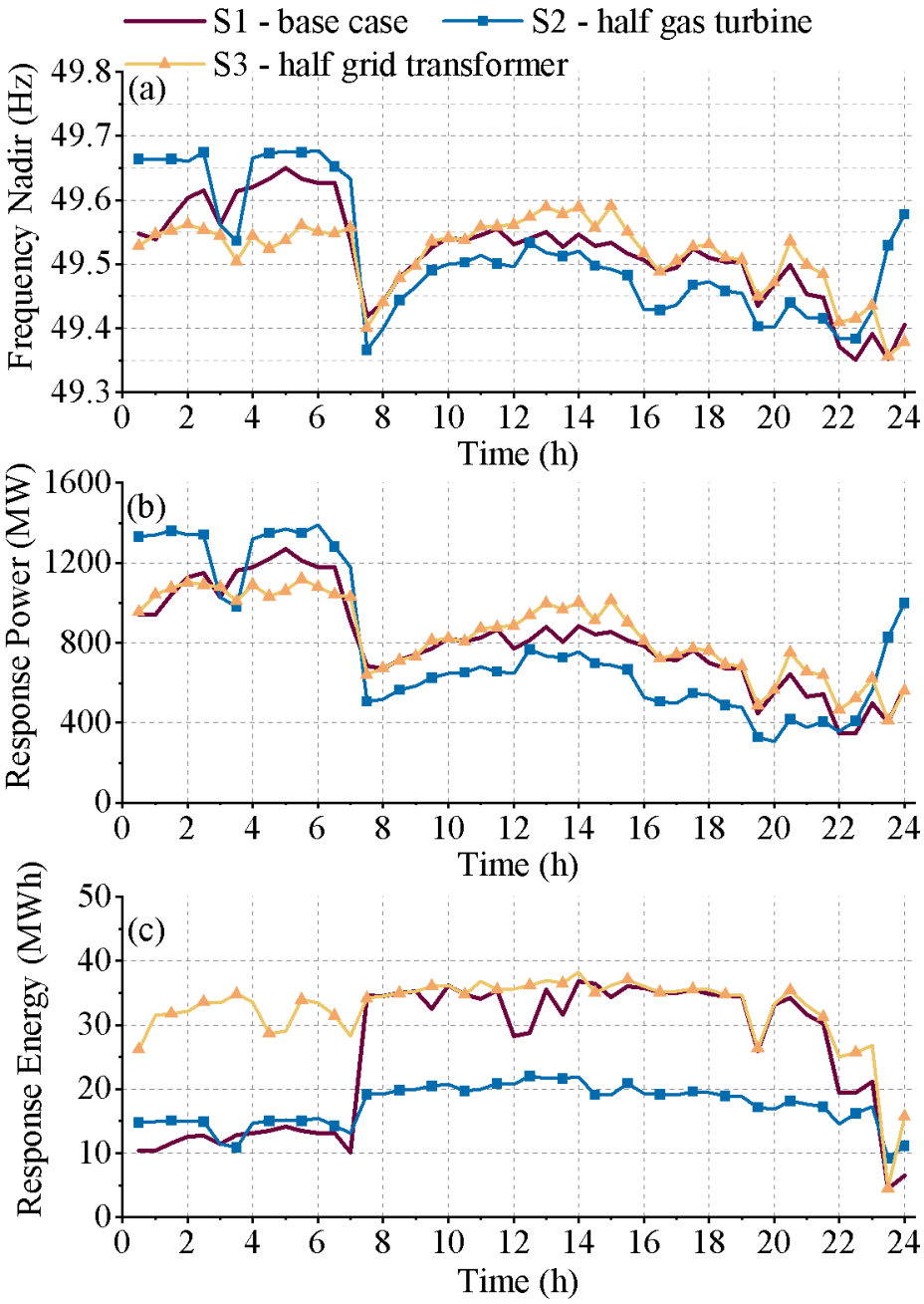

Figure 6-9 Frequency nadir (a), response power (b), and response energy (c) by reduced generation capacity of grid electricity and gas turbine

Scenario 2 (half gas turbine) exhibits an uneven distribution of response power between day and night, as well as less response energy due to the 50% reduction in gas turbine

participation in providing sustained response energy for secondary response timescales. Scenario 3 shows a 0-180 MW lower response power during the night and a 0-160MW higher response power during the day. This is attributed to increased gas turbine participation in energy dispatch when grid supply capacity is halved, resulting in a more balanced distribution of response power and energy between day and night.

However, the base case scenario with balanced grid and gas turbine capacity is still considered the optimal option due to the higher response power provided during low system inertia periods. This frequency phenomenon can be observed in the 24-hour frequency nadir results shown in Figure 6-9 (a), where the base case with balanced generation capacity effectively manages frequency nadirs for both day and night.

6.4.7 Sensitivity analysis of Grid service value

Another sensitivity analysis is conducted to examine the impact of grid service value on energy dispatch strategy and frequency response revenue. Three scenarios are conducted: Scenario 1 as a base case with primary response payment of 8 £/MW and secondary response payment of 10 £/MWh; Scenario 4 representing a lower grid service value with primary response payment of 4 £/MW and secondary response payment of 5 £/MWh; and Scenario 5 representing a higher grid service value with primary response payment of 16 £/MW and secondary response of 20 £/MWh.

Figure 6-10 presents the dispatch results for lower and higher grid service values. In Scenario 4 (Figure 6-10 b), with a lower grid service value, the dispatch strategy tends to rely less on gas turbines during the day, opting to increase grid charging to compensate for the energy shortfall. This is due to the decreased revenue generated from response contracts, causing the dispatch optimisation algorithm to reduce gas turbine usage and increase grid charging to minimise charging costs, taking advantage of lower electricity prices overnight.

Conversely, in Scenario 5 (Figure 6-10 c), with a higher grid service value, gas turbines are dispatched both during the day and at night, enabling a higher share in gas energy dispatch. This strategy maximises the overall revenue of the A2G system by leveraging the higher frequency response payments available.

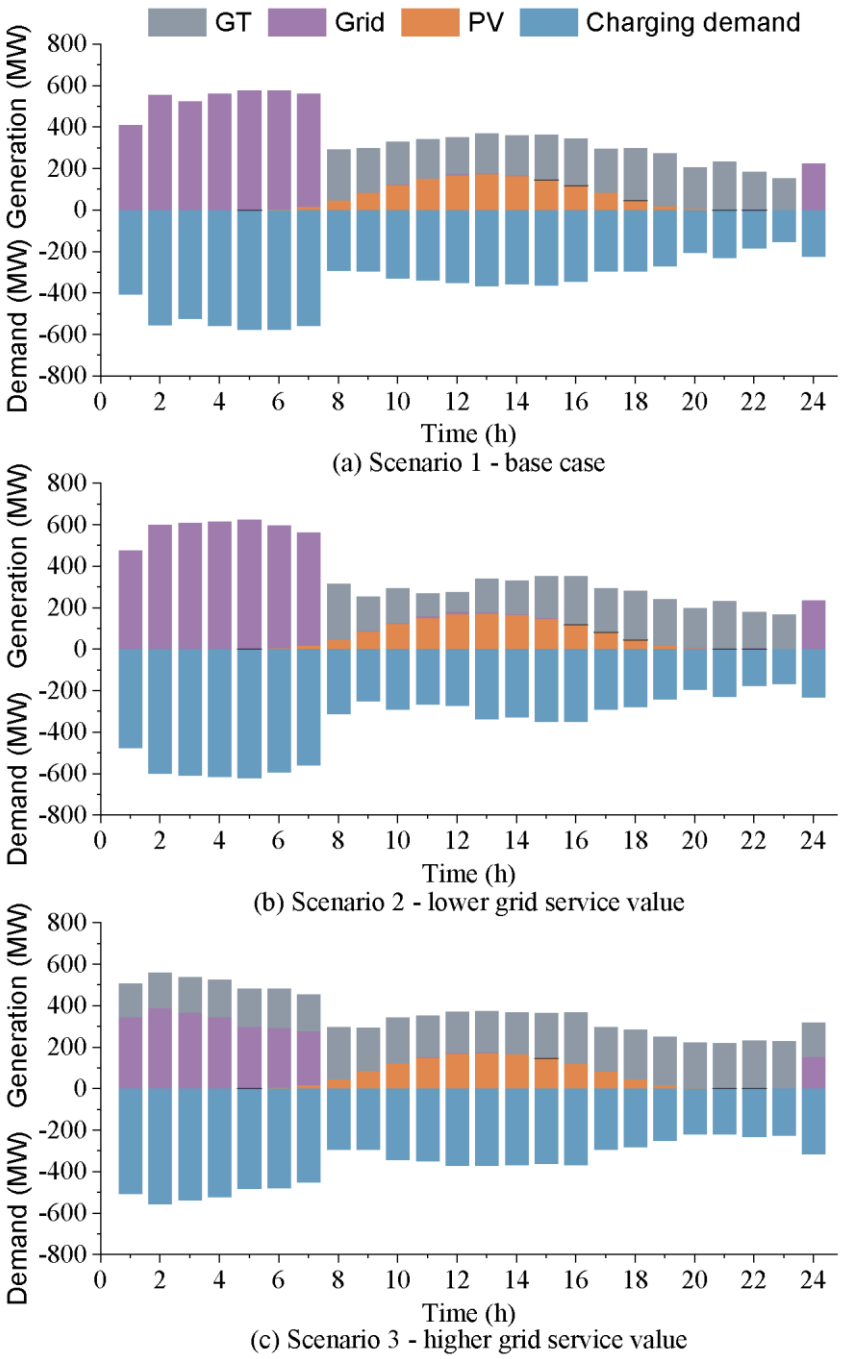

Figure 6-10 Energy dispatch results for case studies with lower and higher grid service values

In Figure 6-11 (a), the impact of varying grid service values on the energy dispatched from A2G system is illustrated. When there is a higher grid service value, the A2G system dispatches more response energy, especially during nighttime hours when the gas turbine provides secondary response. Conversely, a lower grid service value results in a reduction of response energy by half compared to the base case scenario. In Figure 6-11 (b), the

frequency response revenues are analysed across three scenarios with different proportions of primary and secondary response. A higher grid service value attracts greater frequency response revenue, as both the value and capacity of frequency response increase. It is important to note that secondary response revenue, primarily provided by the gas turbines, is more sensitive to changes in grid service value. In summary, higher grid service values result in increased energy dispatch and frequency response revenues, while lower grid service values lead to reduced energy dispatch and revenues.

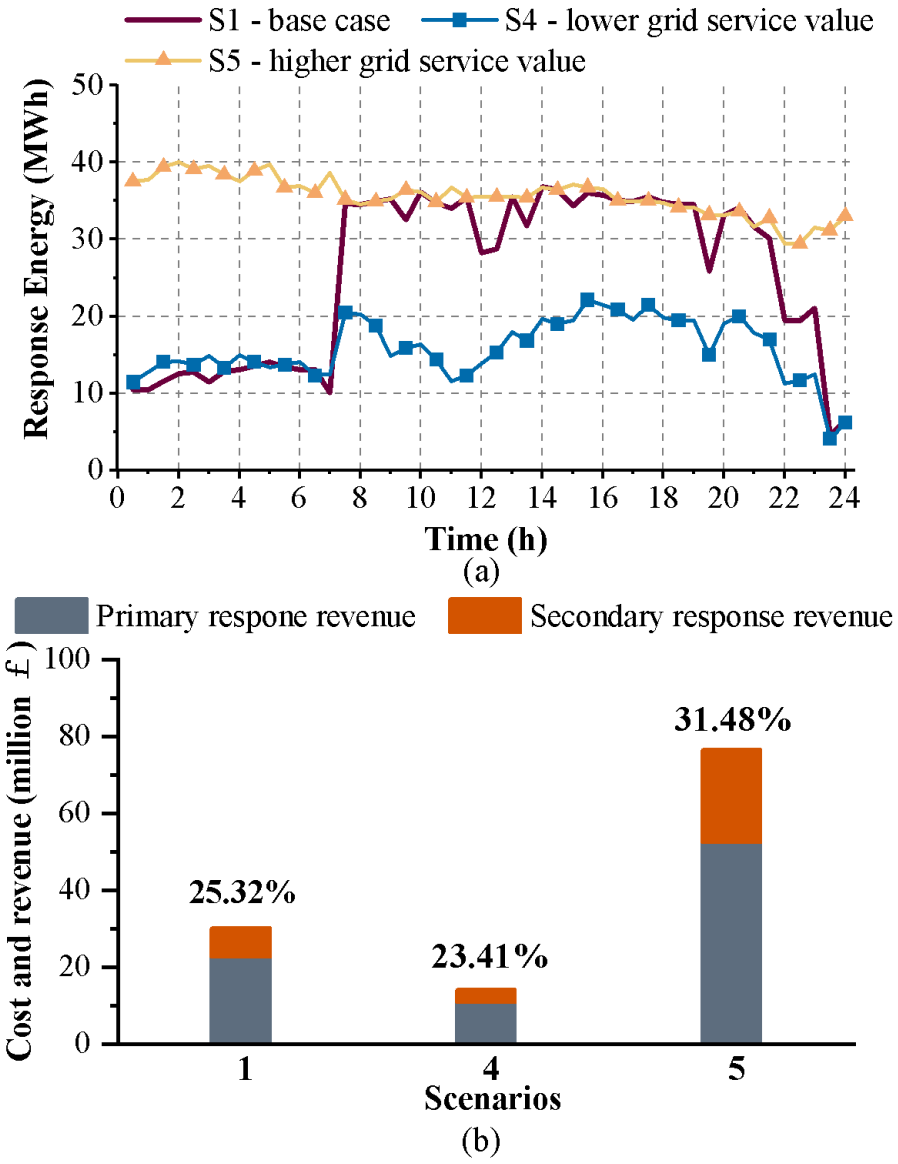

Figure 6-11 Response energy (a) and response revenue (b) of case studies with lower and higher grid service values

6.5 Conclusions

In summary, this chapter proposes a novel approach to A2G flexibility that utilises the EA battery charging system with a battery swap method to provide grid frequency response services. The smart EA charging system is developed to dispatch power from various sources to meet EA charging demand associated with seasonal flight schedules. The A2G frequency response system is designed to coordinate primary and secondary frequency response control with grid inertia estimation.

Case studies were conducted in 8 UK airports serving around 37% of the total UK domestic air passengers. The results show that the typical A2G frequency response services capacity across the 8 UK airports can reach between 900 - 1,300 MW overnight and 200 - 900 MW daytime with seasonal variation. The installed generation capacity has a significant impact on the energy dispatch strategy and response power and energy of the A2G frequency response system.

The study found that EA batteries can provide frequency response power up to six times higher than gas turbines during the day, while 100% of frequency response power is provided by EA batteries overnight. However, gas turbines can provide approximately four times higher frequency response energy than EA batteries due to sustained gas turbine output. The hourly energy dispatch strategy is optimised to achieve minimum operation costs by considering EA charging demand, energy prices, and A2G frequency response revenue.

Moreover, the annual revenue generated from A2G frequency response is estimated to be £46.58 million, covering 19.8% to 30% of energy consumption costs of EA charging in future airports. The average frequency nadir can be improved by 0.31 Hz in summer and 0.23 Hz in winter due to the A2G frequency response services. The likelihood of Infrequent Infeed Loss Risk (defined as power system frequency below 49.5 Hz) can be reduced by 83.33% in summer and 68.75% in winter, indicating significant improvements in the stability of the power grid. Another sensitivity analysis of grid service value reveals that higher grid service value attracts higher frequency response revenue. Specifically, secondary response revenue provided by gas turbines is more sensitive to the variation of grid service value. sensitivity analysis has been performed to study the impacts of

generation capacity on the energy dispatch of EA charging systems, focusing on the A2G frequency response volume, revenue, and costs. Two additional scenarios were analysed: one with half the gas turbine capacity and another with half the grid transformer capacity. The results show that the reduced gas turbine capacity leads to an uneven distribution of response power across day and night, and less response energy due to a 50% reduction in gas turbine participation for providing sustained response energy to secondary response timescales. The scenario with half the grid transformer capacity smooths out the response power and energy between day and night. These findings demonstrate the potential of A2G flexibility to enhance the reliability and efficiency of the power grid while supporting the electrification of aviation, which is crucial for achieving carbon neutrality and reducing greenhouse gas emissions in the aviation industry.

Chapter 7 Aviation-to-Grid Flexibility through Deep Reinforcement Learning

7.1 Introduction

This chapter proposes a novel DRL-based dispatch approach for EA battery recharging systems, designed to provide fast frequency response (FFR) services to power grid. The Deep Q network (DQN) approach is employed to solve the proposed problem. A case study encompassing eight major UK airports and the GB power system demonstrates the feasibility of the proposed approach, utilising the DQN method for problem-solving. The results indicate that UK airport operators could reduce the electricity purchasing cost by 58% by participating in FFR services. To examine the impact of rated EA battery charging power, three scenarios with 5 MW, 7 MW, and 14 MW chargers are explored. The primary contributions of this chapter can be summarized in three main points:

- Developed a Markov decision process (MDP) model to optimise the EA battery swap process within airports. This model considers various factors such as battery charging/discharging rates, state of charge, and the number of available battery packs to provide an efficient and reliable battery management system.
- Developed a model-free DRL approach to tackle the challenges presented by the MDP model. The DRL framework enables real-time decision-making that accommodates dynamic process of the EA battery swap stations within airports.
- The FFR price is updated by incorporating power system inertia and frequency nadir constraints. This allows for a more accurate interaction between the EA battery charging system and the power system FFR price.
- To validate the multi-area impact of A2G frequency response, simulations based on reduced GB power system are performed using DIgSILENT PowerFactory software. These simulations demonstrate the effectiveness of the proposed A2G frequency response system and its influence on power system stability and frequency regulation.

This chapter is organised as follows. Section 7.2 illustrates the concept and motivation of the proposed Aviation-to-Grid frequency response service, Section 7.4 presents the reduced GB power system model and A2G aggregate battery model developed in DIgSILENT PowerFactory. Section 7.3 formulates the A2G fast frequency response as a MDP and proposes the Deep Q Network (DQN) algorithm to solve the problem. The case study is presented in Section 7.5. Section 7.6 concludes this chapter.

7.2 Aviation-to-Grid Framework

The foundational assumptions in this chapter are consistent with those in Chapter 6, concentrating on the conceptual design of an all-electric version A320 to analyse the potential of the A2G FFR strategy. The electric A320 features a passenger capacity of 180, a flight range of 500 nm, and a 28 MWh battery capacity [3]. To prevent flight mission delays due to extended battery charging times, battery swap technology is utilised. The first group of flights to be electrified consists of domestic flights within the eight busiest UK airports, as depicted in Figure 7-1. To ensure the safe operation of the power system, a robust charging infrastructure and efficient recharging scheduling dispatch strategies are essential for EA adoption.

This chapter investigates a DRL approach to establishing A2G as a crucial nexus between electrical power and electrified air transport systems. A2G comprises various levels and locations of integration between the power system and electrified air transport system, including individual airports and national power system operations. A2G flexibility is proposed as the ability of electrified air transport to adjust, within defined boundaries and at acceptable ramp rates, to balance electricity supply and demand within its system and support power systems frequency.

7.3 DRL-Based Aviation-to-Grid Strategy

In this chapter, all the EA batteries at the airport are centrally dispatched. To address the challenges associated with the highly scheduled EA charging problem, a DRL-based dispatch approach is proposed. This approach manages the charging and reserve schedule of EA batteries to provide FFR service, while adhering to the flight schedule for each airport p, as shown in Eq. (7.1).

$$\mathcal{F}_p = \left[F_{p,1}, F_{p,2}, \cdots, F_{p,T}\right] \tag{7.1}$$

7.3.1 Aviation-to-Grid System Model

The A2G system model dispatches the EA batteries to charge or reserve for frequency service, taking into account the interactions between the air transport network and the power system. The objective function of the A2G system model aims to minimise the total cost, which comprises electricity expenses and FFR revenue:

$$\min f = \sum_{t=1}^{T}\sum_{p=1}^{P}\left(\pi_t^e \cdot N_{c,p,t} \cdot P^{charger}\Delta t - p_{rev,t} \cdot P^{charger} \cdot N_{p,r,t}\right) \tag{7.2}$$

where π_t^e is the electricity purchase price, $p_{rev,t}$ is the FFR revenue, $P^{charger}$ is the rated power of EA batteries, $N_{c,p,t}$ is the number of charging batteries for at airport p, $N_{p,r,t}$ is the number of EA batteries reserving for FFR at airport p.

Subject to:

$$SOC_{min} \le SOC_{p,i,t} \le SOC_{max} \tag{7.3}$$

$$0 \le E_{p,i,t} \le \min\left(\frac{E_{batt}^{EA}\left(SOC_{max} - SOC_{p,i,t}\right)}{\eta\Delta t}, P^{charger}\right) \tag{7.4}$$

1) Battery Swap Process: At the start of each step, the battery swap process is carried out if there are flight missions at this step. First, the list of SOC values of EA batteries $SOC_{p,i,t}$ is sorted in ascending order. Next, the first $F_{p,t}$ batteries in the list undergo swapping by exchanging the SOC values with the depleted batteries. The number of EA batteries that are swapped to the arrival flights but not yet fully charged is denoted as $N_{p,u,t}$. The constraint violation is represented by the penalty cost $C_{pen,t}$:

$$C_{pen,t} = \rho^{pen} \cdot N_{p,u,t} \tag{7.5}$$

where ρ^{pen} is the penalty for violating the constraint.

2) Battery Charge and Reserve Process: Once the battery swap process is completed, the updated SOC list is sorted in ascending order again. Based on the action, $N_{c,p,t}$ batteries from the first battery that are not fully charged undergo charging. The charged energy for each battery is constrained to be less than the energy required for a fully charge, as demonstrated in Eq. (7.4). The number of batteries reserved for FFR services at the step

equals the number of batteries that are neither charging nor being swapped, as illustrated in Eq. (7.6). The complete process of EA battery charging scheduling is depicted in Algorithm 7.1.

$$N_{p,r,t} = N_{p,b} - N_{c,p,t} - F_{p,t} \tag{7.6}$$

where $N_{p,b}$ is the total number of batteries in the airport p.

Algorithm 7.1: EA Battery Charging Scheduling Algorithm

Input: $N_{c,p,t}, SOC_{p,i,t}, p = 1,2,\dots,P, i = 1,2,\dots,N_{p,b}, ep_t, F_{p,t}$.
1: Estimate the FFR price through Eq. (7.9) and system inertia.
2: **for** $a = 1,2,\dots,A$ **do**
3: Sort $SOC_{p,i,t}$ in descending order.
4: Replacing first $F_{p,t}$ of batteries with depleted SOC values.
5: Record the number of unsatisfied batteries $N_{p,u,t}$.
6: Sort $SOC_{p,i,t}$ in ascending order.
7: Charge first $N_{c,p,t}$ of batteries through Eq. (7.3) and (7.4).
8: Record the number of reserved batteries $N_{p,r,t}$.
9: Calculate penalty $C_{pen,t}$ through Eq. (7.5).
10: Calculate overall cost f_t through Eq. (7.2).
11: Output the reward r_t through Eq. (7.11).
12: **end for**

7.3.2 Fast Frequency Response Service

FFR service is a potential scheme in the GB power system, where the price should vary over time to reflect the real-time balancing of the power system [194]. In this chapter, the FFR price is calculated every time step (30 minutes time interval) based on the power system inertia. The inertia of the power system is determined by the generation mix:

$$H_{sys} = \sum_g H_g \cdot \frac{S_g}{S_{ND}} \tag{7.7}$$

where H_g is the inertia constant for generation unit g. S_g and S_{ND} are rated generation power of generation unit g and national demand respectively.

After deriving the inertia of the power system, the required amount of PFR and FFR power can be derived by applying the frequency nadir limit [194]. It is important to note that the FFR service must be fully delivered within 1 second after a contingency occurs, while the PFR is required to be fully delivered within 10 seconds following the

contingency. The price of FFR is calculated based on the amount of P_{PFR} can be replaced by the P_{FFR}, as shown in Eq. (7.8). P_{PFR} represents the aggregation of all generators that can provide PFR services.

$$\left(\frac{H_{sys}}{f_0} - \frac{P_{FFR} \cdot T_{FFR}}{4 \cdot \Delta f_{max}}\right) \cdot \frac{P_{PFR}}{T_{PFR}} \geq \frac{(P_{loss} - P_{FFR})^2}{4 \cdot \Delta f_{max}} \tag{7.8}$$

where Δf_{max} is 0.8 Hz, P_{FFR} is 1000 MW initially. T_{FFR} and T_{PFR} equals to 1s and 10s, respectively.

To prevent under-frequency load shedding during the most significant power loss event in the GB power system, the required amount of PFR should be calculated using Equation (7.9), which is presented below:

$$P_{PFR} \geq \frac{(P_{loss} - P_{FFR})^2 \cdot T_{PFR}}{4 \cdot \Delta f_{max}\left(\frac{H_{sys}}{f_0} - \frac{P_{FFR} \cdot T_{FFR}}{4 \cdot \Delta f_{max}}\right)} \tag{7.9}$$

Finally, the price of FFR is determined by calculating the equivalent amount of PFR that an additional megawatt (MW) of FFR can replace, as derived from Eq. (7.9).

7.3.3 Markov Decision Process

Reinforcement learning problems should be formulated as a MDP [148]. The following discussion covers the state, action, state transition function, and reward function of the MDP.

1) State: The system state S, as described by Eq. (7.10), comprises the electricity price, frequency response price, battery swap demand, and the SOC of the EA batteries.

$$S = \left\{s \middle| s_t = \left(\pi_t^e, \mathcal{F}_p, p_{rev,t}, SOC_{p,i,t}\right)\right\} \tag{7.10}$$

2) Action and State Transition Function: To dispatch the number of charging batteries at time *t*, a discrete action space $A = \left\{a \middle| a_t = N_{c,p,t}\right\}$ is established. Once an action is selected, the number of charging batteries $N_{c,p,t}$ is used to compute the next system state following the process described in Section 7.3.1.

3) Reward and State-action Value Function: The real-time reward function is formulated using the objective function Eq. (7.2) and the penalty function Eq. (7.11), defined as follows:

$$r_t = -f_t - C_{pen,t} \tag{7.11}$$

where f_t represents the value of objective function at time *t*.

At each time step *t*, the optimal action A can be determined by solving the corresponding state-action value function:

$$Q^{\pi}(s,a) = E_{\pi}[r_t | s_t = s, a_t = a] \tag{7.12}$$

The objective of the proposed A2G dispatch problem is to find a policy π that maximises the state-action value function Eq. (7.13), which is defined by the following equation:

$$\pi = \arg\min_{\forall a \in A} Q^{\pi}(s,a) \tag{7.13}$$

7.3.4 DQN Algorithm

In this chapter, the DQN algorithm is selected as the method for solving the reinforcement learning optimisation problem. The DQN algorithm trains the agent to learn a dispatch policy based on past observations, iteratively updating the state-value function in accordance with the Bellman equation:

$$Q^{\pi}(s,a) = E_{\pi}[r_t + \gamma Q^{\pi}(s_{t+1}, a_{t+1}) | s_t = s, a_t = a] \tag{7.14}$$

Algorithm 7.2: Training Process of DQN Algorithm

Initialize: replay memory $\mathcal{D}$ to capacity $\mathcal{N}$, action-value function Q with random weights.

Initialize action-value function $\hat{Q}$ with parameter $\hat{\theta} \leftarrow \theta$
for episode $= 1,2,\ldots,M$ **do**
  Initialize sequence s_0 and preprocess $\phi_0 = \phi(s_0)$
  for t $= 1,2,\ldots,T$ **do**
    Select an action a_t based on the current state s_t.
    Execute a_t in the environment **Algorithm 1**.
    Transit to the next stage s_{t+1} and obtain the reward r_t.
    Pre-process next state $\phi_{t+1} = \phi(s_{t+1})$.
    Store transition $(\phi_t, a_t, r_t, \phi_{t+1})$ in $\mathcal{D}$.
    Sample random minibatch of transitions from $\mathcal{D}$.
    Set $y_i = \begin{cases} r_i & , \mathcal{D}_i \neq 0 \\ r_i + \gamma \max_{a'} \hat{Q}(\phi_{i+1}, a'; \hat{\theta}), & \mathcal{D}_i = 0 \end{cases}$
    Perform a gradient descent step on $\left(y_i - Q(\phi_i, a_i; \theta)\right)^2$.
  end for
end for

Algorithm 7.2 presents the training process of the DQN algorithm. The DQN algorithm

enhances the traditional Q learning algorithm in three ways: by incorporating an experience playback mechanism, using a fixed goal Q-value network, and narrowing the reward value range.

7.4 GB Power System Model

Upon acquiring the charging and reserve schedules for EA batteries, the ability of A2G flexibility to provide frequency response services to the grid are evaluated using the simulation proposed in this section.

7.4.1 37-Bus GB Power System Model

In this study, a reduced dynamic equivalent model of the GB power system is employed for the case study analysis. This equivalent model was meticulously developed by the National Grid using DIgSILENT PowerFactory software, specifically for academic research purposes [195][196]. As illustrated in Figure 7-1, the entire transmission network of GB power system comprises 37 distinct zones.

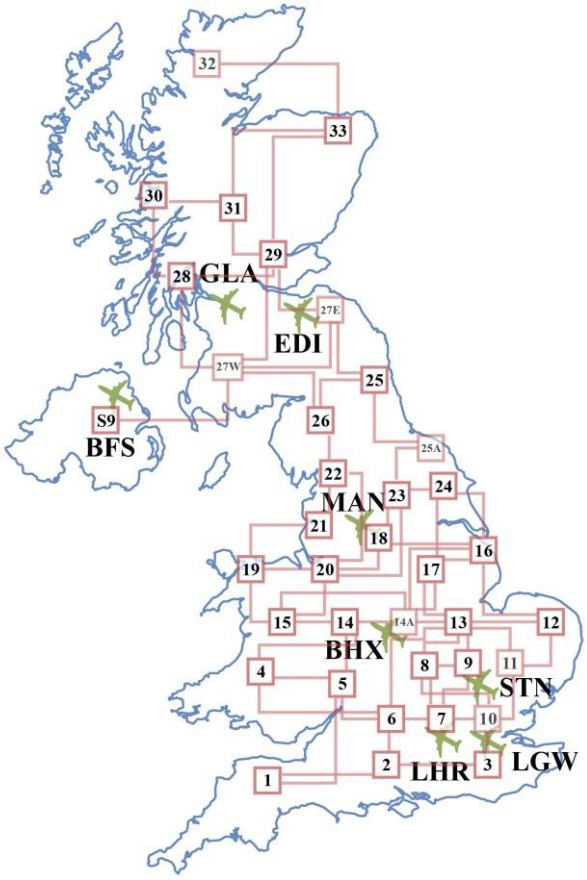

Figure 7-1 Reduced GB 37-bus transmission system and UK airport map

To better reflect future energy scenarios, the generation mix in the dynamic equivalent model has been further modified based on the National Grid's Future Energy Scenario [63] as follows:

- Adjusted the generation mix, specifically by proportionally increasing the renewable generation (solar PV and Wind) capacity, and reducing the generation power of synchronous generators accordingly.
- Incorporated EA batteries connected to each zone based on the geographical distribution of airports. And added an additional zone was to the model to represent Northern Ireland.

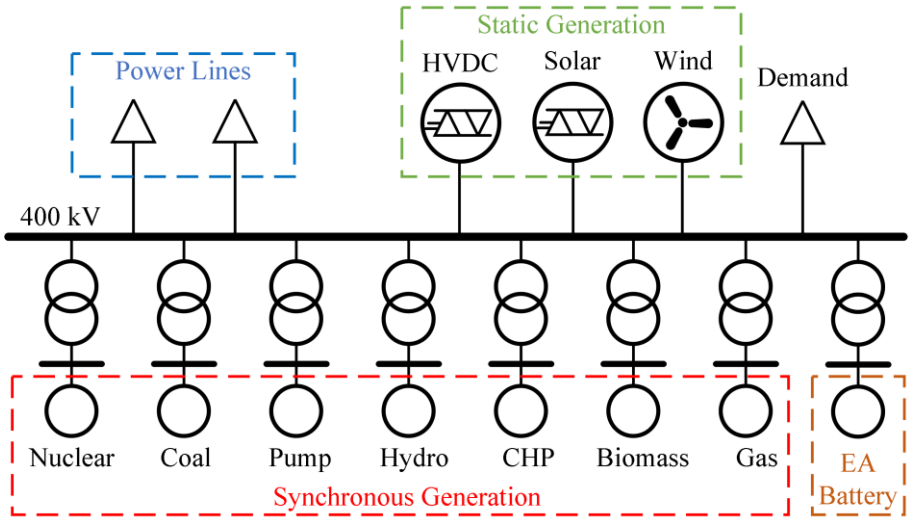

Figure 7-2 Structure of a single zone substation in the reduced GB power system model

Table 7-1 Connections of Major Airports

Airport	IATA Code	Zone
London Heathrow	LHR	7
Edinburgh	EDI	27E
Glasgow	GLA	28
Manchester	MAN	18
Birmingham International	BHX	14A
Belfast International	BFS	S9
London Gatwick	LGW	10
London Stansted	STN	9

This modification ensures that the case study analysis considers the anticipated changes in energy production and consumption, providing a more accurate representation of how the GB power system may evolve over time. The details of modified generation mix can be found in Section 7.5. By utilising this updated model, the case study can more effectively evaluate the impacts and benefits of the proposed A2G FFR strategy within the context of future power system operations and requirements.

Figure 7-2 illustrates the structure of a single-zone substation within the 37-bus reduced GB power system model. Each zone features generators, a load model, and high-voltage direct current (HVDC) interconnectors connected to the busbar. Each synchronous generator is equipped with standard governor control (GOV), automatic voltage regulator (AVR), and power system stabilizer (PSS) [197], ensuring stable and efficient operation of the power system. It is important to note that not all generators and connectors are installed in every bus. In cases where specific types of generators are not present, the power output for those generators will be set to 0. This ensures a more accurate representation of the power system and its components.

Renewable generators, such as PV and WT, are modelled as static generators, meaning they are unable to provide frequency response services in this study. Airports are integrated into the GB power system through the geographical adjacent busbars. For example, London Heathrow (LHR) airport is connected to Zone 7. The specific connections of the airports to the GB power system can be found in Table 7-1, which details the corresponding zones for each of the airports considered in this study. This integration allows for a more realistic and accurate representation of the interactions between the electrified air transport system and the power grid, enabling a comprehensive assessment of the proposed A2G FFR strategy's impacts and benefits.

7.4.2 Aggregate EA Battery Energy Storage Model

The EA batteries are represented by a large-scale battery energy storage model [198], connected to the busbars at the representative airport locations. As depicted in Figure 7-3, the aggregate EA battery is modelled using a DC Voltage Source and a pulse-width modulation (PWM) technique. The PWM enables efficient control of the power electronics, ensuring smooth and responsive operation of the battery system.

The most critical component of this model, in the context of this study, is the frequency controller, highlighted by a red rectangle in Figure 7-3. The frequency controller comprises a proportional controller with a deadband feature. This configuration allows the controller to effectively manage the frequency response provided by the EA batteries, ensuring that they contribute to maintaining the frequency stability of the power system as needed.

By integrating this frequency controller into the EA battery model, the study can thoroughly evaluate the impact of the proposed A2G FFR strategy on the power system's frequency response and overall performance. This detailed representation of the EA battery system provides valuable insights into the potential benefits and challenges of implementing the A2G FFR strategy in real-world power grid environments.

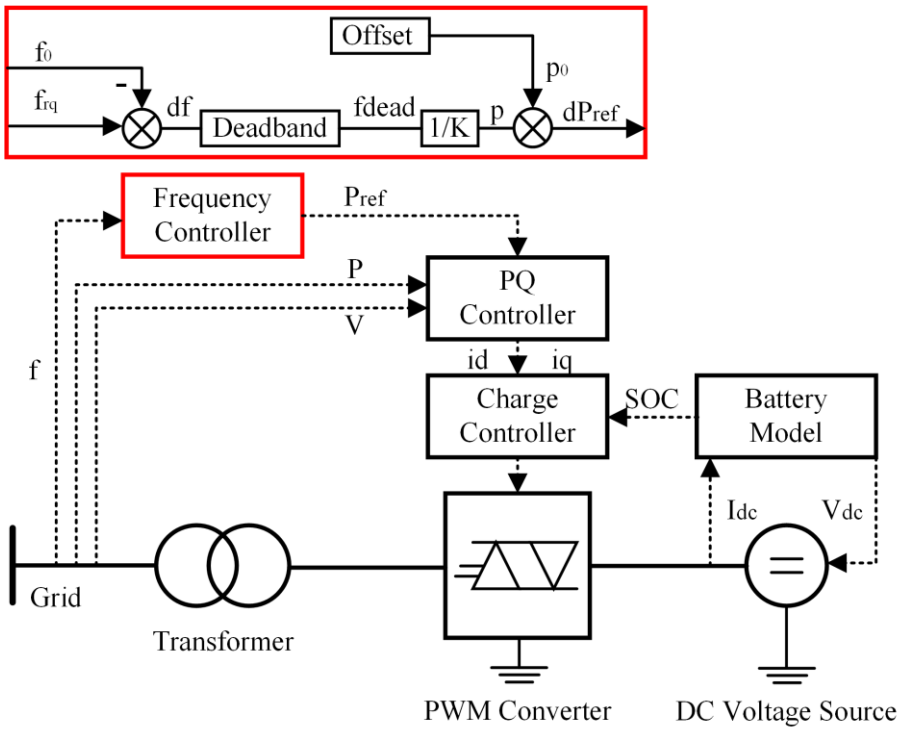

Figure 7-3 EA battery model featuring frequency controller implemented in DIgSILENT PowerFactory

7.5 Case Study

In this section, the proposed DQN network is trained and evaluated using the national demand, which ranges from 20 GW to 60 GW, along with 6.5 GW of wind capacity and 13 GW of PV capacity. The power system connects of 35 inertial generation units

including nuclear power plants, gas turbines, hydraulic generators, biomass generators, and pump storage units. The initial price for PFR is set as £10/MW/h. The 2019 UK peak air transport schedules are utilised as the training database, which is shown in Appendix B. The time-of-use electricity price are as follows: a peak tariff is 200 £/MWh (7:30-10:00, 16:30-21:00), an off-peak tariff is 70 £/MWh (0:00-7:00, 23:30-24:00) and a mid-peak tariff is 150 £/MWh (10:30-16:00, 21:30-23:00).

One critical parameter that significantly impacts the results is the rated charging power of EA batteries. To investigate the differences resulting from various rated charging powers, three case studies are conducted, featuring EA charging powers of 5 MW, 7 MW, and 14 MW. The total number of EA batteries stored at each airport is assumed to be 25% of the daily arrival flight number. This assumption ensures that the operation of flights will not experience delays due to any discrepancies between the availability of fully charged batteries and flight demand. By maintaining an adequate supply of charged batteries, the system can accommodate fluctuations in flight schedules.

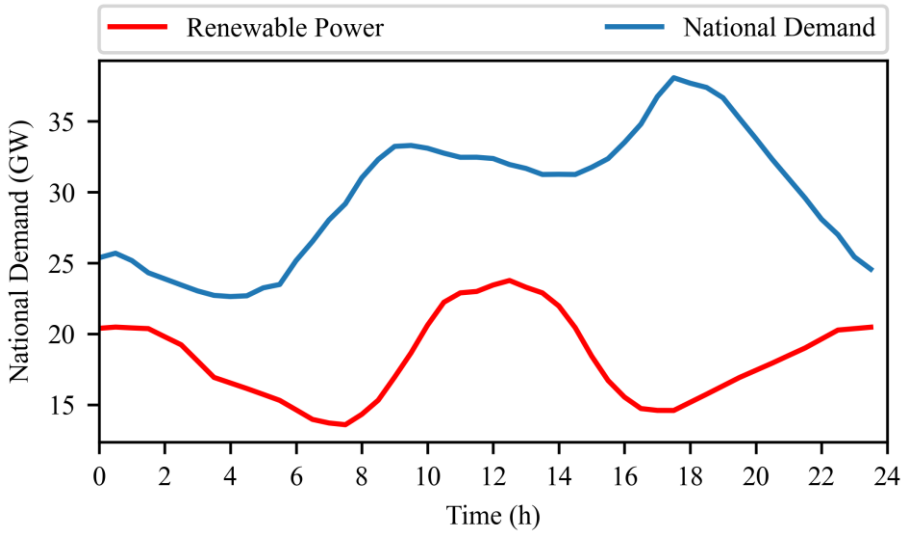

Figure 7-4 National demand and renewable power data for a typical day

To evaluate the performance of the A2G fast frequency response service, a typical day shown in Figure 7-4 is selected for running the test. The simulated system loss for frequency events is assumed at 1800 MW in Zone 3, and the events are assumed to happen every half an hour. The power system simulations are implemented in DIgSILENT PowerFactory.

7.5.1 Training Results

The neural network training process is shown in Figure 7-5, with depicting the average cost for all airports. During the initial stage (first 500 episodes), the average cost experiences fluctuations at a higher level without a significant downward trend. This occurs because the algorithm is still learning the policy through sampling new input data and accumulating experience, with the penalties applied for the failure to provide fully charged EA batteries. Following this process, the algorithm obtains the optimal action strategy, and the overall cost experienced a substantial decrease, from more than 1×10^7 £ to less than 2×10^6 £. After approximately 5,000 training episodes, the average overall costs of the three cases converged at 1.53×10^6 £, 1.28×10^6 £, and 1.16×10^6 £ respectively, as shown in Table 7-2. The converged average cost values demonstrate that higher rated power for EA battery chargers results in lower overall operation costs. The A2G revenues for the three cases account for 3.93%, 6.47%, and 13.2% of their respective charging costs. The results indicate that higher rated charging power leads to a greater proportion of the charging cost being offset by A2G revenue.

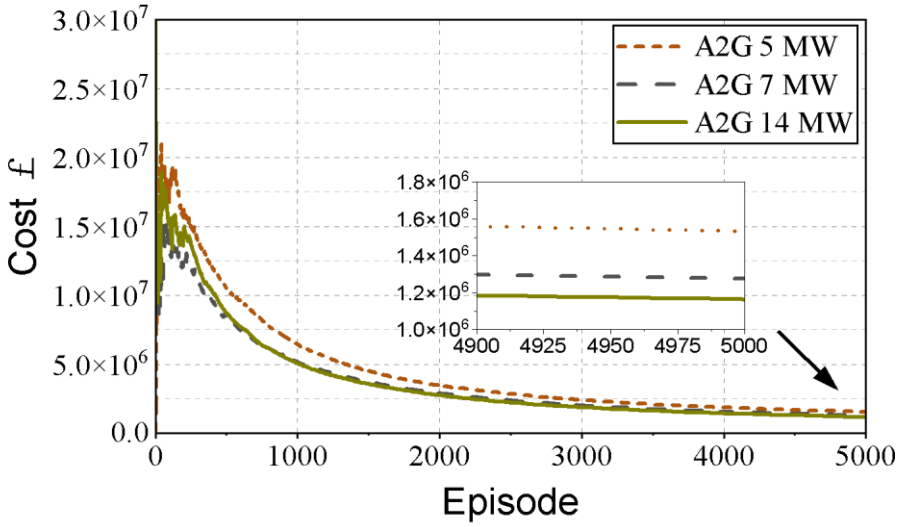

Figure 7-5 Convergence of the average rewards curve for DQN

Table 7-2 Converged Average Charging Cost and A2G Revenue for Three Cases

Capital (£)	5 MW	7 MW	14 MW
Charging Cost	1.60×10^6	1.36×10^6	1.34×10^6
A2G Revenue	6.3×10^4	8.8×10^4	1.77×10^5
Overall Cost	1.53×10^6	1.28×10^6	1.16×10^6

7.5.2 Optimal Dispatch Results

After the training process is finished, the converged neural network is applied in another environment with the selected input data, as shown in Figure 7-4.

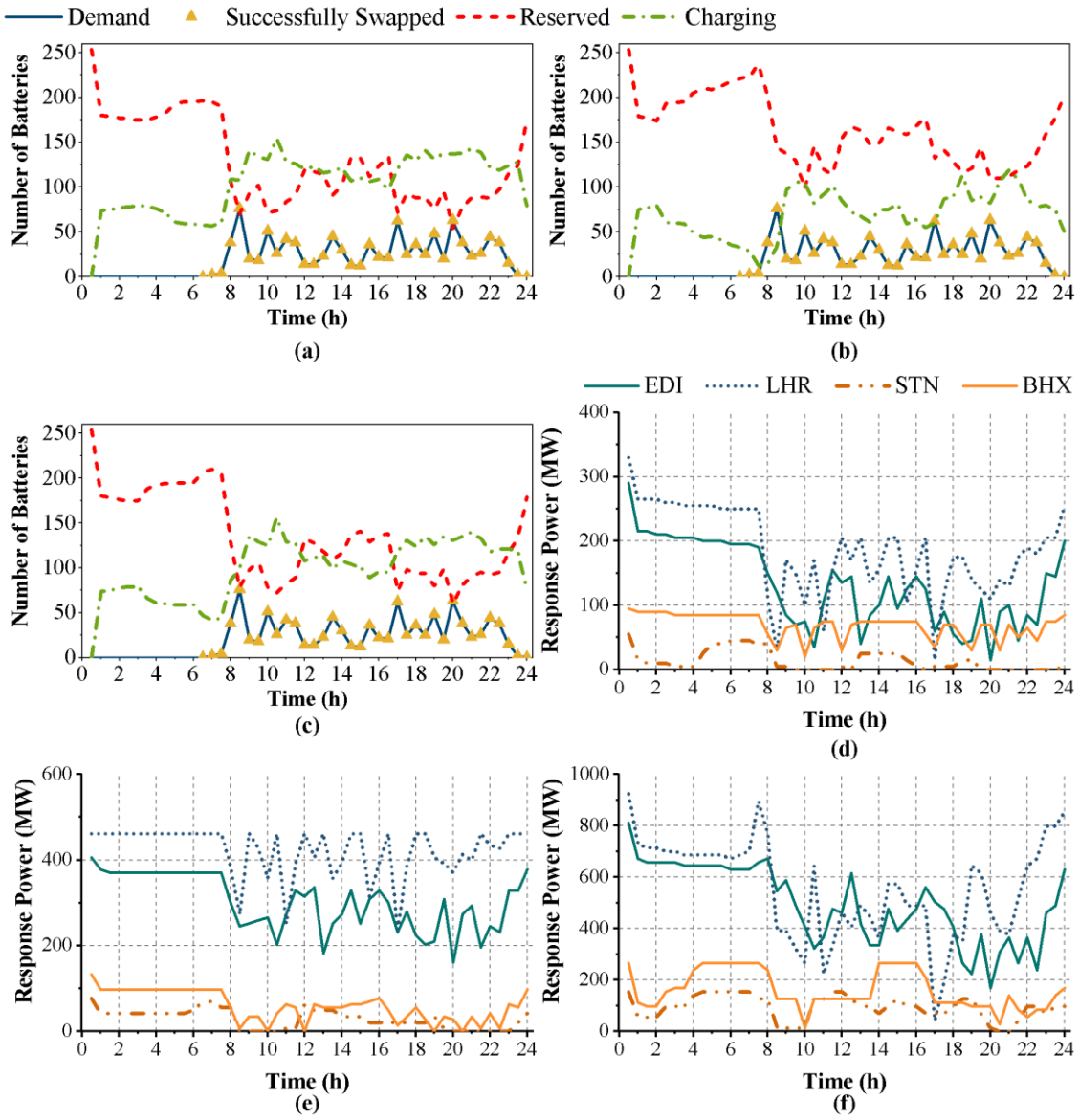

Figure 7-6 Dispatch results obtained by the proposed DQN-based approach: Operation status of EA battery charging system for all airports with 5 MW (a), 7 MW (b), and 14 MW (c) rated charging power; Aggregate response power of EA batteries with 5 MW (d), 7 MW (e), and 14 MW (f) rated charging power for four airports (EDI, LHR, STN, and BHX).

As shown in Figure 7-6 (a)(b)(c), all the flight mission demands for three cases are satisfied. At the beginning of the day, the batteries restored at airports are dispatched to

be fully recharged to satisfy the morning peak flight demand. With the rated EA battery charging power increases, the fewer EA batteries are charging at the same time across the day and the higher number of batteries will be available for participating A2G frequency response reserve. In terms of battery dispatch, the number of charging batteries is significantly high during the daytime from 09:00 to 20:00, indicating that the EA battery charging demand patterns are similar to the flight schedules across the day. The EA charging demand is uniformly distributed during the night time, and the number of reserve batteries reaches a peak at 07:30, which is exactly the time before the morning peak. This is because the cheaper electricity price during the night incentivizes the EA battery charging system to charge the swappable batteries ready for the morning peak flight missions the following day.

The response power from four selected representative airports (EDI, LHR, STN, and BHX) is shown in Figure 7-6 (d)(e)(f). The EDI and LHR represent large airports while STN and BHX represent medium hub airports. The results indicate that large airports (EDI and LHR) can provide higher response power than medium airports. Especially during night time, large airports can provide 2 to 3 times higher response power than medium airports. As shown in Figure 7-6 (d), response powers generated from both large airports and medium airports are fluctuated around the lower level (0 to 200 MW) from 8:00 to 23:00. This is because the lower rated charging power makes it difficult to dispatch more batteries to reserve for FFR services. In the case of 7 MW EA battery chargers, the large airports can provide relatively stable FFR response power during daytime, indicating that the flight mission demand is easier to be satisfied with 7 MW EA battery chargers. In contrast, the response powers from large airports fluctuate from 200 to 600 MW during the daytime in the case of 14 MW EA battery chargers. This is because the power system does not need higher response power to save the frequency during high-inertia time (8:00 to 23:00), and higher response power is concentrated in the night-time to prevent severe frequency drop due to low-inertia.

Figure 7-7 shows the total FFR response power from all 8 major airports for three cases. The trends of response power across the day are similar for three cases: high response power is available during the night, and there is less response power during the morning peak (08:00 – 10:00) and evening peak (18:00 – 23:00). The A2G strategy can provide

around 800 – 3200 MW during the night and 300 – 2400 MW during the daytime to the GB power system.

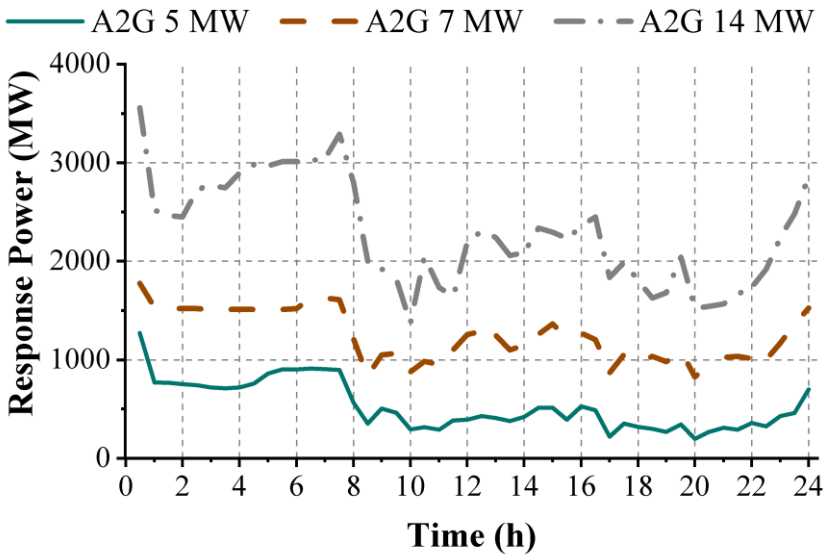

Figure 7-7 Total frequency response power across one day from all 8 airports for three cases

7.5.3 A2G Frequency Response Simulation Results

The A2G frequency response control mechanism is triggered when a large frequency deviation such as a power generation loss event happens. Figure 7-8 compares the frequency deviation profiles with and without the A2G frequency response due to 1800 MW generation loss on the GB power system at 02:00, 07:00, and 14:00 with different rated charging power of EA battery.

The most effective A2G frequency response appears at 07:00 (Figure 7-8 (b) and (f)), which can restore the frequency nadir from 49.15 Hz to 49.75 – 49.9 Hz by comparing it with the non-A2G response case. This is due to the high response power that A2G can provide with no flight schedules at 07:00, together with low system inertia during the minimum national demand period.

During the evening peak period from 18:00 to 20:00, the A2G service provides the least effective frequency response due to the peak flight schedules so the EA charging system will prioritise its reserve charging power to meet aviation requirements instead of grid frequency response.

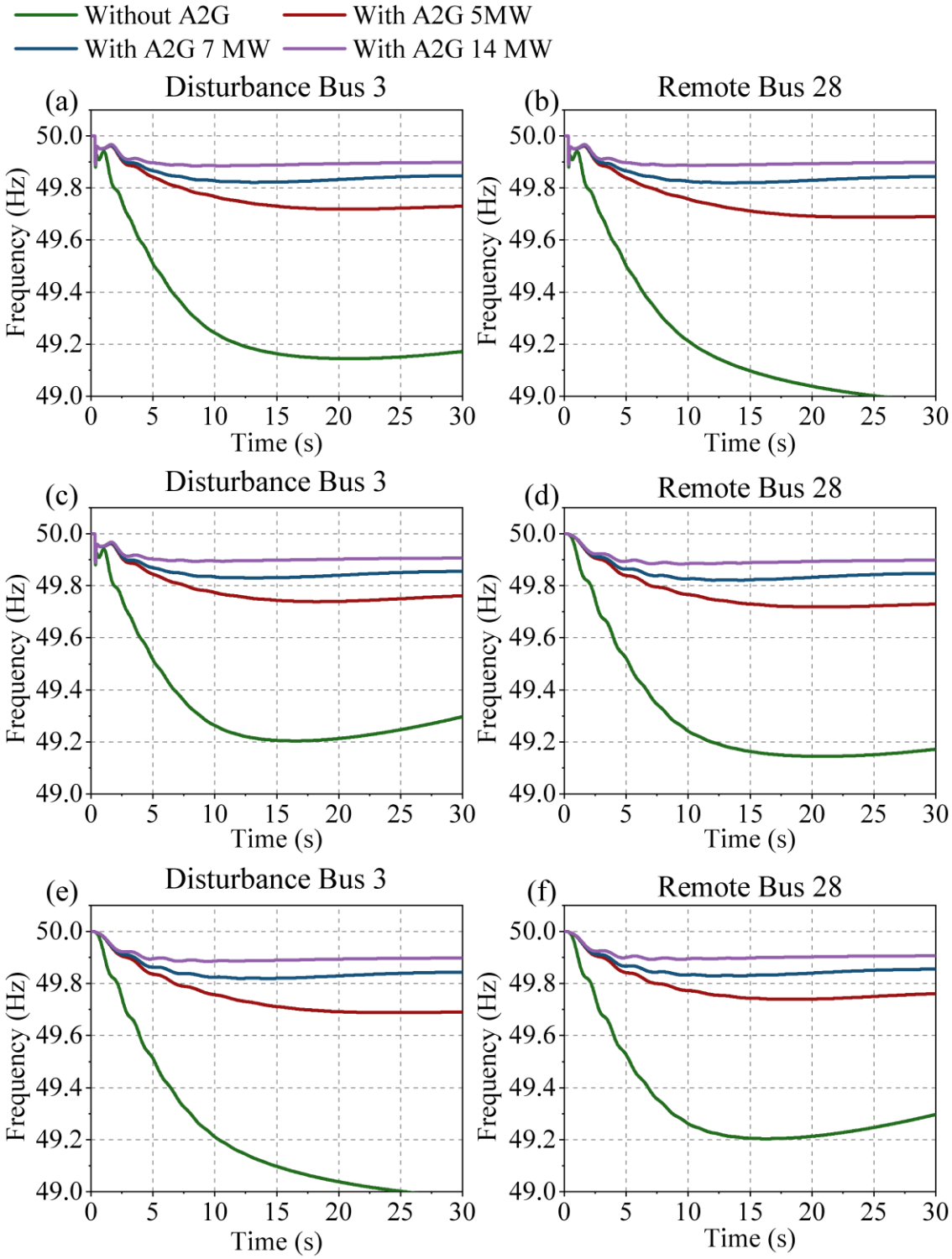

Figure 7-8 Frequency variations in difference cases with and without A2G frequency response at 02:00(a), 07:00 (b), 14:00 (c) at disturbance bus 3, and 02:00(e), 07:00 (f), 14:00 (g) at remote bus 28

Figure 7-9 shows the frequency nadir – the minimum post-contingency frequency after the system suffers a loss of 1800 MW generation every 30 minutes with and without A2G frequency response. Comparing with the non-A2G scenario, the half-hourly frequency nadir in the case with 5 MW EA battery chargers improved significantly by approximately 0.4 – 0.9 Hz during the night and 0.2 – 0.3 Hz in the daytime. However, the results for all cases with different charger power rating shows that the system frequency is always kept within the safe range (higher than 49.5 Hz) in the 1800 MW power loss event across the day. At the same time, the frequency nadir results for 7 MW and 14 MW show that the system frequency A2G response can save the frequency response to a safer frequency range (higher than 49.7 Hz). Most importantly, the A2G frequency response can completely avoid Infrequent Infeed Loss Risk (defined as below 49.5 Hz) [62]. The average frequency nadir across the day of the base case is 49.23 Hz, while the value was improved to 49.66 Hz, 49.80 Hz, and 49.86 Hz by cases with 5 MW, 7 MW, and 14 MW A2G chargers.

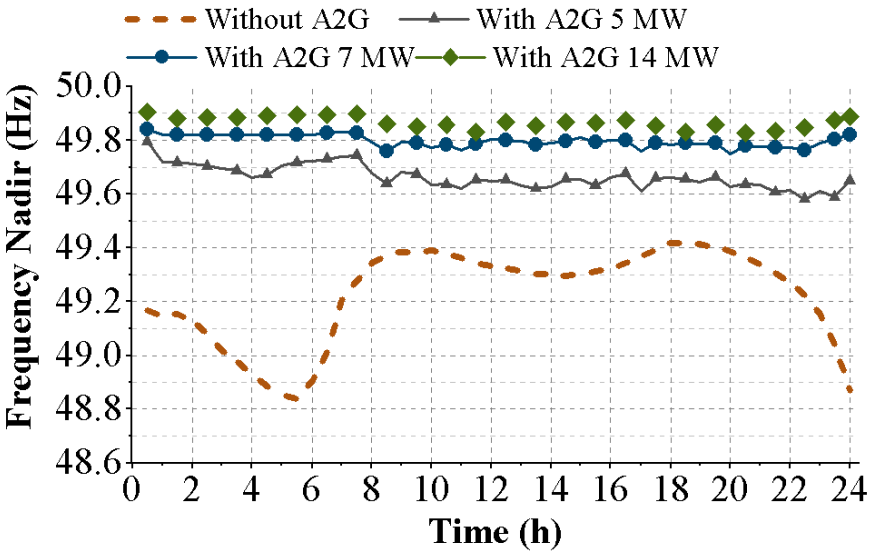

Figure 7-9 Frequency nadirs across the day for different cases

7.6 Conclusions

This chapter proposed a DRL-based approach for dispatching the EA battery recharging system to provide FFR services to the power grid with the A2G capability. The results demonstrated the feasibility of the A2G FFR strategy for providing essential flexibility services to the power grid whilst fulfilling the EA charging demand associated with the flight schedules. Considering the EA charging demand, energy prices, and A2G

frequency response revenue, the hourly energy dispatch strategy is designed to achieve the lowest possible operation costs. Case studies with different levels of rated EA battery charging power of 5 MW, 7 MW, and 14 MW are conducted in 8 UK airports that serve approximately 37% of the total domestic air travellers in the UK. The results show that the typical A2G frequency response services capacity across the 8 UK airports can reach between 800 – 3200 MW overnight and 300 – 2400 MW daytime depending on different rated EA charging power. The response power is essential for the GB power system, especially during the night when the system inertia is low.

The rated EA battery charging power has a significant impact on the energy dispatch results and response power of the A2G frequency response system. The revenues that are generated from A2G frequency response are estimated to be 6.3×10^4 £, 8.8×10^4 £, and 1.77×10^5 £ for 5 MW, 7 MW, and 14 MW EA battery charger, which can cover 3.93%, 6.47%, and 13.2% of charging power consumption costs in the airports, respectively. The average frequency nadir was improved to 49.66 Hz, 49.80 Hz, and 49.86 Hz by cases with 5 MW, 7 MW, and 14 MW A2G chargers, and the likelihood of Infrequent Infeed Loss Risk can be totally avoided.

For future work, the competition mechanism between multi-airport EA charging systems will be built through multi-agent deep reinforcement learning. Future works will also focus on the application of A2G to participate in regional ancillary services for power network constraint management.

In the next chapter, the conclusions of the studies conducted in this thesis are presented, along with suggestions for future works.

Chapter 8 Conclusions and Future Research

This thesis has contributed to the planning and design of electrified energy networks for sustainable aviation considering the ancillary services (A2G) to the grids from electrified aviation technologies including EA, airport parking EVs, and electric airport shuttle buses. In this concluding chapter, section 8.1 summarises the key contributions of this thesis. Section 8.2 outlines the suggestions for future work.

8.1 Summary and Conclusions

The key motivation of the research, as explained in Chapter 1, was to investigate the electricity network infrastructure planning for the electrification of aviation with EA and the airport-based DER resources that can provide ancillary services to the power grid. The key contributions of the thesis are summarised as follows.

8.1.1 Planning framework for the airport microgrid accommodating EA and parking EVs

As reviewed in Section 3.2, existing research has primarily concentrated on designing EA charging system. However, these studies have not investigated the coordinative interactions between EA charging system and airport parking EV charging systems. In this study, a multi-objective infrastructure planning framework for the airport microgrid to simultaneously accommodate parking EVs and EAs is proposed. Additionally, two different scheduling strategies (plug-in charge and battery swap) for charging EA batteries are proposed and compared. The key findings in this research are listed as follows:

The results obtained from the without EV, G2V, and V2G scenarios demonstrate that implementing the V2G strategy can significantly enhance the airport microgrid economic and operational performance. This finding indicates that V2G services from airport parking EVs can bring substantial benefits to airport operators in terms of energy management. At the same time, encouraging the parking EV owners to participate in V2G services is essential for reducing the total operation cost of future electrified aviation, benefiting both EV owners and airport operators.

Comparing the two different EA charging strategies, the Pareto Front results reveal that

the EA battery swap strategy outperforms the EA plug-in charge strategy in terms of microgrid operation performance, regardless of whether airport parking EVs are involved in the microgrid operation or not, particularly in peak-to-valley ratio (PVR) and resilience factor (RF).

The sensitivity analysis on EA implementation levels shows a clear trend of increasing difficulty in airport microgrid operation as the EA implementation level rises. Airport operators should consider adopting a microgrid independent from the airport landside (terminal building) energy system to support higher EA implementation level. The sensitivity analysis on renewable generation uncertainties underscores the importance of adopting hydrogen fuel cells with higher capacity to mitigate the negative effects of renewable generation on the airport microgrid.

Most notably, to the best of the author's knowledge, this is the first study to investigate the coordinative scheduling of EA and airport parking EVs. Our findings provide valuable insights for airport operators striving to decarbonise their air transport activities through the adoption of EA, emphasising the significance of this research in promoting sustainable aviation practices.

8.1.2 Planning approach for the wireless charging system for airport electric shuttle buses

While the existing work in the field of wireless charging systems for EVs primarily focuses on the planning and design of equipment enabling wireless power transfer, these studies have not explored the integration of wireless charging system for EVs from the power system perspective. In this research, a bi-level optimisation framework for allocating WPTs and PSU in the airfield traffic network and distribution power network of a commercial airport is proposed.

The results obtained from the three case studies demonstrate the techno-economic feasibility of wireless charging technology for airport electric shuttle buses. Th economic analysis reveals that, as annualised cost results show, conventional diesel shuttle buses will become a more expensive option compared with electrification options in the future, making the electrification of airport shuttle buses a more promising technical path. The average energy stored in electric buses suggests that wireless charging technology enables

the electric shuttle buses to carry batteries with lower capacity while conducting the same number of tasks.

The findings provide airport designers and operators evidence that adopting electric shuttle buses and wireless charging systems at airports is an economically viable option from the power system integration perspective. The system presented in this research serves as a cost-effective and realistic example. The work expends on prior works by examining an additional aspect: the power network operation perspective thereby contributing valuable insights to the ongoing discourse on wireless charging systems for EVs.

8.1.3 Providing A2G ancillary services to the power system through electric aircraft charging

The literature review in Section 2.5 indicates that prior research works have sought to leverage DER from transportation electrification sectors to provide ancillary services to grids. However, these studies have primarily focused on the potential flexibility provided by EVs, leaving the potential flexibility from aviation electrification unexplored. Additionally, there has been limited research on utilising multiple energy resources to provide both primary and secondary frequency response services.

In this thesis, aviation electrification enables the EA battery charging system to provide valuable flexibility services to the power grid. A novel concept of A2G flexibility that utilises EA charging system with a battery swap method to provide grid frequency response services. A smart EA charging system is developed to dispatch PV, gas turbines and grid electricity to meet EA charging demand associated with the seasonal flight schedules.

The A2G frequency response system is developed to coordinate primary and secondary frequency response control with the grid inertia estimation. The hourly energy dispatch strategy is optimised to achieve the minimum operation costs by considering the EA charging demand, energy prices and A2G frequency response revenue. Case studies are conducted in 8 major UK airports which serve around 37% of the total UK domestic air passengers.

The results show that the typical A2G frequency response services capacity across these

major UK airports can reach between 900 - 1,300 MW overnight and 200 - 900 MW daytime with seasonal variation. EA batteries can provide up to six times more frequency response power than gas turbine during the day, while overnight, EA batteries supply 100% of frequency response power. However, due to sustained gas turbine output, gas turbines can provide roughly four times more frequency response energy than EA batteries. The installed generation capacity significantly impacts on the energy dispatch strategy, response power, and energy of A2G frequency response system. The annual revenue generated from A2G frequency response is estimated at £46.58 million, potentially cover 19.8% to 30% of energy consumption costs of EA charging at future airports. The average frequency nadir can be improved by 0.31 Hz in summer and 0.23 Hz in winter due to the A2G frequency response services, and the likelihood of Infrequent Infeed Loss Risk can be reduced by 83.33% in summer and 68.75% in winter.

The sensitivity analysis of grid service value reveals that the higher grid service value will attract higher frequency response revenue. Specifically, the secondary response revenue which is provided by gas turbine is more sensitive to the variation of grid service value. Another sensitivity analysis examined the impacts of generation capacity on energy dispatch, A2G frequency response, and costs. Two scenarios were evaluated: one with reduced gas turbine capacity and another with reduced grid transformer capacity. Results revealed that a balanced grid and gas turbine capacity is optimal due to its higher night response power and more effective management of frequency nadir events. Although the scenario with half the grid transformer capacity had the highest profitable ratio of revenue over operation costs, the base case had the lowest total cost after the deduction of revenue.

The results obtained in this research reveal that the A2G flexibility provided from EA charging systems can significantly improve the frequency stability of the future power grid. The work also establishes a framework for future studies to investigate the potential A2G flexibility services further.

8.1.4 Deep reinforcement learning-based A2G dispatch approach

Previous work in Chapter 6 has presented the novel concept of A2G flexibility and examined the results of adopting A2G frequency response services to support the grid in frequency drop events. However, the previous work adopted MILP to solve the A2G frequency reserve scheduling problem, which can only make decisions in advance (day-

ahead) rather than react when the situation changes. In this research, the A2G FFR service scheduling problem was formulated as an MDP, and solved with DRL-based approach, by which the real-time management of EA charging system is enabled. The UK domestic air transport and GB power system are combined for testing the proposed strategy.

The results demonstrate the feasibility of the A2G FFR strategy in providing essential flexibility services to the power grid while meeting the EA charging demands associated with the flight schedules. By taking the EA charging demand, energy prices, and A2G frequency response revenue into account, the hourly energy dispatch strategy is designed to achieve the lowest possible operation costs efficiently.

To test the impact of EA battery charger capacity on the results, case studies with different levels of rated EA battery charging power of 5 MW, 7 MW, and 14 MW are conducted. in 8 UK airports that serve approximately 37% of the total domestic air travellers in the UK. The results show that the typical A2G frequency response services capacity across the 8 UK airports can reach between 800 – 3200 MW overnight and 300 – 2400 MW daytime depending on different rated EA charging power. The response power is essential for the GB power system, especially during the night when the system inertia is low.

The rated EA battery charging power has a significant impact on the energy dispatch results and response power of the A2G frequency response system. The revenues that are generated from A2G frequency response are estimated to be 6.3×10^4 £, 8.8×10^4 £, and 1.77×10^5 £ for 5 MW, 7 MW, and 14 MW EA battery charger, which can cover 3.93%, 6.47%, and 13.2% of charging power consumption costs in the airports, respectively. The average frequency nadir was improved to 49.66 Hz, 49.80 Hz, and 49.86 Hz by cases with 5 MW, 7 MW, and 14 MW A2G chargers, and the likelihood of Infrequent Infeed Loss Risk can be totally avoided.

This research expands on prior work by employing DRL-based approaches to dispatch the EA battery charging system for FFR services, offering an innovative scheduling method.

8.2 Future Research

The research aims and objectives have been satisfied through the presented works. However, the work can be extended in several potential research directions. This section

suggests further works as a continuation of development on the presented work in the thesis as follows.

8.2.1 Integrating more DER resources in airports

Future works can further explore the impact of integrating more flexible DER located in the airport into the airport microgrids and the main grid, such as controllable thermal load, electric ground support vehicles, and electric air conditioning systems. All these DER resources can potentially provide demand-side response services to the microgrid and the main grid.

8.2.2 Renewable-powered hydrogen-electric aviation

There is an alternative technical path of sustainable aviation named “hydrogen-electric aircraft”. More and more airport operators are evaluating the applicability of installing on-site hydrogen production devices to accommodate hydrogen-electric aircraft. The utility-scale hydrogen electrolyser and airport-based renewable generation can also provide massive flexibility to the grids as well. Future work can be focused on the integration of large-scale hydrogen production devices into the grid and the potential ancillary services provided by airport on-site hydrogen electrolysers. Alternatively, the airport integrated renewable energy systems planning and design for accommodating hydrogen-electric aircraft is also a significant topic.

8.2.3 Uncertainty parameters and analysis

In this research, it can be seen that several underlying parameters in the developed planning and scheduling approaches contain uncertainties, including the stochastic behaviours of EV owners, flight mission punctuality, availability of shuttle buses, and renewable power output. There are many recent approaches designated for handling the uncertainties in optimisation problems: stochastic optimisation methods, robust optimisation methods, chance-constrained programming-based methods, Interval optimisation, fuzzy techniques, information gap decision theory, and hybrid techniques. One of the potential future directions is adopting these advanced techniques for optimal dispatch of the proposed airport energy system planning and design.

8.2.4 Advanced reinforcement learning technologies

The reinforcement learning theory and algorithms have been developing fast in the past few years, more advanced algorithms such as multi-agent deep reinforcement learning, federated learning, multi-task reinforcement learning, etc., are developed to solve more complex problems. These advanced reinforcement learning technologies can be adopted in more complicated and realistic situations, such as the privacy of data sharing between airport operators, the competition mechanism between different airports in terms of providing ancillary services to the grid, and multi-airport collaboration in grid frequency restoration tasks.

8.2.5 More types of A2G ancillary services to the grid

Current work is focused on A2G frequency response services. However, frequency response is one of the most essential ancillary services that are desired by the grid operators, but it is not the only one. There are multiple types of ancillary services that are becoming more and more important since the grid operators are facing unprecedented system balancing challenges due to the increasing penetration level of renewable generation. Future work can explore the potential of A2G flexibility in providing multiple types of ancillary services, such as reactive power services, reserve services, regional inertial support services, voltage constraint management, etc.

Appendix A

Table A-1 UK Airport PV Installation Capacity

Airport Name	IATA Code	Total Area (acres)	Available Area (acres)	PV (MW)
London Heathrow	LHR	3,032	250	50
Edinburgh	EDI	1,300	85	17
Glasgow	GLA	1,028	37	7
Manchester	MAN	1,384	88	17
Birmingham International	BHX	820	108	21
Belfast International	BFS	1,198	58	11
London Gatwick	LGW	1,665	217	43
London Stansted	STN	1,796	95	19

An example of PV installation capacity calculation:

Airport-based solar PV system becomes a promising technology to achieve low emission in aviation. There are three main types of airport-based PV plants: ground-mounted, parking canopy-supported, and building rooftop-mounted [199].

The roof-mounted PV system is the most demanding one, as a result, only the flat-roof buildings are selected. The capacity of the solar plant can be calculated on the basis of available land area in the selected zone. The plant capacity varies with the selection of PV module technology and type of mounting system. Many factors will affect the capacity of installed PV. Latitude, tilt angle, azimuth of the PV panels. This work is only for a rough estimation; therefore, these influence factors are neglected. The worldwide norm of PV land size over installed capacity is 1 MW per 2ha (5 acres) [182]. The capacity of the PV plant is estimated using Eq. (A.1). However, the norm is based on the land-based situation. If this assumption is going to be used for estimating the capacity of roof-mounted and canopy-mounted PV systems, there will be a deduction rate. The deduction rate is 0.8 for roof-mounted, 0.7 for canopy-mounted.

$$P_c = \frac{A_{PV} \times r_d}{5} \qquad \text{A.1}$$

where, P_c is the estimated capacity of installed PV. A_{PV} is the area of the selected PV sites. r_d is the deduction rate of each type of PV plant.

To investigate the solar PV installation potential in a specific airport, the first step is to identify the boundary and applicable area, as shown in Figure A-1. There is a runway protect zone in airport, the land near this zone is not recommended for PV installation due to the reflective hazard when the airplane taking off and landing. According to the expansion plan of LGW airport

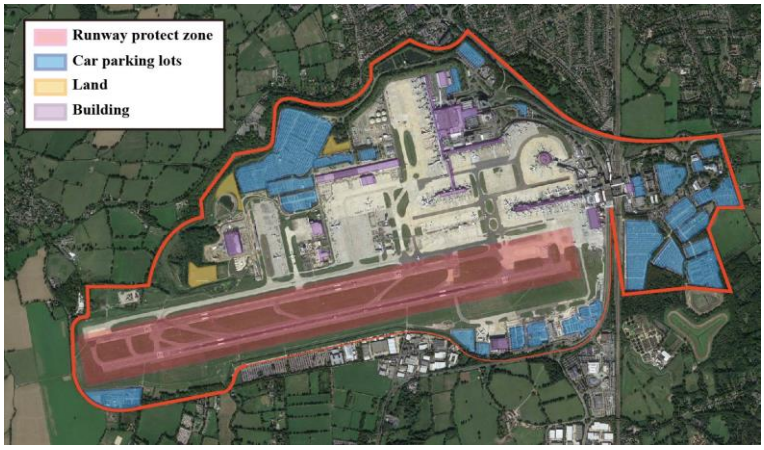

Figure A-1 LGW airport boundary and selected sites for solar PV installation

The areas of each type of selected zones are listed in Table A-2.

Table A-2 Areas of selected zones for PV installation

Zone	Area	
	In km^2	In acres
Building rooftop	0.1563	38.62
Land based	0.0488	12.06
Solar car park	0.7223	178.5

The total installation potential PV installation capacity in LGW airport is 43 MW. In order to reduce the complexity, the assumption that the PV installation capacity is proportional to the total area of the airport. In following research, the spare land for PV installation in each airport is calculated according to the total area of the airports over that of the LGW airport.

Appendix B

Seasonal domestic arrival flight schedules:

Two weeks' flight schedules in summer peak month (May) and winter peak month (November) are investigated. Figure B-1 shows the domestic arrival flight schedules of the 8 major airports over 24 hours in summer and winter. The selected summer and winter dates are 1st May 2019 and 15th November 2018 respectively, which are determined by the highest number of flights in the respective season. The flight schedules normally have a double peak characteristic, one peak occurs in the morning (07:00 am to 10:00 am), the other peak happens in the afternoon to the early evening (16:00 to 21:00) dependent on season. There is no flight scheduled from midnight to early morning for the duration of 6 hours.

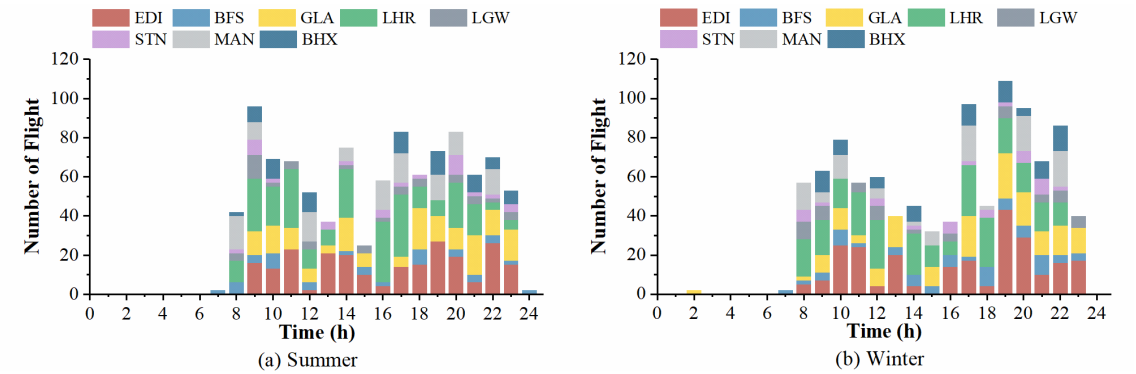

Figure B-1 Seasonal domestic arrival flight schedules of the 8 UK airports. (a) summer schedule, (b) winter schedule

Appendix C

Flight demand forecasting considering the effect of COVID:

The flight schedule is formulated as a time-series data, which includes the number of flights arriving at half-hour time slots in a specific airport. For flight schedule forecasting, the common assumption is that the existing growth rate of passengers will persist due to the demand inertia under the right economic conditions [42].

According to the forecast for future UK domestic air traffic [200], the domestic passengers in the UK can be expected to continuously increase 0.9% - 1.1% annually from 2016 to 2050. But under the impact of the COVID-19, the air travel is severely impacted. In this thesis, it is assumed that the economy and air travel will be recovered to the status before COVID (2019) by the year 2023. As shown in Figure C-1, the UK domestic flight passengers are expected to continuously increase 1% annually from 2023 to 2050. In this thesis, the flight schedule in 2050 is formulated as a linear relationship with the year of passengers based on the Eq. (C.1) [201].

$$FS_{t,2050} = FS_{t,2019} \times \frac{Pax_{2050}}{Pax_{2019}} \qquad \text{C.1}$$

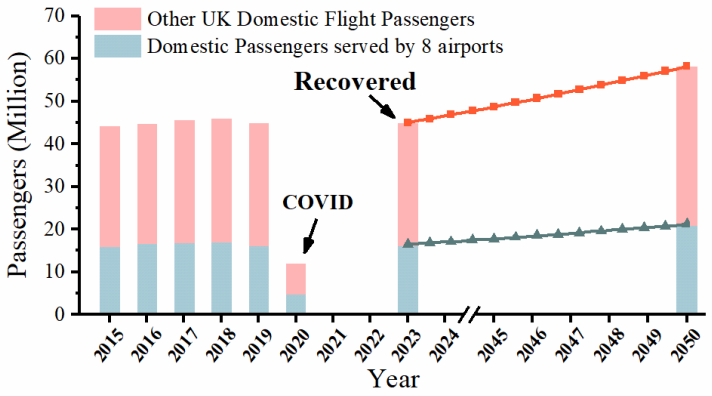

Figure C-1 Prediction of the UK domestic flight passengers to the year 2050

References

[1] "Flightpath 2050: Europe's Vision for Aviation; Maintaining Global Leadership and Serving Society's Needs: Report of the High-Level Group on Aviation Research," Publications Office of the European Union: Luxembourg, 2012. doi: doi/10.2777/50266.

[2] Sustainable Aviation, "Sustainable aviation progress report," 2017. https://www.sustainableaviation.co.uk/progress-reports/ (accessed Sep. 08, 2022).

[3] A. R. Gnadt, R. L. Speth, J. S. Sabnis, and S. R. H. Barrett, "Technical and environmental assessment of all-electric 180-passenger commercial aircraft," *Progress in Aerospace Sciences*, vol. 105, no. November 2018, pp. 1–30, 2019, doi: 10.1016/j.paerosci.2018.11.002.

[4] A. Bills, S. Sripad, W. L. Fredericks, M. Singh, and V. Viswanathan, "Performance Metrics Required of Next-Generation Batteries to Electrify Commercial Aircraft," *ACS Energy Lett*, pp. 663–668, 2020, doi: 10.1021/acsenergylett.9b02574.

[5] A. W. Schäfer *et al.*, "Technological, economic and environmental prospects of all-electric aircraft," *Nat Energy*, vol. 4, no. 2, pp. 160–166, 2019, doi: 10.1038/s41560-018-0294-x.

[6] A. Schwab, A. Thomas, J. Bennett, E. Robertson, and S. Cary, "Electrification of Aircraft: Challenges, Barriers, and Potential Impacts," *National Renewable Energy Laboratory*, no. October, 2018, [Online]. Available: https://www.nrel.gov/docs/fy22osti/80220.pdf.

[7] M. Alruwaili and L. Cipcigan, "Airport electrified ground support equipment for providing ancillary services to the grid," *Electric Power Systems Research*, vol. 211, no. June, p. 108242, 2022, doi: 10.1016/j.epsr.2022.108242.

[8] L. Badesa, C. Matamala, Y. Zhou, and G. Strbac, "Assigning Shadow Prices to Synthetic Inertia and Frequency Response Reserves From Renewable Energy Sources," *IEEE Trans Sustain Energy*, vol. 14, no. 1, pp. 12–26, 2023, doi: 10.1109/TSTE.2022.3198324.

[9] C. O'Malley, L. Badesa, F. Teng, and G. Strbac, "Frequency Response From Aggregated V2G Chargers With Uncertain EV Connections," *IEEE Transactions on Power Systems*, 2022, doi: 10.1109/TPWRS.2022.3202607.

[10] ICAO, "Renewable Energy for Aviation: Practical Applications To Achieve Carbon Reductions and Cost Savings," 2017, [Online]. Available: https://www.icao.int/environmental-protection/Documents/ICAO_UNDP_GEF_RenewableEnergyGuidance.pdf

[11] The Geography of Transport Systems, "Airport Components and Terminal Configurations." https://transportgeography.org/contents/chapter6/airport-terminals/airport-terminals-configuration/ (accessed Aug. 07, 2023).

[12] European Commission, *Innovation for sustainable aviation in a global environment : proceedings of the sixth European Aeronautics Days, Madrid, 30 March-1 April 2011*. IOS Press, 2012. doi: doi/10.2777/69176.

[13] J. Zhang, I. Roumeliotis, and A. Zolotas, "Sustainable Aviation Electrification: A Comprehensive Review of Electric Propulsion System Architectures, Energy Management, and Control," *Sustainability (Switzerland)*, vol. 14, no. 10. MDPI, May 01, 2022. doi: 10.3390/su14105880.

[14] B. J. Brelje and J. R. R. A. Martins, "Electric, hybrid, and turboelectric fixed-wing aircraft: A review of concepts, models, and design approaches," *Progress in Aerospace Sciences*, vol. 104, no. June 2018, pp. 1–19, 2019, doi: 10.1016/j.paerosci.2018.06.004.

[15] R. Hickman and D. Banister, "Looking over the horizon: Transport and reduced CO2 emissions in the UK by 2030," *Transp Policy (Oxf)*, vol. 14, no. 5, pp. 377–387, 2007, doi: 10.1016/j.tranpol.2007.04.005.

[16] A. Benito and G. Alonso, *Energy Efficiency in Air Transportation*. Butterworth-Heinemann, 2018. doi: https://doi.org/10.1016/B978-0-12-812581-6.00005-3.

[17] National Academies of Sciences Engineering and and Medicine, *Commercial Aircraft Propulsion and Energy Systems Research: Reducing Global Carbon Emissions*. Washington, DC: The National Academies Press, 2016. doi: 10.17226/23490.

[18] "Alice – Eviation." https://www.eviation.co/alice/ (accessed May 16, 2021).

[19] M. Broadbent, "All about Alice for DHL," *Air International*, vol. 101, no. 3, p. 6, 2021.

[20] A. W. Schäfer *et al.*, "Technological, economic and environmental prospects of all-electric aircraft," *Nat Energy*, vol. 4, no. 2, 2019, doi: 10.1038/s41560-018-0294-x.

[21] J. Benzaquen, J. He, and B. Mirafzal, "Toward more electric powertrains in aircraft: Technical challenges and advancements," *CES Transactions on Electrical Machines and Systems*, vol. 5, no. 3, 2021, doi: 10.30941/cestems.2021.00022.

[22] S. Karpuk and A. Elham, "Influence of novel airframe technologies on the feasibility of fully-electric regional aviation," *Aerospace*, vol. 8, no. 6, 2021, doi: 10.3390/aerospace8060163.

[23] "Airbus E-Fan." https://www.airbus.com/en/innovation/zero-emission/electric-flight (accessed Sep. 13, 2022).

[24] "Electric Sport and Training Aircraft." e: https://www.rolls-royce.com/products-and-services/electrical/ propulsion/light-sport-and-training-aircraft (accessed Sep. 13, 2022).

[25] " NASA X-57 Maxwell." https://www.nasa.gov/specials/X57/ (accessed Sep. 13, 2022).

[26] "Rolls-Royce ACCEL." https://www.rolls-royce.com/products-and-services/electrical/propulsion/light-sport-and-training-aircraft.aspx#accel (accessed Sep. 13, 2022).

[27] Technology | Wright Electric, "Wright Electric/Easy jet." weflywright.com (accessed Sep. 13, 2022).

[28] "CleanSky 2 Project ELICA (ELectric Innovative Commuter Aircraft)." https://www.elica-cleansky-project.eu/ (accessed Sep. 13, 2022).

[29] M. Schmidt, A. Paul, M. Cole, and K. O. Ploetner, "Challenges for ground operations arising from aircraft concepts using alternative energy," *J Air Transp Manag*, 2016, doi: 10.1016/j.jairtraman.2016.04.023.

[30] U. Sultana, A. B. Khairuddin, B. Sultana, N. Rasheed, S. H. Qazi, and N. R. Malik, "Placement and sizing of multiple distributed generation and battery swapping stations using grasshopper optimizer algorithm," *Energy*, 2018, doi: 10.1016/j.energy.2018.09.083.

[31] W. Jie, J. Yang, M. Zhang, and Y. Huang, "The two-echelon capacitated electric vehicle routing problem with battery swapping stations: Formulation and efficient methodology," *Eur J Oper Res*, 2019, doi: 10.1016/j.ejor.2018.07.002.

[32] C. Y. Justin, A. P. Payan, S. I. Briceno, B. J. German, and D. N. Mavris, "Power optimized battery swap and recharge strategies for electric aircraft operations," *Transp Res Part C Emerg Technol*, vol. 115, no. July 2019, p. 102605, 2020, doi: 10.1016/j.trc.2020.02.027.

[33] Y. Cheng and C. Zhang, "Configuration and operation combined optimization for EV battery swapping station considering PV consumption bundling," *Protection and Control of Modern Power Systems*, vol. 2, no. 1, Dec. 2017, doi: 10.1186/s41601-017-0056-y.

[34] N. Liu, Q. Chen, X. Lu, J. Liu, and J. Zhang, "A Charging Strategy for PV-Based Battery Switch Stations Considering Service Availability and Self-Consumption of PV Energy," *IEEE Transactions on Industrial Electronics*, vol. 62, no. 8, pp. 4878–4889, 2015, doi: 10.1109/TIE.2015.2404316.

[35] B. Sun, X. Sun, D. H. K. Tsang, and W. Whitt, "Optimal battery purchasing and charging strategy at electric vehicle battery swap stations," *Eur J Oper Res*, vol. 279, no. 2, pp. 524–539, 2019, doi: 10.1016/j.ejor.2019.06.019.

[36] M. Sari, W. M. W. Mohamed, and S. A. Jalil, "The Optimization Using Electric Ground Support Equipment in Aviation Industry," *International Journal of Energy Economics and Policy*, vol. 12, no. 1, pp. 401–406, Jan. 2022, doi: 10.32479/ijeep.11711.

[37] J. A. Stockford, C. Lawson, and Z. Liu, "Benefit and performance impact analysis of using hydrogen fuel cell powered e-Taxi system on A320 class airliner," *Aeronautical Journal*, vol. 123, no. 1261, pp. 378–397, Mar. 2019, doi: 10.1017/aer.2018.156.

[38] M. N. Postorino, L. Mantecchini, and F. Paganelli, “Improving taxi-out operations at city airports to reduce CO2 emissions,” *Transp Policy (Oxf)*, vol. 80, no. May 2018, pp. 167–176, 2019, doi: 10.1016/j.tranpol.2018.09.002.

[39] C. Yang, X.-Q. Jin, Z.-M. Du, B. Fan, and X.-B. Yang, “Modeling and simulation of the airport terminal air conditioning system based on energyplus,” *Shanghai Jiaotong Daxue Xuebao/Journal of Shanghai Jiaotong University*, vol. 44, pp. 745-748+754, Jun. 2010.

[40] S. O. Alba and M. Manana, “Energy research in airports: A review,” *Energies (Basel)*, vol. 9, no. 5, pp. 1–19, 2016, doi: 10.3390/en9050349.

[41] C. Lau, J. Stromgren, and D. Green, “Synthesis 21: Airport Energy Efficiency and Cost Reduction. Airport Cooperative Research Program,” Washington, DC, USA, 2010.

[42] Richard de Neufville, “Airport systems planning, design, and management,” in *Air Transport Management*, 2013. doi: 10.4324/9780429299445-6.

[43] F. Bigoni *et al.*, “Design of Airport Infrastructures in Support of the Transition To a Hybrid-Electric Fleet,” no. 1, pp. 1–30, 2018.

[44] Federal Aviation Administration (FAA), “Aeronautical Information Manual (AIM),” 2022. https://www.faa.gov/air_traffic/publications/atpubs/aim_html/index.html (accessed Sep. 07, 2022).

[45] X. Liu, L. Li, X. Liu, and T. Zhang, “Analysis of passenger flow and its influences on HVAC systems: An agent based simulation in a Chinese hub airport terminal,” *Build Environ*, vol. 154, no. December 2018, pp. 55–67, 2019, doi: 10.1016/j.buildenv.2019.03.011.

[46] A. A. Kebede, T. Kalogiannis, J. Van Mierlo, and M. Berecibar, “A comprehensive review of stationary energy storage devices for large scale renewable energy sources grid integration,” *Renewable and Sustainable Energy Reviews*, vol. 159. Elsevier Ltd, May 01, 2022. doi: 10.1016/j.rser.2022.112213.

[47] S. Sreenath, K. Sudhakar, A. F. Yusop, E. Solomin, and I. M. Kirpichnikova, "Solar PV energy system in Malaysian airport: Glare analysis, general design and performance assessment," *Energy Reports*, vol. 6, pp. 698–712, 2020, doi: 10.1016/j.egyr.2020.03.015.

[48] S. Sreenath, K. Sudhakar, A. F. Yusop, E. Cuce, and E. Solomin, "Analysis of solar PV glare in airport environment: Potential solutions," *Results in Engineering*, vol. 5, no. October 2019, p. 100079, 2020, doi: 10.1016/j.rineng.2019.100079.

[49] S. Sreenath, K. Sudhakar, and A. F. Yusop, "Solar PV in the airport environment: A review of glare assessment approaches & metrics," *Solar Energy*, vol. 216. Elsevier Ltd, pp. 439–451, Mar. 01, 2021. doi: 10.1016/j.solener.2021.01.023.

[50] A. Dagar, P. Gupta, and V. Niranjan, "Microgrid protection: A comprehensive review," *Renewable and Sustainable Energy Reviews*, vol. 149, no. July, p. 111401, 2021, doi: 10.1016/j.rser.2021.111401.

[51] S. Sreenath, K. Sudhakar, and A. F. Yusop, "Airport-based photovoltaic applications," *Progress in Photovoltaics: Research and Applications*, vol. 28, no. 8, pp. 833–853, 2020, doi: 10.1002/pip.3265.

[52] A. Anurag, J. Zhang, J. Gwamuri, and J. M. Pearce, "General Design Procedures for Airport-Based Solar Photovoltaic Systems," *Energies (Basel)*, vol. 10, no. 8, pp. 1–19, 2017, doi: 10.3390/en10081194.

[53] IEEE Joint Task Force on QER, "Utility and Other Energy Company Business Case Issues Related to Microgrids and Distributed Generation (DG), Especially Rooftop Photovoltaics," 2014.

[54] M. M. Esfahani and O. Mohammed, "Real-time distribution of en-route Electric Vehicles for optimal operation of unbalanced hybrid AC/DC microgrids," *eTransportation*, vol. 1, p. 100007, 2019, doi: 10.1016/j.etran.2019.100007.

[55] X. Huang, K. Wang, J. Qiu, L. Hang, G. Li, and X. Wang, "Decentralized Control of Multi-Parallel Grid-Forming DGs in Islanded Microgrids for Enhanced Transient Performance," *IEEE Access*, vol. 7, pp. 17958–17968, 2019, doi: 10.1109/ACCESS.2019.2896594.

[56] B. Zhao *et al.*, "Energy management of multiple microgrids based on a system of systems architecture," *IEEE Transactions on Power Systems*, vol. 33, no. 6, pp. 6410–6421, Nov. 2018, doi: 10.1109/TPWRS.2018.2840055.

[57] S. Obara, S. Fujimoto, K. Sato, and Y. Utsugi, "Planning renewable energy introduction for a microgrid without battery storage," *Energy*, vol. 215, Jan. 2021, doi: 10.1016/j.energy.2020.119176.

[58] M. Javadi, Y. Gong, and C. Y. Chung, "Frequency Stability Constrained Microgrid Scheduling Considering Seamless Islanding," *IEEE Transactions on Power Systems*, vol. 8950, no. c, pp. 1–11, 2021, doi: 10.1109/TPWRS.2021.3086844.

[59] R. H. and E. Mannarino, *Microgrids and Their Application for Airports and Public Transit*. Washington, D.C.: Transportation Research Board, 2018. doi: 10.17226/25233.

[60] G. Emanuella, O. Jon, P. Madison, and Z. Christina, "Atlanta's Hartsfield-Jackson airport restores power after crippling outage," *CNN*, 2017.

[61] N. Hatziargyriou *et al.*, "Definition and Classification of Power System Stability - Revisited & Extended," *IEEE Transactions on Power Systems*, vol. 36, no. 4, pp. 3271–3281, 2021, doi: 10.1109/TPWRS.2020.3041774.

[62] National Grid ESO, "Technical Report on the events of 9 August 2019," 2019. https://www.nationalgrideso.com/document/152346/download (accessed Oct. 08, 2021).

[63] National Grid, "Future Energy Scenarios Navigation," 2020. https://www.nationalgrideso.com/future-energy/future-energy-scenarios/fes-2020-documents (accessed Nov. 13, 2020).

[64] L. Badesa, F. Teng, and G. Strbac, "Conditions for Regional Frequency Stability in Power System Scheduling - Part II: Application to Unit Commitment," *IEEE Transactions on Power Systems*, vol. 36, no. 6, pp. 5567–5577, 2021, doi: 10.1109/TPWRS.2021.3073077.

[65] L. Badesa, F. Teng, and G. Strbac, "Conditions for Regional Frequency Stability in Power System Scheduling - Part II: Application to Unit Commitment," *IEEE*

Transactions on Power Systems, vol. 36, no. 6, pp. 5567–5577, 2021, doi: 10.1109/TPWRS.2021.3073077.

[66] L. Meng *et al.*, "Fast Frequency Response from Energy Storage Systems - A Review of Grid Standards, Projects and Technical Issues," *IEEE Trans Smart Grid*, vol. 11, no. 2, pp. 1566–1581, Mar. 2020, doi: 10.1109/TSG.2019.2940173.

[67] J. Ekanayake and N. Jenkins, "Comparison of the response of doubly fed and fixed-speed induction generator wind turbines to changes in network frequency," *IEEE Transactions on Energy Conversion*, vol. 19, no. 4, pp. 800–802, 2004, doi: 10.1109/TEC.2004.827712.

[68] N. R. Ullah, T. Thiringer, and D. Karlsson, "Temporary Primary Frequency Control Support by Variable Speed Wind Turbines— Potential and Applications," *IEEE Transactions on Power Systems*, vol. 23, no. 2, pp. 601–612, 2008, doi: 10.1109/TPWRS.2008.920076.

[69] "Operability Strategy Report," *National Grid*, 2019. https://www.nationalgrideso.com/document/159726/download (accessed Oct. 10, 2021).

[70] National Grid, "Operability Strategy Report," 2022. Accessed: Aug. 11, 2023. [Online]. Available: https://www.nationalgrideso.com/document/273801/download

[71] B. Mantar Gundogdu, S. Nejad, D. T. Gladwin, M. P. Foster, and D. A. Stone, "A battery energy management strategy for U.K. enhanced frequency response and triad avoidance," *IEEE Transactions on Industrial Electronics*, vol. 65, no. 12, pp. 9509–9517, 2018, doi: 10.1109/TIE.2018.2818642.

[72] J. Guo, F. Luis Badesa, B. C. Teng, S. Yuen, R. Hui, and G. Strbac, "Value of Point-of-load Voltage Control for Enhanced Frequency Response in Future GB Power System."

[73] S. I. Nanou, A. G. Papakonstantinou, and S. A. Papathanassiou, "A generic model of two-stage grid-connected PV systems with primary frequency response and inertia emulation," *Electric Power Systems Research*, vol. 127, pp. 186–196, 2015, doi: 10.1016/j.epsr.2015.06.011.

[74] J. Undrill, "Primary Frequency Response and Control of Power System Frequency," *Energy Analysis and Environmental Impacts Division Lawrence Berkeley National Laboratory*, no. February, 2018.

[75] Di. Chakravorty, B. Chaudhuri, and S. Y. R. Hui, "Rapid Frequency Response from Smart Loads in Great Britain Power System," *IEEE Trans Smart Grid*, vol. 8, no. 5, pp. 2160–2169, 2017, doi: 10.1109/TSG.2016.2517409.

[76] "The grid code - UK," 2017. https://www.nationalgrid.com/sites/default/files/documents/8589935310-Complete Grid Code.pdf

[77] P. Kundur, *Power System Stability And Control*, 1st ed. McGraw-Hill Education, 1994.

[78] L. Mehigan, D. Al Kez, S. Collins, A. Foley, B. Ó'Gallachóir, and P. Deane, "Renewables in the European power system and the impact on system rotational inertia," *Energy*, vol. 203, p. 117776, 2020, doi: 10.1016/j.energy.2020.117776.

[79] F. Teng, Y. Mu, H. Jia, J. Wu, P. Zeng, and G. Strbac, "Challenges on primary frequency control and potential solution from EVs in the future GB electricity system," *Appl Energy*, vol. 194, pp. 353–362, 2017, doi: 10.1016/j.apenergy.2016.05.123.

[80] Z. A. Obaid, L. M. Cipcigan, and M. T. Muhssin, "Fuzzy hierarchal approach-based optimal frequency control in the Great Britain power system," *Electric Power Systems Research*, vol. 141, pp. 529–537, 2016, doi: 10.1016/j.epsr.2016.08.032.

[81] M. A. Gonzalez-salazar, T. Kirsten, and L. Prchlik, "Review of the operational flexibility and emissions of gas- and coal-fired power plants in a future with growing renewables," *Renewable and Sustainable Energy Reviews*, vol. 82, no. July 2017, pp. 1497–1513, 2018, doi: 10.1016/j.rser.2017.05.278.

[82] C. Henderson, A. Egea-Alvarez, J. Rull-Duran, M. Nedd, P. Papadopoulos, and L. Xu, "Inertia and Frequency Support from Britain's AC Powered Trains," *IEEE Trans Sustain Energy*, pp. 1–10, 2022, doi: 10.1109/TSTE.2022.3221192.

[83] National Grid ESO, "Markets Roadmap," 2022. https://www.nationalgrideso.com/document/247136/download

[84] Z. Guo, J. Zhang, R. Zhang, and X. Zhang, "Aviation-to-Grid Flexibility through Electric Aircraft Charging," *IEEE Trans Industr Inform*, p. 1, 2021, doi: 10.1109/TII.2021.3128252.

[85] M. Chaoxu, L. Weiqiang, and X. Wei, "Hierarchically Adaptive Frequency Control for an EV-Integrated Smart Grid With Renewable Energy," *IEEE Trans Industr Inform*, vol. 14, no. 9, pp. 4254–4263, 2018.

[86] O. Fallah-Mehrjardi, M. H. Yaghmaee, and A. Leon-Garcia, "Charge Scheduling of Electric Vehicles in Smart Parking-Lot under Future Demands Uncertainty," *IEEE Trans Smart Grid*, vol. 11, no. 6, pp. 4949–4959, 2020, doi: 10.1109/TSG.2020.3000850.

[87] H. Lin, Y. Liu, Q. Sun, R. Xiong, H. Li, and R. Wennersten, "The impact of electric vehicle penetration and charging patterns on the management of energy hub – A multi-agent system simulation," *Appl Energy*, vol. 230, 2018, doi: 10.1016/j.apenergy.2018.08.083.

[88] Y. Xiang, H. Cai, J. Liu, and X. Zhang, "Techno-economic design of energy systems for airport electrification: A hydrogen-solar-storage integrated microgrid solution," *Appl Energy*, vol. 283, no. December, p. 116374, 2021, doi: 10.1016/j.apenergy.2020.116374.

[89] H. Zhao *et al.*, "Resilience Assessment of Hydrogen Integrated Energy System for Airport Electrification," *IEEE Trans Ind Appl*, 2021, doi: 10.1109/TIA.2021.3127481.

[90] A. Molavi, J. Shi, Y. Wu, and G. J. Lim, "Enabling smart ports through the integration of microgrids: A two-stage stochastic programming approach," *Appl Energy*, vol. 258, 2020, doi: 10.1016/j.apenergy.2019.114022.

[91] X. Wu, S. Qi, Z. Wang, C. Duan, X. Wang, and F. Li, "Optimal scheduling for microgrids with hydrogen fueling stations considering uncertainty using data-driven approach," *Appl Energy*, vol. 253, 2019, doi: 10.1016/j.apenergy.2019.113568.

[92] G. Pan, W. Gu, Y. Lu, H. Qiu, S. Lu, and S. Yao, "Optimal Planning for Electricity-Hydrogen Integrated Energy System Considering Power to Hydrogen and Heat and Seasonal Storage," *IEEE Trans Sustain Energy*, vol. 11, no. 4, pp. 2662–2676, 2020, doi: 10.1109/TSTE.2020.2970078.

[93] M. Wang, H. Yu, R. Jing, H. Liu, P. Chen, and C. Li, "Combined multi-objective optimization and robustness analysis framework for building integrated energy system under uncertainty," *Energy Convers Manag*, vol. 208, 2020, doi: 10.1016/j.enconman.2020.112589.

[94] H. Yang, T. Xiong, J. Qiu, D. Qiu, and Z. Y. Dong, "Optimal operation of DES/CCHP based regional multi-energy prosumer with demand response," *Appl Energy*, vol. 167, 2016, doi: 10.1016/j.apenergy.2015.11.022.

[95] X. Ding, W. Sun, G. P. Harrison, X. Lv, and Y. Weng, "Multi-objective optimization for an integrated renewable, power-to-gas and solid oxide fuel cell/gas turbine hybrid system in microgrid," *Energy*, vol. 213, p. 118804, 2020, doi: 10.1016/j.energy.2020.118804.

[96] S. Davarzani, R. Granell, G. A. Taylor, and I. Pisica, "Implementation of a novel multi-agent system for demand response management in low-voltage distribution networks," *Appl Energy*, vol. 253, Nov. 2019, doi: 10.1016/j.apenergy.2019.113516.

[97] S. Liu *et al.*, "Operational optimization of a building-level integrated energy system considering additional potential benefits of energy storage," *Protection and Control of Modern Power Systems*, vol. 6, no. 1, 2021, doi: 10.1186/s41601-021-00184-0.

[98] M. Zhu, C. Xu, S. Dong, K. Tang, and C. Gu, "An integrated multi-energy flow calculation method for electricity-gas-thermal integrated energy systems," *Protection and Control of Modern Power Systems*, vol. 6, no. 1, pp. 2–13, 2021, doi: 10.1186/s41601-021-00182-2.

[99] Z. Guo, X. Zhang, and R. Zhang, "A MULTI-AGENT MICROGRID ENERGY MANAGEMENT SOLUTION FOR AIR TRANSPORT ELECTRIFICATION." doi: https://doi.org/10.1049/icp.2021.2351.

[100] Z. Guo, X. Zhang, N. Balta-Ozkan, and P. Luk, “Aviation to Grid: Airport Charging Infrastructure for Electric Aircraft,” in *International Conference on Applied Energy* , 2020. Accessed: Oct. 05, 2021. [Online]. Available: http://www.energy-proceedings.org/wp-content/uploads/enerarxiv/1607610466.pdf

[101] B. Al-Hanahi, I. Ahmad, D. Habibi, and M. A. S. Masoum, “Smart charging strategies for heavy electric vehicles,” *eTransportation*, vol. 13, p. 100182, 2022, doi: 10.1016/j.etran.2022.100182.

[102] F. Zhu *et al.*, “Does the battery swapping energy supply mode have better economic potential for electric heavy-duty trucks?,” *eTransportation*, vol. 15, no. November 2022, p. 100215, 2023, doi: 10.1016/j.etran.2022.100215.

[103] Q. Yan *et al.*, “Many-objective charging optimization for electric vehicles considering demand response and multi-uncertainties based on Markov chain and information gap decision theory,” *Sustain Cities Soc*, vol. 78, no. January, p. 103652, 2022, doi: 10.1016/j.scs.2021.103652.

[104] P. J. Chacko and M. Sachidanandam, “Optimization & validation of Intelligent Energy Management System for pseudo dynamic predictive regulation of plug-in hybrid electric vehicle as donor clients,” *eTransportation*, vol. 3, p. 100050, 2020, doi: 10.1016/j.etran.2020.100050.

[105] X. Li *et al.*, “A cost-benefit analysis of V2G electric vehicles supporting peak shaving in Shanghai,” *Electric Power Systems Research*, vol. 179, 2020, doi: 10.1016/j.epsr.2019.106058.

[106] H. S. Das, M. M. Rahman, S. Li, and C. W. Tan, “Electric vehicles standards, charging infrastructure, and impact on grid integration: A technological review,” *Renewable and Sustainable Energy Reviews*, vol. 120, no. November 2019, 2020, doi: 10.1016/j.rser.2019.109618.

[107] R. Shi, S. Li, P. Zhang, and K. Y. Lee, “Integration of renewable energy sources and electric vehicles in V2G network with adjustable robust optimization,” *Renew Energy*, vol. 153, 2020, doi: 10.1016/j.renene.2020.02.027.

[108] A. Zakariazadeh, S. Jadid, and P. Siano, "Multi-objective scheduling of electric vehicles in smart distribution system," *Energy Convers Manag*, vol. 79, 2014, doi: 10.1016/j.enconman.2013.11.042.

[109] K. Uddin, T. Jackson, W. D. Widanage, G. Chouchelamane, P. A. Jennings, and J. Marco, "On the possibility of extending the lifetime of lithium-ion batteries through optimal V2G facilitated by an integrated vehicle and smart-grid system," *Energy*, vol. 133, 2017, doi: 10.1016/j.energy.2017.04.116.

[110] A. Ahmadian, M. Sedghi, B. Mohammadi-Ivatloo, A. Elkamel, M. Aliakbar Golkar, and M. Fowler, "Cost-Benefit Analysis of V2G Implementation in Distribution Networks Considering PEVs Battery Degradation," *IEEE Trans Sustain Energy*, vol. 9, no. 2, 2018, doi: 10.1109/TSTE.2017.2768437.

[111] M. J. E. Alam, K. M. Muttaqi, and D. Sutanto, "Effective Utilization of Available PEV Battery Capacity for Mitigation of Solar PV Impact and Grid Support with Integrated V2G Functionality," *IEEE Trans Smart Grid*, vol. 7, no. 3, 2016, doi: 10.1109/TSG.2015.2487514.

[112] C. Peng, J. Zou, L. Lian, and L. Li, "An optimal dispatching strategy for V2G aggregator participating in supplementary frequency regulation considering EV driving demand and aggregator's benefits," *Appl Energy*, vol. 190, 2017, doi: 10.1016/j.apenergy.2016.12.065.

[113] H. S. V. S. Kumar Nunna, S. Battula, S. Doolla, and D. Srinivasan, "Energy Management in Smart Distribution Systems with Vehicle-To-Grid Integrated Microgrids," *IEEE Trans Smart Grid*, vol. 9, no. 5, 2018, doi: 10.1109/TSG.2016.2646779.

[114] Fuel Cells and Hydrogen 2 Joint Undertaking, "Hydrogen-powered aviation: a fact-based study of hydrogen technology, economics, and climate impact by 2050," McKinsey & Company, 2020. doi: doi/10.2843/766989.

[115] S. Hemavathi and A. Shinisha, "A study on trends and developments in electric vehicle charging technologies," *J Energy Storage*, vol. 52, no. PC, p. 105013, 2022, doi: 10.1016/j.est.2022.105013.

[116] A. Ahmad, M. S. Alam, and R. Chabaan, "A Comprehensive Review of Wireless Charging Technologies for Electric Vehicles," *IEEE Transactions on Transportation Electrification*, vol. 4, no. 1, pp. 38–63, 2017, doi: 10.1109/TTE.2017.2771619.

[117] J. Sun *et al.*, "A novel charging and active balancing system based on wireless power transfer for Lithium-ion battery pack," *J Energy Storage*, vol. 55, no. PC, p. 105741, 2022, doi: 10.1016/j.est.2022.105741.

[118] H. S. Das, M. M. Rahman, S. Li, and C. W. Tan, "Electric vehicles standards, charging infrastructure, and impact on grid integration: A technological review," *Renewable and Sustainable Energy Reviews*, no. February, 2019, doi: 10.1016/j.rser.2019.109618.

[119] Y. J. Jang, "Survey of the operation and system study on wireless charging electric vehicle systems," *Transp Res Part C Emerg Technol*, vol. 95, no. November 2017, pp. 844–866, 2018, doi: 10.1016/j.trc.2018.04.006.

[120] S. Lukic and Z. Pantic, "Cutting the Cord: Static and Dynamic Inductive Wireless Charging of Electric Vehicles," *IEEE Electrification Magazine*, vol. 1, no. 1, pp. 57–64, 2013, doi: 10.1109/MELE.2013.2273228.

[121] A. Mahesh, B. Chokkalingam, and L. Mihet-Popa, "Inductive Wireless Power Transfer Charging for Electric Vehicles-A Review," *IEEE Access*, vol. 9, pp. 137667–137713, 2021, doi: 10.1109/ACCESS.2021.3116678.

[122] X. Lu, P. Wang, D. Niyato, D. I. Kim, and Z. Han, "Wireless Charging Technologies: Fundamentals, Standards, and Network Applications," *IEEE Communications Surveys and Tutorials*, vol. 18, no. 2, pp. 1413–1452, 2016, doi: 10.1109/COMST.2015.2499783.

[123] K. Van Schuylenbergh and R. Puers, Eds., "Primary coil drivers," in *Inductive Powering: Basic Theory and Application to Biomedical Systems*, Dordrecht: Springer Netherlands, 2009, pp. 103–143. doi: 10.1007/978-90-481-2412-1_4.

[124] L. A., J. Jiang, A. Maglaras, F. V., and S. Moschoyiannis, "Dynamic wireless charging of electric vehicles on the move with Mobile Energy Disseminators,"

International Journal of Advanced Computer Science and Applications, vol. 6, no. 6, pp. 239–251, 2015, doi: 10.14569/ijacsa.2015.060634.

[125] P. K. Joseph and D. Elangovan, "A review on renewable energy powered wireless power transmission techniques for light electric vehicle charging applications," *J Energy Storage*, vol. 16, pp. 145–155, 2018, doi: 10.1016/j.est.2017.12.019.

[126] Y. D. Ko and Y. J. Jang, "The optimal system design of the online electric vehicle utilizing wireless power transmission technology," *IEEE Transactions on Intelligent Transportation Systems*, vol. 14, no. 3, pp. 1255–1265, 2013, doi: 10.1109/TITS.2013.2259159.

[127] Y. D. Ko and Y. J. Jang, "Efficient design of an operation profile for wireless charging electric tram systems," *Comput Ind Eng*, vol. 127, no. March 2018, pp. 1193–1202, 2019, doi: 10.1016/j.cie.2018.03.042.

[128] R. Riemann, D. Z. W. Wang, and F. Busch, "Optimal location of wireless charging facilities for electric vehicles: Flow capturing location model with stochastic user equilibrium," *Transp Res Part C Emerg Technol*, vol. 58, no. Part A, pp. 1–12, 2015, doi: 10.1016/j.trc.2015.06.022.

[129] R. Tavakoli, E. M. Dede, C. Chou, and Z. Pantic, "Cost-Efficiency Optimization of Ground Assemblies for Dynamic Wireless Charging of Electric Vehicles," *IEEE Transactions on Transportation Electrification*, vol. 8, no. 1, pp. 734–751, 2022, doi: 10.1109/TTE.2021.3105573.

[130] Y. J. Jang, S. Jeong, and M. S. Lee, "Initial energy logistics cost analysis for stationary, quasi-dynamic, & dynamicwireless charging public transportation systems," *Energies (Basel)*, vol. 9, no. 7, 2016, doi: 10.3390/en9070483.

[131] Z. Chen, F. He, and Y. Yin, "Optimal deployment of charging lanes for electric vehicles in transportation networks," *Transportation Research Part B: Methodological*, vol. 91, pp. 344–365, 2016, doi: 10.1016/j.trb.2016.05.018.

[132] H. Liu and D. Z. W. Wang, "Locating multiple types of charging facilities for battery electric vehicles," *Transportation Research Part B: Methodological*, vol. 103, pp. 30–55, 2017, doi: 10.1016/j.trb.2017.01.005.

[133] C. A. García-Vázquez, F. Llorens-Iborra, L. M. Fernández-Ramírez, H. Sánchez-Sainz, and F. Jurado, "Comparative study of dynamic wireless charging of electric vehicles in motorway, highway and urban stretches," *Energy*, vol. 137, no. 2017, pp. 42–57, 2017, doi: 10.1016/j.energy.2017.07.016.

[134] R. C. Majhi, P. Ranjitkar, and M. Sheng, "Assessment of dynamic wireless charging based electric road system: A case study of Auckland motorway," *Sustain Cities Soc*, vol. 84, no. February, p. 104039, 2022, doi: 10.1016/j.scs.2022.104039.

[135] G. Duarte, A. Silva, and P. Baptista, "Assessment of wireless charging impacts based on real-world driving patterns: Case study in Lisbon, Portugal," *Sustain Cities Soc*, vol. 71, no. December 2020, 2021, doi: 10.1016/j.scs.2021.102952.

[136] X. Huang, H. Qiang, Z. Huang, Y. Sun, and J. Li, "The interaction research of smart grid and EV based wireless charging," *2013 9th IEEE Vehicle Power and Propulsion Conference, IEEE VPPC 2013*, pp. 354–358, 2013, doi: 10.1109/VPPC.2013.6671718.

[137] Y. Sun, P. Zhao, L. Wang, and S. M. Malik, "Spatial and temporal modelling of coupled power and transportation systems: A comprehensive review," *Energy Conversion and Economics*, vol. 2, no. 2, pp. 55–66, 2021, doi: 10.1049/enc2.12034.

[138] M. Mohammad *et al.*, "Bidirectional LCC–LCC-Compensated 20-kW Wireless Power Transfer System for Medium-Duty Vehicle Charging," *IEEE Transactions on Transportation Electrification*, vol. 7, no. 3, pp. 1205–1218, 2021, doi: 10.1109/TTE.2021.3049138.

[139] S. Sachan, S. Deb, S. N. Singh, P. P. Singh, and D. D. Sharma, "Planning and operation of EV charging stations by chicken swarm optimization driven heuristics," *Energy Conversion and Economics*, vol. 2, no. 2, pp. 91–99, 2021, doi: 10.1049/enc2.12030.

[140] H. Nasr Esfahani, Z. Liu, and Z. Song, "Optimal pricing for bidirectional wireless charging lanes in coupled transportation and power networks," *Transp Res Part C Emerg Technol*, vol. 135, no. September 2021, p. 103419, 2022, doi: 10.1016/j.trc.2021.103419.

[141] M. Lukic, P. Giangrande, A. Hebala, S. Nuzzo, and M. Galea, "Review, Challenges, and Future Developments of Electric Taxiing Systems," *IEEE Transactions on Transportation Electrification*, vol. 5, no. 4, pp. 1441–1457, 2019, doi: 10.1109/TTE.2019.2956862.

[142] Federal Aviation Administration Press Office, "FAA Awards Another $20.4M to Electrify Airport Equipment, Latest in $300M Investment This Year," Aug. 24, 2021. https://www.faa.gov/newsroom/faa-awards-another-204m-electrify-airport-equipment-latest-300m-investment-year (accessed Jul. 30, 2023).

[143] S. Helber, J. Broihan, Y. J. Jang, P. Hecker, and T. Feuerle, "Location planning for dynamicwireless charging systems for electric airport passenger buses," *Energies (Basel)*, vol. 11, no. 2, pp. 1–16, 2018, doi: 10.3390/en11020258.

[144] L. Soares and H. Wang, "Economic feasibility analysis of charging infrastructure for electric ground fleet in airports," *Transp Res Rec*, vol. 2675, no. 12, pp. 1–12, 2021, doi: 10.1177/03611981211033859.

[145] K. P. Murphy, *Machine Learning - A Probabilistic Perspective*. 2012.

[146] V. François-lavet *et al.*, "An Introduction to Deep Reinforcement Learning," *Foundations and trends in machine learning*, vol. II, no. 3–4, pp. 1–140, 2018, doi: 10.1561/2200000071.Vincent.

[147] R. Bellman, "A Markovian Decision Process," *Indiana University Mathematics Journal*, vol. 6, no. 4, pp. 679–684, 1957, doi: 10.1512/iumj.1957.6.56038.

[148] D. Hao *et al.*, *Deep Reinforcement Learning: Fundamentals, Research, and Applications*. Springer, 2020.

[149] Y. Lecun, Y. Bengio, and G. Hinton, "Deep learning," *Nature*, vol. 521, no. 7553, pp. 436–444, 2015, doi: 10.1038/nature14539.

[150] Y. Wang, D. Qiu, and G. Strbac, "Multi-agent deep reinforcement learning for resilience-driven routing and scheduling of mobile energy storage systems," *Appl Energy*, vol. 310, Mar. 2022, doi: 10.1016/j.apenergy.2022.118575.

[151] T. Yang, L. Zhao, W. Li, and A. Y. Zomaya, "Dynamic energy dispatch strategy for integrated energy system based on improved deep reinforcement learning," *Energy*, vol. 235, Nov. 2021, doi: 10.1016/j.energy.2021.121377.

[152] F. Sanchez Gorostiza and F. M. Gonzalez-Longatt, "Deep Reinforcement Learning-Based Controller for SOC Management of Multi-Electrical Energy Storage System," *IEEE Trans Smart Grid*, vol. 11, no. 6, pp. 5039–5050, 2020, doi: 10.1109/TSG.2020.2996274.

[153] S. Wang, S. Bi, and Y. A. Zhang, "Reinforcement Learning for Real-Time Pricing and Scheduling Control in EV Charging Stations," *IEEE Trans Industr Inform*, vol. 17, no. 2, pp. 849–859, Feb. 2021, doi: 10.1109/TII.2019.2950809.

[154] Y. Wang, D. Qiu, G. Strbac, and Z. Gao, "Coordinated Electric Vehicle Active and Reactive Power Control for Active Distribution Networks," *IEEE Trans Industr Inform*, vol. 3203, no. c, pp. 1–11, 2022, doi: 10.1109/TII.2022.3169975.

[155] Q. Yuan, Y. Ye, Y. Tang, Y. Liu, and G. Strbac, "A novel deep-learning based surrogate modeling of stochastic electric vehicle traffic user equilibrium in low-carbon electricity–transportation nexus," *Appl Energy*, vol. 315, no. April, p. 118961, 2022, doi: 10.1016/j.apenergy.2022.118961.

[156] D. Qiu, Y. Wang, T. Zhang, M. Sun, and G. Strbac, "Hybrid Multi-Agent Reinforcement Learning for Electric Vehicle Resilience Control Towards a Low-Carbon Transition," *IEEE Trans Industr Inform*, vol. 18, no. 11, pp. 8258–8269, 2022, doi: 10.1109/TII.2022.3166215.

[157] S. Ortega Alba and M. Manana, "Characterization and analysis of energy demand patterns in airports," *Energies (Basel)*, vol. 10, no. 1, pp. 1–35, 2017, doi: 10.3390/en10010119.

[158] S. Ison, I. Humphreys, and T. Rye, "UK airport employee car parking: The role of a charge?," *J Air Transp Manag*, vol. 13, no. 3, pp. 163–165, 2007, doi: 10.1016/j.jairtraman.2006.12.001.

[159] J. West, "How Early Should You Get to the Airport? [A Complete Guide]." https://upgradedpoints.com/travel/airports/how-early-should-you-get-to-the-airport/ (accessed Aug. 07, 2023).

[160] H. Zhao *et al.*, "Resilience Assessment of Hydrogen-Integrated Energy System for Airport Electrification," *IEEE Trans Ind Appl*, vol. 58, no. 2, pp. 2812–2824, 2022, doi: 10.1109/TIA.2021.3127481.

[161] M. K. Deshmukh and S. S. Deshmukh, "Modeling of hybrid renewable energy systems," *Renewable and Sustainable Energy Reviews*, vol. 12, no. 1, pp. 235–249, 2008, doi: 10.1016/j.rser.2006.07.011.

[162] J. Jiang *et al.*, "Optimal sizing, operation strategy and case study of a grid-connected solid oxide fuel cell microgrid," *Appl Energy*, vol. 307, no. December 2021, p. 118214, 2022, doi: 10.1016/j.apenergy.2021.118214.

[163] Department of Energy, "DOE Hydrogen and Fuel Cells Program Record 9013: Energy requirements for hydrogen gas compression and liquefaction as related to vehicle storage needs," 2009. [Online]. Available: http://www.eere.energy.gov/hydrogenandfuelcells/hydrogen_publications.html#h2_storage

[164] H. Liang, Y. Liu, F. Li, and Y. Shen, "Dynamic Economic/Emission Dispatch Including PEVs for Peak Shaving and Valley Filling," *IEEE Transactions on Industrial Electronics*, vol. 66, no. 4, pp. 2880–2890, 2019, doi: 10.1109/TIE.2018.2850030.

[165] K. Deb, A. Pratap, S. Agarwal, and T. Meyarivan, "A fast and elitist multiobjective genetic algorithm: NSGA-II," *IEEE Transactions on Evolutionary Computation*, vol. 6, no. 2, pp. 182–197, 2002, doi: 10.1109/4235.996017.

[166] H. Wei, J. Liang, C. Li, and Y. Zhang, "Real-time Locally Optimal Schedule for Electric Vehicle Load via Diversity-maximization NSGA-II," *Journal of Modern Power Systems and Clean Energy*, vol. 9, no. 4, pp. 940–950, 2021, doi: 10.35833/MPCE.2020.000093.

[167] JUSTWE, "Time of Use Tariff UK." https://justwe-gpi.com/energy-economy/time-of-use-tariff-uk/ (accessed Aug. 01, 2023).

[168] K. Berman, J. Dziuba, C. Hamilton, R. Carlson, J. Jackson, and P. Sklar, "The Lithium Ion Battery and the EV Market," no. February, 2018.

[169] O. Bucovetchi, A. Georgescu, D. Badea, and R. D. Stanciu, "Agent-based modeling (ABM): Support for emphasizing the air transport infrastructure dependence of space systems," *Sustainability (Switzerland)*, vol. 11, no. 19, 2019, doi: 10.3390/su11195331.

[170] K. Deb, A. Pratap, S. Agarwal, and T. Meyarivan, "A fast and elitist multiobjective genetic algorithm: NSGA-II," *IEEE Transactions on Evolutionary Computation*, vol. 6, no. 2, pp. 182–197, 2002, doi: 10.1109/4235.996017.

[171] K. Deb and H. Jain, "An evolutionary many-objective optimization algorithm using reference-point-based nondominated sorting approach, Part I: Solving problems with box constraints," *IEEE Transactions on Evolutionary Computation*, vol. 18, no. 4, pp. 577–601, 2014, doi: 10.1109/TEVC.2013.2281535.

[172] I. Das and J. E. Dennis, "Normal-Boundary Intersection: A New Method for Generating the Pareto Surface in Nonlinear Multicriteria Optimization Problems," *SIAM Journal on Optimization*, vol. 8, no. 3, pp. 631–657, 1998, doi: 10.1137/S1052623496307510.

[173] F. Hameed, M. Al Hosani, and H. H. Zeineldin, "A Modified Backward/Forward Sweep Load Flow Method for Islanded Radial Microgrids," *IEEE Trans Smart Grid*, vol. 10, no. 1, pp. 910–918, Jan. 2019, doi: 10.1109/TSG.2017.2754551.

[174] G. W. Chang, S. Y. Chu, and H. L. Wang, "An improved backward/forward sweep load flow algorithm for radial distribution systems," *IEEE Transactions on Power Systems*, vol. 22, no. 2, pp. 882–884, 2007, doi: 10.1109/TPWRS.2007.894848.

[175] M. Potkány, M. Hlatká, M. Debnár, and J. Hanzl, "Comparison of the lifecycle cost structure of electric and diesel buses," *Nase More*, vol. 65, no. 4 Special issue, pp. 270–275, Oct. 2018, doi: 10.17818/NM/2018/4SI.20.

[176] "Fuel price calculator: How much do you pay? - BBC News." https://www.bbc.co.uk/news/business-21238363 (accessed Feb. 11, 2023).

[177] "Kg CO2 per litre of diesel vehicles | Comcar." https://comcar.co.uk/emissions/co2litre/?fueltype=diesel (accessed Feb. 11, 2023).

[178] “ESO Data Portal: National Carbon Intensity Forecast - Dataset| National Grid Electricity System Operator.” https://data.nationalgrideso.com/carbon-intensity1/national-carbon-intensity-forecast (accessed Feb. 11, 2023).

[179] “CO_2 emission performance standards for cars and vans.” https://climate.ec.europa.eu/eu-action/transport-emissions/road-transport-reducing-co2-emissions-vehicles/co2-emission-performance-standards-cars-and-vans_en (accessed Feb. 11, 2023).

[180] “UK Civil Aviation Authority (CAA).” https://www.caa.co.uk/home/

[181] “FlightStats - Global Flight Status & Tracker, Airport Weather and Delays.” https://www.flightstats.com/v2/ (accessed Jun. 27, 2020).

[182] “Topic 13 – Solar Power Plant Installations In Malaysia | AER.” http://aer.global/topic-13-solar-power-plant-installations-in-malaysia/ (accessed Sep. 13, 2020).

[183] S. Pfenninger and I. Staffell, “Long-term patterns of European PV output using 30 years of validated hourly reanalysis and satellite data,” *Energy*, 2016, doi: 10.1016/j.energy.2016.08.060.

[184] B. I. Ayuyev, P. M. Yerokhin, N. G. Shubin, V. G. Neujmin, and A. A. Alexandrov, “Unit commitment with network constraints,” *2005 IEEE Russia Power Tech, PowerTech*, 2005, doi: 10.1109/PTC.2005.4524780.

[185] Z. Liu, Q. Wu, M. Shahidehpour, C. Li, S. Huang, and W. Wei, “Transactive real-time electric vehicle charging management for commercial buildings with PV on-site generation,” *IEEE Trans Smart Grid*, vol. 10, no. 5, pp. 4939–4950, 2019, doi: 10.1109/TSG.2018.2871171.

[186] “THE GRID CODE ISSUE 6 REVISION 6,” *National Grid*, 2021. https://www.nationalgrideso.com/document/162271/download (accessed Sep. 12, 2021).

[187] “Appendices to the Technical Report on the events of 9 August 2019,” 2019. https://www.nationalgrideso.com/document/152351/download (accessed Oct. 08, 2021).

[188] J. Morren, S. W. H. De Haan, and J. A. Ferreira, "Contribution of DG units to primary frequency control," *European Transactions on Electrical Power*, vol. 16, no. 5, pp. 507–521, 2006, doi: 10.1002/etep.113.

[189] "Firm frequency response (FFR) | National Grid ESO." https://www.nationalgrideso.com/industry-information/balancing-services/frequency-response-services/firm-frequency-response-ffr?overview (accessed Sep. 19, 2021).

[190] Y. Mu, J. Wu, J. Ekanayake, N. Jenkins, and H. Jia, "Primary frequency response from electric vehicles in the Great Britain power system," *IEEE Trans Smart Grid*, 2013, doi: 10.1109/TSG.2012.2220867.

[191] National Grid ESO, "Operating a Low Inertia System," 2020. https://www.nationalgrideso.com/research-publications/system-operability-framework-sof (accessed Oct. 10, 2021).

[192] J. Meng, Y. Mu, H. Jia, J. Wu, X. Yu, and B. Qu, "Dynamic frequency response from electric vehicles considering travelling behavior in the Great Britain power system," *Appl Energy*, vol. 162, pp. 966–979, 2016, doi: 10.1016/j.apenergy.2015.10.159.

[193] Y. Zhu and K. Tomsovic, "Development of models for analyzing the load-following performance of microturbines and fuel cells," *Electric Power Systems Research*, vol. 62, no. 1, pp. 1–11, 2002, doi: 10.1016/S0378-7796(02)00033-0.

[194] L. Badesa, G. Strbac, M. Magill, and B. Stojkovska, "Ancillary services in Great Britain during the COVID-19 lockdown: A glimpse of the carbon-free future," *Appl Energy*, vol. 285, no. December 2020, p. 116500, 2021, doi: 10.1016/j.apenergy.2021.116500.

[195] H. Urdal, R. Ierna, J. Zhu, C. Ivanov, A. Dahresobh, and D. Rostom, "System strength considerations in a converter dominated power system," in *IET Renewable Power Generation*, Institution of Engineering and Technology, Jan. 2015, pp. 10–17. doi: 10.1049/iet-rpg.2014.0199.

[196] P. Imris, M. Bradley, G. Taylor, and Y. Li, "Development of a Great Britain Transmission System Reduced Model for Hardware-In-the-Loop Studies."

[197] P. Imris, G. A. Taylor, M. E. Bradley, and Y. Li, “A Novel Hardware-in-the-Loop Approach to Investigate the Impact of Low System Inertia on RoCoF Relay Settings,” *Energies (Basel)*, vol. 15, no. 17, Sep. 2022, doi: 10.3390/en15176386.

[198] G. Nuhic Mirza and Yang, “Battery Energy Storage System Modelling in DIgSILENT PowerFactory,” in *Modelling and Simulation of Power Electronic Converter Dominated Power Systems in PowerFactory*, J. L. Gonzalez-Longatt Francisco M. and Rueda Torres, Ed., Cham: Springer International Publishing, 2021, pp. 177–200. doi: 10.1007/978-3-030-54124-8_7.

[199] S. Sukumaran and K. Sudhakar, “Fully solar powered airport: A case study of Cochin International airport,” *J Air Transp Manag*, vol. 62, pp. 176–188, 2017, doi: 10.1016/j.jairtraman.2017.04.004.

[200] “Aviation 2050 - The future of UK aviation,” 2018. https://assets.publishing.service.gov.uk/government/uploads/system/uploads/attachment_data/file/769695/aviation-2050-web.pdf

[201] P. Bießlich, “Developing Generic Flight Schedules for Airport Clusters,” in *5th CEAS conference*, 2015, pp. 1–16.